Forest of Giants : understanding the role of intact tropical forests as natural climate solutions by the abundance, distribution and biomass of their large trees

Mathieu Guillemette

Faculty of Science, Department of Biology

McGill University

Montréal, Québec, Canada

A thesis submitted to McGill University in partial fulfillment of the requirements of the degree of Master of Science

Table of Contents

Abstract **5**

Résumé **7**

Acknowledgments **9**

Preface **11**

List of Tables **13**

List of Figures **15**

List of Abbreviations **20**

General Introduction **22**

Chapter 1 : A new compartmentalized model to estimate large tropical tree aboveground biomass with terrestrial laser scanning technology **26**

- Introduction 29
- Materials and Methods 32
  - Study sites and datasets 32
  - AGB estimations 34
  - Analyses 40
- Results 41
  - QSM's challenges 41
  - Models' agreement to QSM 44
  - AGB's distribution in large tropical trees 47
- Discussion 50
  - The future of TLS, QSM and the Compartmentalized Model 50
  - Challenges in estimating large trees' AGB 52

Conclusion 55

References 56

Supplementary Information 65

Data acquisition and tree measurements 65

Other QSM studies in tropical forests 66

Theories for tree crown development 67

Challenges in computing QSM 68

Models' performances 70

First-order branches' biomass 73

Linking Statement 76

Chapter 2: Large tree density, distribution pattern and carbon stocks' spatial variation in a neotropical intact forest 77

Introduction 78

Materials and Methods 81

Study site 81

Bacurú Drõa Permanent Plot 82

Landscape analyses 86

Results 90

Bacurú Drõa Permanent Plot's tree diversity and forest structure 90

RS trees false-negative analysis 93

Landscape giant tree abundance, distribution pattern and carbon stocks 94

Discussion 96

Abundance and distribution pattern of large trees 96

Large tree distribution pattern's impacts on sampling protocols 99

Conclusion 101
References 102
Supplementary information 109
  ForestGEO forest plot design 109
  Poisson distribution point pattern 110
  The area of interest within the *Tierras Colectivas del Rio Balsas* 111
  Large tree density analysis 112
  The *Bacurú Drõa* Permanent Plot between clusters of RS trees 113
  Research limits 115
General Discussion and Conclusion 117
Master’s Reference List 122

Abstract

It has been suggested that conserving standing tropical forests might be the most cost-effective and fastest way to mitigate the impacts of climate change. Over the past few years, numerous initiatives putting tropical forests at the forefront of the climate agenda have been deployed. However, monitoring forest carbon stocks is still a science in progress. Recently, large tropical trees have attracted increased attention as they hold the bulk of forest carbon stocks, but accurately estimating large trees' carbon content remains challenging. Moreover, the global distribution, abundance and factors influencing the distribution of large trees remain elusive. This thesis (1) focuses on a new method to estimate large tropical trees' aboveground biomass (AGB) (a proxy for carbon stocks) using terrestrial laser scanning technology (TLS) and (2) investigates large tropical tree distribution patterns and its impact on the spatial variation of forest carbon stocks.

Recent literature has suggested that TLS combined with Quantitative Structure Models (QSM) was the most accurate way to estimate large trees' AGB. However, in tropical evergreen forests, QSMs have only been applied at the scale of only a few hundred trees, never providing estimates of AGB at the plot level. Estimates of AGB at the plot level are essential to extrapolate to the landscape level or to calibrate remote sensing tools and develop forest carbon maps. In chapter 1, I tested the applicability of QSM to 104 scans of large tropical trees. I found that QSM were successfully applied to only 36 trees due to occlusion problems, preventing QSM from providing AGB estimates for entire forest plots. To answer this gap, I developed a new method that I called the Compartmentalized Model. This method considers trees as fractal objects where tree trunks and branches are separate elements from which biomass can be estimated using TLS

point clouds. I then discuss the opportunities for TLS to measure different tree components from the ground and to improve AGB estimates of large tropical trees.

In chapter 2, using three different forest inventory datasets that cover a total area of ~ 20 ha and one remote sensing dataset containing large tropical tree locations across the Emberá Territory of the Balsas River, Panama, I found that large trees had a clustered distribution. This distribution of large trees resulted in a heterogenous forest landscape characterized by small pockets of high carbon density surrounded by areas of lower carbon density. In addition, I used the inventory datasets to demonstrate how plot size and plot distribution in a heterogenous forest landscape can lead to significantly different carbon density values and affect carbon payments in forest carbon finance programs. These results advance our knowledge of large tropical tree distribution patterns and abundance values. They also raise concerns about accurately monitoring forest carbon stocks in intact forest landscapes.

Résumé

Il a été suggéré que conserver les forêts tropicales pourrait être le moyen le plus rentable et le plus rapide pour atténuer les impacts du changement climatique. Au cours des dernières années, de nombreuses initiatives plaçant les forêts tropicales au premier plan de l'agenda climatique ont été déployées. Cependant, le suivi des stocks de carbone forestier est encore une science en évolution. Récemment, les gros arbres tropicaux ont attiré une attention accrue, car ils détiennent, à eux seuls, la majorité du carbone forestier. Toutefois, estimer avec précision la quantité de carbone contenue dans les gros arbres reste difficile. De plus, la répartition mondiale, l'abondance et les facteurs influençant ceux-ci restent méconnus pour les gros arbres. Ce mémoire (1) propose une nouvelle méthode pour estimer la biomasse aérienne des gros arbres tropicaux (un proxy pour les stocks de carbone) en utilisant le Lidar Terrestre (T-Lidar) et (2) étudie la distribution des gros arbres tropicaux et son impact sur la variation spatiale des stocks de carbone forestier.

La littérature récente suggère que le T-Lidar combiné aux modèles de structure quantitative (QSM) est présentement le moyen le plus précis d'estimer la biomasse aérienne des gros arbres. Cependant, dans les forêts tropicales humides, les QSM n'ont été appliqués qu'à quelques centaines d'arbres, ne fournissant jamais d'estimations de biomasse pour des parcelles de forêts. Les estimations de la biomasse aérienne au niveau de la parcelle sont essentielles pour extrapoler ces données au niveau du paysage ou pour calibrer les outils de télédétection afin de développer des cartes du carbone forestier. Dans le chapitre 1, j'ai testé l'applicabilité des QSM à 104 numérisations de gros arbres tropicaux. Mes résultats démontrent que les QSM ont été appliqués avec succès qu'à 36 arbres en raison de problèmes d'occlusion. Cela empêche les QSM

de fournir des estimations de biomasse au niveau de parcelles forestières. Pour répondre à cette problématique, j'ai développé une nouvelle méthode que j'appelle le Modèle Compartimenté. Celle-ci considère les arbres comme des objets fractals où le tronc et les branches des arbres sont des éléments séparés à partir desquels la biomasse peut être estimée à l'aide de nuage de points provenant de numérisations T-Lidar. Je discute ensuite des opportunités du T-Lidar pour mesurer différentes composantes d'arbre à partir du sol et pour améliorer les estimations de biomasse aérienne des gros arbres tropicaux.

Dans le chapitre 2, en utilisant trois jeux de données d'inventaire forestier différents couvrant une superficie totale d'environ 20 ha et un jeu de données de télédétection contenant l'emplacement de gros arbres tropicaux à travers le territoire Emberá de la rivière Balsas, au Panama, j'ai constaté que les gros arbres avaient une distribution groupée. Cette distribution résulte en un paysage forestier hétérogène caractérisé par de petites pochettes à haute densité de carbone entourées de zones à densité plus faible de carbone. De plus, j'ai utilisé ces jeux de données pour démontrer comment, dans un paysage forestier hétérogène, la taille et la distribution des parcelles d'inventaire forestier peuvent conduire à des valeurs de densité de carbone significativement différentes et affecter les estimés de paiements de carbone dans les programmes de financement du carbone forestier. Ces résultats avancent nos connaissances sur la distribution et les valeurs d'abondance des gros arbres tropicaux et soulèvent des inquiétudes quant à la manière de surveiller avec précision les stocks de carbone forestier dans les forêts intactes.

Acknowledgments

I would like to start by thanking my supervisor Dr. Catherine Potvin for her support throughout my graduate studies. I was fortunate to meet Catherine for the first time in 2014 when I was a young undergraduate student, ambitious to work in the tropics. At the time, Catherine took me under the umbrella of her lab and showed me the fantastic reality of working in tropical forest ecology with the collaboration of Indigenous People. It was a very rich and exciting experience that led me to pursue graduate studies on that path. I am deeply grateful for the opportunity that Catherine has given me. This thesis would not have been possible without Catherine's 25+ years of experience working in the tropics and with the collaboration of the Emberá People. Catherine, thank you for sharing your experience and knowledge, for being incredibly supportive, and for giving me these opportunities.

I am extremely grateful to my committee members, Dr. Matthias Kunz, Dr. Helene Muller-Landau and Dr. Jérôme Chave. Without them, this Master's thesis wouldn't have been possible. Dr. Matthias Kunz has been of tremendous help since the beginning of my graduate studies. He taught me how to work with terrestrial laser scan data, how to navigate graduate studies and how to find where I stand in science. Matthias, you are a source of inspiration, a mentor and a friend. Moreover, Dr. Helene Muller-Landau and Dr. Jérôme Chave have been helpful with all their advices and feedbacks on my research ideas and manuscripts. Thank you!

Muchas gracias to all the technicians and people of the *Tierras Colectivas del Rio Balsas*. You have been extremely generous to welcome me into your territory and it was a privilege walking alongside you in your forests. I wish you the best with the *Bacurú Drõa* forest observatory and hope to visit you again.

Finally, thank you to my friends, lab mates and family. Graduate studies are made of questions, answers, doubts, accomplishments, ups and downs. But, no matter what, you were always there to share the ups and downs, and I feel fortunate to have you. Now, I look forward to sharing this new accomplishment with you!

Financial Support

Thank you to the National Science and Engineering Research Council for funding the first year of my graduate studies and to the Fonds de Recherche du Québec for funding the last two years of my studies. Also, thank you to McGill University for adding extra financial support with the with a welcoming graduate student award and with a Covid-19 and inflationary award. Finally, thank you to Dr. Potvin's lab for supporting me financially in addition to these scholarships.

Preface

Thesis Format Style

This manuscript-based thesis includes two manuscripts following scientific publication formatting. The first chapter explores the challenges in estimating the aboveground biomass (AGB) of large tropical trees and develops a new estimation method using Terrestrial Laser Scanning technology. This chapter was submitted to Methods in Ecology and Evolution. The second chapter extends the analysis of AGB at the landscape level to understand the spatial variation of carbon stocks and the implications for monitoring forests. Part of this chapter (i.e., the analyses using data from the *Bacurú Drõa* Permanent Plot) will join another manuscript to present the *Bacurú Drõa* Permanent Plot forest structure in an upcoming submission to a scientific journal.

Contribution of Authors

Thesis

Mathieu Guillemette developed the original idea of this thesis with the help of Dr. Catherine Potvin. Catherine Potvin, Matthias Kunz and Alexis Ortega participated in collecting the *Ceiba pentandra* trunk slice used in the discussion. Fabio Gennaretti performed the growth ring analysis on the *Ceiba pentandra*. Mathieu Guillemette analyzed the growth ring data to transform it into carbon content. Mathieu Guillemette led the writing of this thesis with the guidance of Catherine Potvin.

Chapter 1

Mathieu Guillemette, Matthias Kunz and Catherine Potvin conceived the original idea for this study. Karl Friedrich Reich, Goddert von Oheimb and Jose Gonzalez de Tanago contributed to the ideas and further refinement. Alexis Ortega, Catherine Potvin, Francisco Solis, José Pari-Pari, Jose Gonzalez de Tanago and Matthias Kunz are responsible for collecting the field data. Alexandra Koller, Inga Freshse, Jose Gonzalez de Tanago, Matthias Kunz and Mathieu Guillemette performed that data processing and analysis. Dr. Karl Friedrich Reich, Dr. Goddert von Oheimb and Dr. Gonzalez de Tanago contributed to this chapter's ideas and further refinement. Mathieu Guillemette led the writing of the manuscript, with all other co-authors making significant contributions.

Chapter 2

Mathieu Guillemette developed the original idea behind this chapter with the contribution of Dr. Catherine Potvin, Dr. Matthias Kunz. Dr. Potvin, Dr. Kunz, Rolando Perez, Salomon Aguilar, David Mitre, Jorge Valdez, Alexis Ortega and Mathieu Guillemette contributed significantly to the design and establishment of the Bacurú Drõa Permanent Plot and to the data collection from the *Bacurú Drõa* Permanent plot used in this chapter. Dr. Kunz and Mathieu Guillemette collected the remote sensing data of potential giant trees over the landscape analysis. Mathieu Guillemette performed the statistical and spatial analyses with the help of Dr. Camilo Alejo and Dr. Kunz. Dr. Helene Muller-Landau contributed significantly to the idea and refinement of this chapter. Finally, with the help and guidance of mentioned co-authors, Mathieu Guillemette led the redaction of this chapter.

List of Tables

Chapter 1

Table 1: Study sites and data.

Table 2: The different allometric equations used to estimate trees' AGB. Chave et al. (2005) equation 07 (Ch.05 eq.07), Chave et al. (2014) equation 04 (Ch.14 eq.04), Ploton et al. (2016) model 3 (Plo.16M3) and the Compartmentalized Model (Compartmentalized).

Table 3: Models performance against QSM reconstructions. SE = standard error. R2 = coefficient of determination RMSE = root mean square error. CCC = concordance correlation coefficient. In all cases, the regression model has 38 points and, thus, 36 degrees of freedom.

Table S1: Previously published scientific articles with Quantitative Structure Models (QSM) for tropical trees.

Table S2: Summary of theories behind tree crown size and architecture.

Table S3: Models performance against QSM reconstructions. SE = standard error. R2 = coefficient of determination RMSE = root mean square error. CCC = concordance correlation coefficient. In all cases, trees of QSM AGB > 25 Mg were removed and there are 34 points and, thus, 32 degrees of freedom in the regression model.

Chapter 2

Table 1: The six most dominant tree species and families for all the trees and the large tree community of the *Bacurú Drõa* Permanent Plot with their respective number of trees, DBH average and standard deviation and their population's proportion of individuals in the large tree community. Species are presented by order of the highest number of large trees to the lowest.

Table 2: Average carbon stocks for all the plots inventoried inside Balsa river territory and total carbon stocks following the Stratify and Multiply method for the area covered by intact forests according to Global Forest Watch data (Hansen *et al.* 2013).

List of Figures

Chapter 1

Figure 1: The Emberá Traditional Territory of the Balsas River in eastern Panama and the locations of 20 plots where TLS data was collected (i.e., Panama Plots).

Figure 2: The different tree measurements (diameter at breast height (DBH), trunk height (Ht), top trunk diameter (Dtt), branch “i” diameter (Db_i) and branch “i” length (Lb_i)) taken on terrestrial laser scan trees (DBH ≥ 50 cm) to estimate their AGB using the Compartmentalized Model.

Figure 3: Unsuccessful Leaf-Wood Separation computation where the initial point cloud (panel A) was split into a soft-tissue point cloud (panel B) and a hard-tissue point cloud (panel C). In this example the separation led to removing too much of the point cloud considered as soft tissue, thus adding occlusion in the point cloud and affecting tree structure significantly.

Figure 4: A successful Leaf-Wood Separation computation where the initial point cloud (panel A) was split into a soft-tissue point cloud (panel B) and a hard-tissue point cloud (panel C). The resulting hard-tissue point cloud represents the entire tree architecture but still contains soft tissues that were removed manually using the segmentation tool in CloudCompare.

Figure 5: The process of extracting and measuring (top fork) or reconstructing QSM (bottom fork) for large trees using TLS plot scan to obtain plot AGB estimates with the Compartmentalized Model (top fork) and QSM (bottom fork).

Figure 6: Scattered plot of the predicted tree AGB from (a) Chave et al. (2005) pantropical equation, (b) Chave et al. (2014) pantropical equation, (c) Ploton et al. (2016) model 3 and (d) the compartmentalized Model against the reference values of the quantitative structure models (QSM) AGB estimates. The solid black line represents a fitted linear regression between the predicted values from the equation or model and the reference value of the QSMs. The dashed grey line represents a 1:1 relationship. Tree measurements come from TLS scans of the Panama dataset and Gonzalez de Tanago (2018) dataset ($n = 38$). (see Table 3 for linear models' parameters).

Figure 7: Log-transformed individual tree trunk biomass values are represented in green dots and green linear regression line ($F = 381.4$; $p < 0.05$). Log-transformed individual tree crown biomass values are in dark grey dots and dark grey linear regression line ($F= 116.1$; $p < 0.05$).

Figure 8: First-order branch biomass estimates coming from the Compartmentalized Model. The Boxplots are categorized and colored based on the number of branches in a tree crown. Boxes represent the interquartile range (25th and 75 percentile) with the median value represented by the middle line. Grey dots represent individual first-order branch biomass estimates within 1.5 times interquartile range and the black dots are individual first-order branch biomass outliers found outside 1.5 times interquartile range.

Figure 9: Estimated AGB (Mg) for all 104 TLS large trees coming from Chave et al. (2005) pantropical equation, Chave et al. (2014) pantropical equation, Ploton et al. (2016) model 3 and the Compartmentalized Model.

Figure S1: Example of TLS scan design inside 30 x 30 m plots (dashed line). Triangles show regular scan positions (blue stroke) and additional freely selected scan positions (orange stroke) for optimized scan coverage.

Figure S2: QSM reconstruction (dark colored cylinders) and tree point cloud (yellow) of tree17_02 where we see missing reconstruction of a second order branch in the crown center, a limited definition of crown reconstruction and the difficulty in capturing the buttressed trunk.

Figure S3: Residuals from Chave et al. (2005) pantropical equation estimates compared to the reference values of the QSM reconstruction (panel a) and for Chave et al. (2014) pantropical equation (panel b), Ploton et al. (2016) model 3 (panel 3) and the Compartmentalized Model (panel c).

Figure S4: Scattered plot of the predicted tree AGB from (a) Chave et al. (2005) pantropical equation, (b) Chave et al. (2014) pantropical equation, (c) Ploton et al. (2016) model 3 and (d) the compartmentalized method against the reference values of the quantitative structure models (QSM) AGB estimates. The solid black line represents a fitted linear regression between the predicted values from the equation or model and the reference value of the QSMs. The dashed grey line represents a 1:1 relationship. Tree measurements come from TLS scans of the Panama dataset and Gonzalez de Tanago et al. (2018) dataset. Trees of QSM AGB > 25 Mg were removed (n = 34) (see Table S3 for linear models' parameters).

Figure S5: Biomass (Mg) distribution of first-order branches following trees' DBH for the 104 TLS trees.

Chapter 2

Figure 1: Map close-up on the *Tierras Colectivas del Rio Balsas* with the centroids of the 0.09-ha plots presented in Kunz et al. (2022), 1-ha plots from Mateo-Vega et al. (2019) and the *Bacurú Drõa* Permanent Plot (10 ha) as well as the main villages and rivers. Marker size is not to scale.

Figure 2: Map of the *Bacurú Drõa* Permanent Plot, showing censused trees by DBH size class category.

Figure 3: Location of the RS trees (pink dots) and ground-validated RS trees (White/blue dots) within the concave hull area of interest (20 100 ha). Data from Kunz *et al.* (2022) with the additional 92 RS trees. Slope quantiles are flat (0 – 2.9°), semi-flat (2.9 - 8.6°), moderate (8.6 – 17.3°) and steep (17.3 – 60.9°).

Figure 4: Large trees (DBH ≥ 50 cm) distribution and overlayed quadrat-count (panel a). Very large trees (DBH ≥ 70 cm) distribution and overlayed quadrat-count (panel b). Giant trees (DBH ≥ 100 cm) distribution and overlayed quadrat-count+ (panel c).

Figure 5: The *Bacurú Drõa* Permanent Plot with the RS trees identified (red dots) using satellite image analysis on the left and the evaluation against ground census data for trees of DBH ≥ 100 cm from inventory data of the *Bacurú Drõa* Permanent Plot with their DBH measurements identified in centimeters on the right. The satellite image on this map comes from PlanetScope 4-Band Scene (10/13/2018).

Figure S1 : ForestGEO forest plot design. Panel a shows the 10 ha *Bacurú Drõa* Permanent Plot with each subplot of 1 ha. Panel b shows a zoom-in on the 20 x 20 m squares surveyed on the ground and marked with PVC tubes to move north until completing a 1-ha-subplot.

Figure S2: Map of the *Tierras Colectivas del Rio Balsas* categorized by the area above 500 m (black) and below 500 m (blue) and with the location of the inventory data plots.

Figure S3: Kernel density plot of the large tree community of the *Bacurú Drõa* Permanent plot. Warm colors represent a higher density of large trees and cold colors represent a lower density.

Figure S4: The *Bacurú Drõa* Permanent Plot location between clusters of giant trees presented using a Kernel Density interpolation using the RS trees.

General Discussion and Conclusion

Figure 1: The fallen *Ceiba pentandra* yearly carbon uptake according to its growth ring analysis.

List of Abbreviations

AGB – Aboveground biomass

BCI – Barro Colorado Island

CCC – Concordance correlation coefficient

CO_2 – Carbon dioxide

CTFS – Center for tropical forest studies

CV – Coefficient of variation

DBH – Diameter at breast height

FAO – Food and Agriculture Organization

GFW – Global Forest Watch

IPCC – Intergovernmental Panel on Climate Change

LeWoS – Leaf-Wood Separation

MRV – Monitoring, reporting and verifying

MST – Metabolic Scaling Theory

NCS – Natural climate solutions

QSM – Quantitative Structure Models

REDD+ – Reducing emissions from deforestation and forest degradation in developing countries

R2 – Coefficient of determination

RMSE – Root mean square error

RS – Remote Sensing

SD – Standard deviation

SE – Standard error

TLS – Terrestrial Laser Scan

General Introduction

Climate change mitigation requires both a rapid reduction in emissions from anthropogenic fossil fuels and maximizing the mitigation potential of natural ecosystems (Dooley K. *et al.* 2022). Natural climate solutions (NCS) propose a combination of conservation, improved management and restoration actions to increase natural ecosystems' carbon dioxide (CO_2) storing capacities, reduce greenhouse gas emissions and mitigate climate change (Griscom *et al.* 2017; Drever *et al.* 2021). Actions from NCS can also provide various environmental co-benefits (Fargione *et al.* 2018). For example, protecting forests for their carbon sequestration potential also ensure enhancing air and water quality (Smith *et al.* 2013), conserving biodiversity (Lindenmayer & Laurance 2017; Bastin *et al.* 2018) and supporting human well-being (Berkes & Davidson-Hunt 2006).

Historically, humans have had a negative impact on the world's forests through deforestation and forest degradation (Potapov *et al.* 2017; FAO 2018). However, this narrative could change as countries around the globe focus on mitigating their carbon emissions to slow down global warming (Allan *et al.* 2021) and NCS pathways involving forests attract the attention of forested countries (Griscom *et al.* 2017; Fargione *et al.* 2018; Drever *et al.* 2021). Globally, NCS forest pathways (e.g., reforestation and forest conservation) are allegedly the most cost-effective to achieve the global mitigation needed by 2030 (Griscom *et al.* 2017). This is because forests have a dual role as NCS (Drever *et al.* 2021). Forest conservation prevents emitting into the atmosphere carbon that is stored into forests' above and belowground carbon stocks. At the same time, reforestation activities aim to augment forest land cover by planting trees, increasing forests' atmospheric CO_2 storage capacities (Drever *et al.* 2021).

Tropical forests store significant amounts of carbon and grow quickly to absorb more (Redondo-Brenes 2007). However, even with rapidly growing tree species, tree growth can take years to offset today's emissions, and it is argued that the biggest land-based climate mitigation potential for achieving our short-term climate objectives resides in conserving intact forest ecosystems (Mackey *et al.* 2020). Yet, despite the urgent need to reduce global warming below 1.5°C (Atwoli *et al.* 2022), the last decade has seen an infatuation with planting trees compared to conserving intact ecosystems (Watson *et al.* 2018). For example, the Bonn Challenge, the New York Declaration on Forests and the Trillion Tree Campaign, amongst other NCS initiatives, aim at reforesting millions of hectares of land (Seymour 2020). But, ecosystem restoration to offset carbon emissions of today creates a lag in atmospheric CO_2 removal (Dooley K. *et al.* 2022). Conserving long-lived and resilient standing forests ensures keeping current forest carbon stocks and serves to keep greenhouse gases out of the atmosphere, an immediate climate benefit (Mackey *et al.* 2008; Dooley K. *et al.* 2022). Intact forests are defined as forested land of at least 500 km^2 with no detectable signs of human intervention from remote sensing (Potapov *et al.* 2017). They hold the highest carbon density compared to other forest types (Mackey *et al.* 2020) and the recent Land-Gap Report by Dooley K. *et al.* (2022) amongst others (e.g., Funk *et al.* 2019; Mackey *et al.* 2020; Seymour 2020) suggest that land-based policies aiming at achieving climate change mitigation should focus primarily on preserving carbon stocks from intact forests.

To ensure the climate benefits of conserving standing forests and to track the world's greenhouse gas emissions, it is essential to accurately monitor forest carbon stocks (Grassi *et al.* 2008; Mackey *et al.* 2008). Monitoring, Reporting and Verifying (MRV) was developed as a key element of the Reducing Deforestation and forest Degradation program (REDD+). MRV aims to provide accurate and verified data on forest carbon stocks to inform decision-making and ensure the climate mitigation effectiveness of REDD+ actions (Goetz *et al.* 2015). Jurisdictions wanting to participate in REDD+ must prove that they have a reliable MRV system (Sills *et al.* 2014). In fact, MRV is essential for any forest carbon accounting system aiming at conserving standing forests (Mascaro *et al.* 2014). However, even with recent technological advances, accurately estimating forest carbon stocks remains challenging (Pelletier, Busch & Potvin 2015). In 2021, global land-use change emissions still had the highest uncertainties of all categories of emissions (Friedlingstein *et al.* 2022). The use of allometric equations to transform tree measurements into aboveground biomass (AGB) estimates combined with the expansion factors to transform AGB into carbon content and the sampling protocols used to monitor entire ecosystems are identified as the primary factors affecting forest carbon stock uncertainties (Pelletier, Kirby & Potvin 2012). This thesis seeks to advance our understanding of the methods and sampling protocols to estimate trees' AGB, particularly for large tropical trees.

The abundance of large tropical trees characterizes old-growth forests compared to other forest types (Mateo-Vega, Arroyo-Mora & Potvin 2019) and large trees' contribution to forest carbon stocks is undeniable as they hold the bulk of tropical forests AGB (Slik *et al.* 2013; Bastin *et al.* 2014; Ali *et al.* 2019; Mateo-Vega, Arroyo-Mora & Potvin 2019). However, accurately estimating large trees AGB is challenging because the traditionally used allometric equations were developed using harvested biomass datasets that were skewed towards small trees, creating larger uncertainties in large tree AGB estimates using these equations (Chave *et al.* 2014; Goodman, Phillips & Baker 2014; Gonzalez de Tanago *et al.* 2018; Lutz *et al.* 2018). In addition, large tropical trees control the spatial distribution of forest carbon stocks and affect forest structure heterogeneity (Slik *et al.* 2013; Bastin *et al.* 2018; Lutz *et al.* 2018). Yet, their distribution and abundance have been studied in only a few forest regions, and globally, they remain poorly understood (Lutz *et al.* 2012; Lutz *et al.* 2018; Clark *et al.* 2019; de Lima *et al.* 2022). Therefore, it is important to extend our understanding of large tropical tree distribution patterns to other forest regions to inform us about the global distribution of terrestrial carbon stocks (Muller-Landau *et al.* 2006) while orienting forest monitoring protocols (e.g., MRV) and improve forest carbon stock estimates (Baraloto *et al.* 2013).

In chapter one, I focus on the difficulty of estimating large tropical trees AGB and propose a new method to estimate entire forest plot AGB using Terrestrial Laser Scans (TLS). I call this method the Compartmentalized Model. In chapter two, I present the distribution pattern and abundance value of the large trees found inside the intact tropical forest of the *Tierras Colectivas del Rio Balsas*. The *Tierras Colectivas del Rio Balsas* are located in the Darién Province of Panama and within Central America's largest intact tropical forest (Kunz *et al.* 2022). I also present the impact of large tree distribution patterns on the spatial variation of carbon stocks. Finally, I propose solutions to improve forest carbon monitoring protocols to capture the spatial variation of forest carbon stocks adequately. My findings are of particular importance in today's reality because large trees and intact tropical forests are rapidly declining (Lindenmayer, Laurance & Franklin 2012; Lindenmayer, Messier & Sato 2016; Potapov *et al.* 2017) and we still don't fully understand their contribution the world's carbon budget (Ali & Wang 2021). I hope this thesis will help improve forest carbon stock estimates to ensure the mitigation benefits of forest conservation and restoration.

Chapter 1 : A new compartmentalized model to estimate large tropical tree aboveground biomass with terrestrial laser scanning technology

Authors: Mathieu Guillemette[1*], Matthias Kunz[2], Alexis Ortega[3], Jose Pari-Pari[3], Francisco Solis[3], Inga Freshse[2], Alexandra Koller[2], Karl Friedrich Reich[2], Goddert von Oheimb[2], Jose Gonzalez de Tanago[4], Catherine Potvin[1,5]

Affiliations:

[1]Department of Biology, McGill University, Montréal, Québec, Canada

[2]Institute of General Ecology and Environmental Protection, Technische Universität Dresden, Germany

[3]Tierras Colectivas Emberá del Rio Balsas, Manené, Panama

[4]Environment and Water Agency of Andalusia (AMAYA), Seville, Spain

[5]Smithsonian Tropical Research Institute, Luis Clement Avenue, Bldg. 401 Tupper, Balboa, Panama

*** Correspondance:**

Mathieu Guillemette

mathieu.guillemette@mail.mcgill.ca

Abstract

1. As the world is transitioning towards a carbon-neutral economy and looking at ways to mitigate its carbon emissions, tropical forests are attracting particular attention. Large tropical trees represent the bulk of the aboveground biomass (AGB) in tropical forests. However, accurately estimating large tropical trees' AGB can be challenging. This size class is underrepresented in the harvested biomass data used for developing allometric equations. It is important to improve large tropical trees' AGB estimates to quantify forest carbon stocks accurately.

2. In this study, we developed a new method using Terrestrial Laser Scan (TLS) data that seeks to improve AGB estimates for large tropical trees (DBH ≥ 50 cm). We call this method the "Compartmentalized Model". The Compartmentalized Model considers trees as fractal objects where tree trunks and branches are separate elements from which biomass can be estimated. The Compartmentalized Model uses a simplified approach that is less dependent on point cloud quality than Quantitative Structure Models (QSM), which are currently considered the best estimation method.

3. We found that QSM faced some challenges, preventing its successful application to all TLS scans of large tropical trees and preventing it from providing plot-level AGB estimates. In comparison, the Compartmentalized Model was applied successfully to all TLS scans of large tropical trees from the datasets used in this study. It also offered AGB estimates with the best agreement with the QSM for the largest trees compared to the other allometric equations tested in this study. Furthermore, we found that tree trunks' and crowns' biomass increased non-linearly with DBH, leading to higher absolute biomass value for each of these components and suggesting using tailored AGB estimation methods for large trees.

4. We conclude that given the current technologies, computation tools, and challenges faced by QSM, estimating plots' AGB in tropical evergreen forests using TLS data depends on finding the right balance between the level of detail in tree compartmentalization and availability in point cloud quality. The Compartmentalize Model seems to have found this balance providing AGB estimates for all the large trees of our forest plots with the closest estimates to the reference values.

Keywords: Allometric equations, Tree allometry, Tropical forests, Forest carbon, Carbon stocks, Quantitative Structure Models, REDD+, MRV.

Introduction

Large tropical trees (diameter at breast height (DBH) ≥ 50 cm) play a key role in forest structure, diversity, and complexity (Lutz *et al.* 2012). They serve as a habitat refugia for wildlife (Lindenmayer, Laurance & Franklin 2012), influence forest regrowth patterns (Keeton & Franklin 2005), and account for the bulk of tropical forest carbon stocks (Slik *et al.* 2013; Bastin *et al.* 2014; Ali *et al.* 2019; Mateo-Vega, Arroyo-Mora & Potvin 2019). However, around the world, their number is rapidly declining (Lindenmayer, Laurance & Franklin 2012; Lindenmayer, Messier & Sato 2016; Lindenmayer & Laurance 2017). Large trees face many threats (Lindenmayer, Laurance & Franklin 2012; Meakem *et al.* 2018). They are more susceptible to dying from cavitation and water deficits during drought than smaller trees (Nepstad *et al.* 2007; Bennett *et al.* 2015; Clark *et al.* 2019). The rising temperatures, extended drought periods, and severe El Niño events will affect large tropical trees more than smaller trees (Allen *et al.* 2010; Lindenmayer, Laurance & Franklin 2012; Bennett *et al.* 2015; Clark *et al.* 2019), likely reducing tropical forests' carbon stocks (Slik *et al.* 2013; Gora & Esquivel-Muelbert 2021). Esquivel-Muelbert *et al.* (2019) have already found an increase in tree mortality and a climate-induced community shift in the Amazonian forest, raising the alarm about the carbon sink that tropical forests represent. Although in recent years, large tropical trees have received increased attention due to their significant contribution to the AGB (Slik *et al.* 2013; Bastin *et al.* 2014; Ali *et al.* 2019; Mateo-Vega, Arroyo-Mora & Potvin 2019), their AGB is still challenging to estimate and little is known about their abundance and distribution (Lutz *et al.* 2012; Clark *et al.* 2019). With the increasing initiatives to conserve carbon stocks, it is more and more important to accurately estimate the reduction of forest carbon stocks by the loss of its largest trees (Asner *et al.* 2005).

AGB is typically estimated from allometric equations calibrated from harvested tree biomass data. Large trees are under-represented in harvested tree samples (Clark & Kellner 2012; Chave *et al.* 2014), resulting in a potential bias when estimating large trees' AGB using allometric equations (Chave *et al.* 2014; Goodman, Phillips & Baker 2014; Gonzalez de Tanago *et al.* 2018; Lutz *et al.* 2018). Recent studies using Terrestrial Laser Scan (TLS) technology opened the door to improve estimates of large trees' AGB. TLS is a non-destructive surveying technology that captures, from the ground, three-dimensional (3D) point clouds representing trees individually or entire forest plots (Henning & Radtke 2006; Dassot, Constant & Fournier 2011). It has been used in tropical forests to extract tree measurements such as DBH (Hopkinson *et al.* 2004; Srinivasan *et al.* 2014; Calders *et al.* 2015), height (Hopkinson *et al.* 2004; Burt *et al.* 2013; Srinivasan *et al.* 2014), crown size (Holopainen *et al.* 2011; Srinivasan *et al.* 2014) and AGB estimates from allometric equations (Hopkinson *et al.* 2004; Holopainen *et al.* 2011; Srinivasan *et al.* 2014; Guillemot *et al.* 2020). Lau *et al.* (2019) have also used TLS to develop new national allometric models to estimate Guyana's large tropical trees' AGB.

A key strength of TLS technology is its flexibility to measure any part of a tree. Therefore, TLS allows rethinking the way we estimate AGB and to go beyond allometric equations (Newnham *et al.* 2015). Quantitative Structure Models (QSM) is a method based on individual tree point cloud data retrieved from TLS scans that fit many cylinders to replicate a tree's 3D structure and obtain an estimated tree volume (Hackenberg *et al.* 2015; Raumonen *et al.* 2015). QSM reconstructs a tree's architecture and provides a tailored estimate of its AGB. Some consider this model the best way to currently estimate trees' AGB (Disney *et al.* 2018) and different studies have accurately estimated large tropical trees' AGB using QSMs (Gonzalez de Tanago *et al.* 2018; Lau *et al.* 2018; Momo Takoudjou *et al.* 2018; Lau *et al.* 2019). Previous studies (e.g., Bastin *et al.* 2015; Bastin *et al.* 2018) have shown that forest plots' AGB in the tropics can be estimated using only the largest trees. However, to our knowledge, all studies providing QSM AGB estimates for large tropical trees have focused on individual trees and have used relatively small sample sizes (i.e., n < 61, except for Brede *et al.* (2022) where n = 171) (Supp. Info. Table S1) and none have provided QSM estimates for entire forest plots in evergreen tropical forests. Yet, calibration data for remote sensing tools rely on plot AGB estimates and not on individual trees (Goetz *et al.* 2009). A major milestone awaiting QSM is to scale up the estimate of tree AGB to the plot level to calibrate and improve the accuracy of landscape biomass estimates.

Here, we developed a new estimation method that seeks to overcome the challenges faced by QSM reconstruction while providing AGB estimates comparable to the accuracy achieved by QSM estimates. The idea is to develop a model that is accessible and applicable at large scales in order to estimate the AGB of entire tropical forest plots using only its largest trees. We call this method the "Compartmentalized Model". Like the "LoD3" model of Liang *et al.* (2016), the Compartmentalized Model takes advantage of TLS data to segment and measure tree components without fully reconstructing their architecture. And, similar to QSM, this model aims to provide estimates tailored to each tree but with the right level of detail so that the model is not as affected as QSM by occlusion problems (i.e., missing points in the point cloud because of hidden or obstructed regions from the scanner). We ensured that the Compartmentalized Model is accessible to current technologies, user-friendly and that it is applicable at large scales so it can improve tropical forest plots' AGB estimates.

Materials and Methods

Study sites and datasets

Panama Plots

The project is part of the *Bacurú Drõa* initiative developed in partnership with the *Emberá* People of the Balsas River to establish an old-growth forest observatory (Kunz *et al.* 2022). Ten sampling sites, each presenting two sampling plots, were established in the Emberá Traditional Territories of the Balsas River (*Emberá Tierras Collectivas del Rio Balsas*) in Darién (Figure 1). Each site was selected by the local *Emberá* technicians and authorities to showcase what they consider to be their best old-growth forests. Each sampling site contained two 30 x 30 m plots (total area of 1.8 ha). In each plot, we collected between 8-13 TLS scans with a RIEGL 400zi and extracted all large tropical trees. Each plot contained between one to four large trees (Supp. Info. Section 1 for more details on the data acquisition). We define large trees as trees of DBH ≥ 50 cm. Hereafter, we refer to this dataset as the “Panama Plots”.

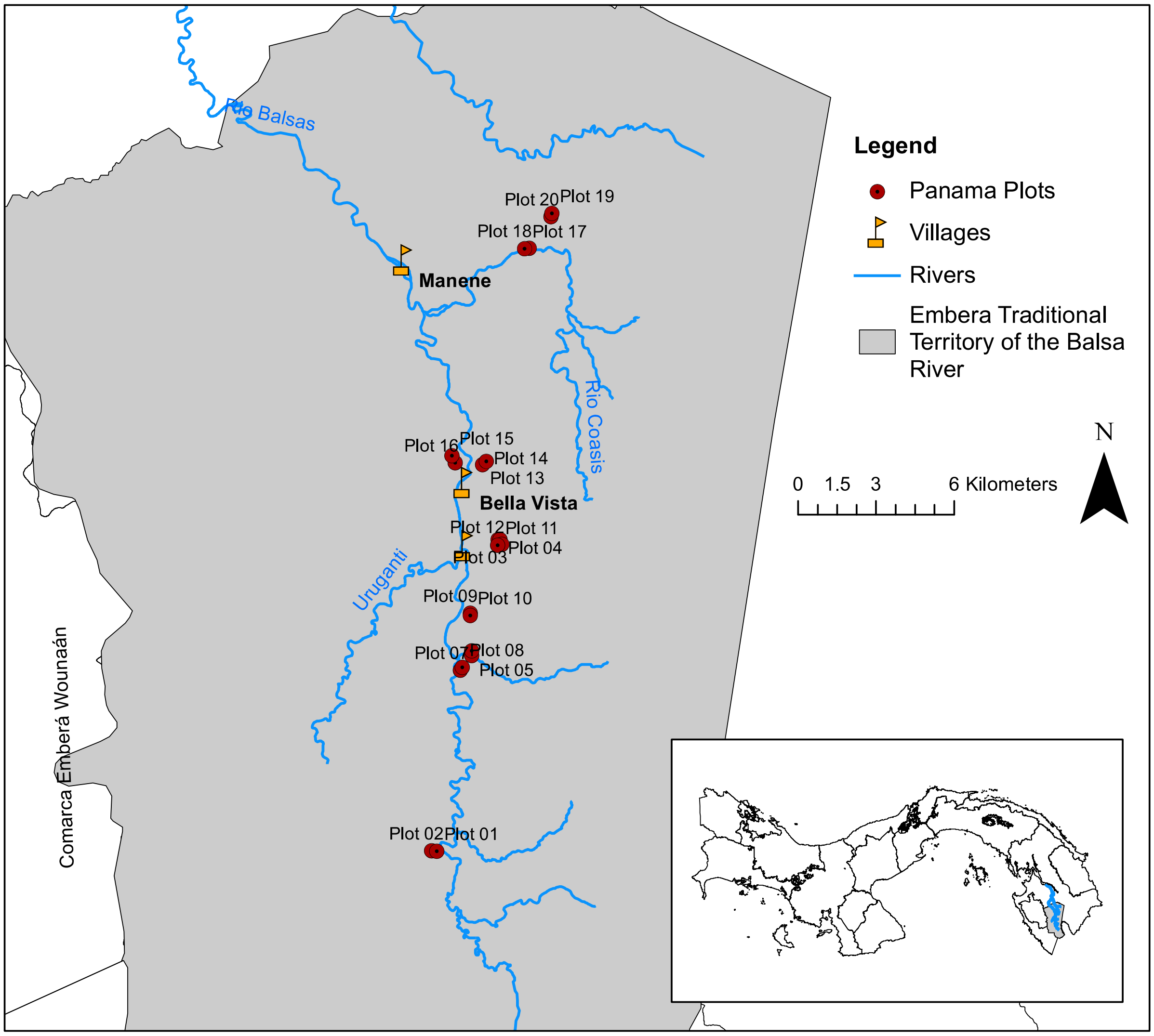

Figure 1: The Emberá Traditional Territory of the Balsas River in eastern Panama and the locations of 20 plots where TLS data was collected (i.e. Panama Plots).

Peru, Indonesia and Guyana Plots

We complemented the Panama Plot dataset with open-access data from Gonzalez de Tanago *et al.* (2018) (available at http://lucid.wur.nl/datasets/terrestrial-lidar-of-tropical-forests). This dataset contains manual field measurements, TLS scans, and QSM reconstructions for 26 large tropical trees (DBH ≥ 50 cm) coming from 26 tropical forest plots in Peru, Indonesia, and

Guyana (Table 1). Similar to the Panama Plots, Gonzalez de Tanago *et al.* (2018) plots were 30 x 50 m in Peru and 30 x 40 m in Indonesia and Guyana.

Table 1: Study sites and data.

	Panama	Peru	Indonesia	Guyana
Forest Type	Moist tropical forest	Moist tropical forest	Peat swamp forest	Moist tropical forest
Region	Balsas River (Darien)	Madre de Dios (SW Amazon)	Mentaya River (Central Kalimentan)	Vaitarna Holding's concession
Mean Elevation (m)	123	312[1]	22[1]	117[1]
Mean Annual Precipitation (mm)	2741[2]	2074[1]	2616[1]	2195[1]
n manually and TLS-measured large trees	78	9	7	10
n QSM	12	9	7	10

AGB estimations

Quantitative Structure Models

In this study, we estimated large tropical trees' AGB using three different methods (i.e., QSM, Compartmentalized Model and allometric equations) and compared the performance of the Compartmentalized Model and allometric equations to the reference values of QSM reconstructions. To model trees' architecture using cylinders, QSM requires removing leaves or other vegetation from the TLS point cloud retaining only woody tissues. To do so, we used the

---

[1] Data from Gonzalez de Tanago *et al.* (2018)

[2] Data from Kunz *et al*. (2022)

Leaf-Wood-Separation (LeWoS) algorithm (Wang, Momo Takoudjou & Casella 2020) with Matlab's R2019b plugin (https://github.com/dwang520/LeWoS). After trying different Feature Threshold values (i.e., 0.1, 0.15, 0.2, and 0.25), we selected the Feature Threshold value at 0.2 to process all Panama Plots' large tropical trees. Given the size of our trees and the quality of the point clouds, we found that this Feature Threshold provided the best separation of leaf and woody tissues. LeWoS results were judged either as good or bad following a visual inspection in CloudCompare (Figure 3 and Figure 4). From the 78 large tropical trees scanned with TLS, we retained only 17 LeWoS segmentations; the others were unsuitable for QSM reconstruction. A LeWoS was judged unsuited when it led to an unsuccessful separation of leaf and woody tissue, resulting in too much leaf tissue still present on the point cloud or in removing too much woody tissue, thus affecting the structure of the tree.

We computed QSMs for the 17 large trees of the Panama Plots dataset that were judged to have a good LeWoS segmentation. QSMs were computed in Matlab v.2021a using TreeQSM v.2.4 (Raumonen *et al.* 2015). Following communication with Pasi Raumonen (Tampere University, personal communication), to improve QSM results, we set PatchDiam1 at 0.25, 0.35, 0.5; PatchDiam2min at 0.1, 0.15, 0.2; and PatchDiam2max at 0.25, 0.4, 0.6 due the large trees. BallRad 1 value was equal to PathDiam1 + 0.05 and BallRad2 value was equal to PatchDiam2max + 0.05. We also triangulated buttressed trunks using the "inputs.Tria" function of TreeQSM v.2.4 (Raumonen *et al.* 2015). Following the method of Gonzalez de Tanago *et al.* (2018), we did 20 reconstructions per tree and recorded the average volume for each tree. We transformed tree volume in AGB value by multiplying it by the tree species-specific wood density using values from the Global Wood Density Database (Zanne *et al.* 2009). We retained only 12 QSM reconstructions out of the 17. The other five missed important crown parts due to occlusion problems (Supp. Info. Figure S2).

Gonzalez de Tanago *et al.* (2018) open-access dataset comes with results for the QSM reconstruction of 26 large tropical trees. As for the Panama Plot QSM reconstructions, cylinders smaller than 10 cm in diameter were filtered out and 20 reconstructions were computed for each tree to avoid random generations of the QSM patches (point cloud partition into small segments) (Calders *et al.* 2015; Raumonen *et al.* 2015). In total, we had QSM reconstruction for 38 large tropical trees.

Compartmentalized Model

The Compartmentalized Model assumes that trees are fractal objects (Guzmán Q *et al.* 2020; Ehbrecht *et al.* 2021) where the tree trunk is modelized as a tapered cylinder and each first-order branch is akin to an individual tree. (Figure 2). The predictive equation of the Compartmentalized Model is divided into two parts (Eq. 1). The first part of the equation estimates the trunk's biomass with the geometrical equation for a tapered cylinder using DBH and trunk height. It then transforms the volume to biomass using the species-specific wood density value (Zanne *et al.* 2009). The second part of the equation represents the sum of first-order branches' biomass, estimated using the pantropical allometric equation n.04 (Chave *et al.* 2014). The basis behind the choice of this equation is that, as trees are fractal objects, first-order branches should follow the same allometry as the entire tree. Moreover, the pantropical equation is the most robust tropical allometric equation and it provides more accurate AGB estimates with smaller DBH and height measurements (Chave *et al.* 2014). Therefore, by using the diameter and length of first-order branches, the measurements fed into the pantropical equation will be smaller. Finally, to calculate the plot AGB with the Compartmentalized Model, we summed all large trees AGB found within each plot. The calculations for the Compartmentalized Model were performed in R4.2.1 (R Development Core Team 2022).

Equation 1. The Compartmentalized Model equation. DBH = diameter at breast height, WD = wood density (g/cm^3) Ht = trunk height, Dtt = top trunk diameter, Db$_i$ = branch "i" diameter and Db$_i$ = branch "i" length. a = 0.0673. b = 0.976.

$$\left(\frac{\boldsymbol{Ht}}{\mathbf{3}} * \left(\boldsymbol{\pi} * \boldsymbol{DBH} + \sqrt{\boldsymbol{DBH} * \boldsymbol{Dtt}} + \boldsymbol{Dtt}\right)\right) * \boldsymbol{WD} + \sum_{\boldsymbol{b}=\boldsymbol{i}}^{\boldsymbol{k}} \mathbf{a} * \left(\boldsymbol{WD} * \boldsymbol{Lb_i} * \boldsymbol{Db_i^2}\right)\hat{}\,\boldsymbol{b}$$

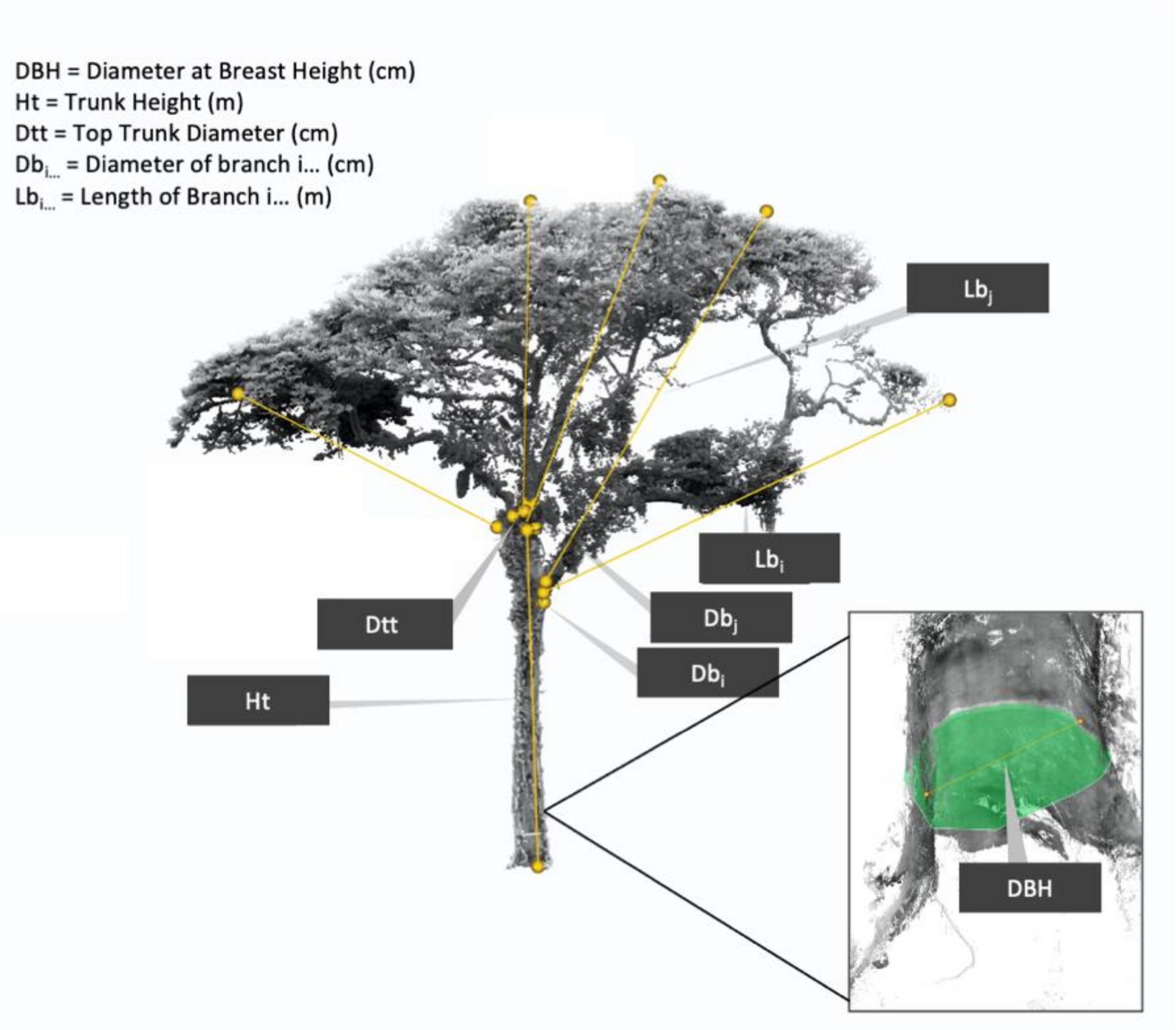

Figure 2: The different tree measurements (diameter at breast height (DBH), trunk height (Ht), top trunk diameter (Dtt), branch "i" diameter (Db_i) and branch "i" length (Lb_i)) taken on terrestrial laser scan trees (DBH ≥ 50 cm) to estimate their AGB using the Compartmentalized Model.

Allometric equations

We compared the results from the Compartmentalized Model against the reference value of the 38 QSM reconstructions. In addition, we also compared the estimates from three different allometric equations (Table 2) to the reference value of the 38 QSM reconstructions. We selected

Chave *et al.* (2005) pantropical equation for moist tropical forests using only DBH and Chave *et al.* (2014) pantropical equation n.04 using DBH and height. To our knowledge, those two equations are derived from the largest harvested biomass dataset. We also chose to compare Ploton *et al.* (2016) model 3 because these authors argue that taking crown mass into account improved large trees' AGB estimates and that their model 3 "closes the gap" in estimating large tropical trees' AGB. We, therefore, tested each allometric equation and the Compartmentalized Model's performance against the QSM reference values.

The AGB estimates from the two pantropical equations were obtained using the R package BIOMASS (Réjou-Méchain *et al.* 2017) and species-specific wood density were obtained from the Global Wood Density Database (Zanne *et al.* 2009).

Table 2: The different allometric equations used to estimate trees' AGB. Chave et al. (2005) equation 07 (Ch.05 eq.07), Chave et al. (2014) equation 04 (Ch.14 eq.04), Ploton et al. (2016) model 3 (Plo.16M3) and the Compartmentalized Model (Compartmentalized).

	Equations	a	b	c	d
Ch.05 eq.07	$\exp\left(-\mathrm{a} + \mathrm{b} * \ln(\mathrm{D}) + \mathrm{c} * \ln(D)^2 - \mathrm{d} * (\ln(D)^3)\right) * WD$	1.499	2.148	0.207	0.0281
Ch.14 eq.04	$a * (WD * H * D^2)\verb|^|b$	0.0673	0.976		
Plo.16M3	$\exp(a + b * (D^2 * Ht * WD) + c * (D^2 * Cs * WD)^2)$	0.58	0.4263	0.0283	
Compartment-alized	$\left(\frac{Ht}{3} * \left(\pi * DBH + \sqrt{DBH * Dtt} + Dtt\right)\right) * WD + \sum_{b=i}^{k} \mathrm{a} * (WD * Lb_i * Db_i^2)\verb|^|b$	0.0673	0.976		

Analyses

Models' performance against QSM

Usually, to test the performance of new AGB estimation methods or allometric equations, the predicated AGB estimates are compared with harvested biomass data. However, in this study, we did not want and could not cut trees in the Panama Plots. Instead, we used the results from the QSM estimates as the reference value since QSMs are currently considered the most accurate method to estimate trees' AGB (Calders *et al.* 2015). For instance, Gonzalez de Tanago *et al.* (2018) volume estimates from QSM reconstruction showed remarkably high agreement (CCC = 0.95) to the harvested values. The concordance correlation coefficient (CCC) measures the agreement of the scatterplot points to a 1:1 line with the prediction's variability. The CCC measures both the accuracy and precision of a model. A 1:1 linear model (slope = 1, intercept = 0) would reflect a perfect fit or CCC = 1, while a CCC = 0 would reflect no fit between models (slope = ±∞, intercept = ±∞). Comparable results were found by Lau *et al.* (2019) and Momo Takoudjou *et al.* (2018). Moreover, large tropical trees are increasingly rare worldwide and we should avoid cutting more (Lindenmayer, Laurance & Franklin 2012). Finally, Kaasalainen *et al.* (2014) advanced that QSMs can be an option to replace harvested data preventing cutting down more trees and this was recently successfully applied by Brede *et al.* (2022).

To judge the fit of every model against the QSM reference values, we computed linear models for each estimation method. We extracted the slope and the intercept from each regression as well as the R-square (R^2) and the Root Mean Square Error (RMSE) to assess the general model's accuracy (Table 6). We compared the agreement of the AGB predictions from each model to the QSM reference values using the CCC. Furthermore, absolute and relative biases were calculated to assess further each AGB estimation method's ability to produce an accurate estimate when all trees' AGB is counted together. All calculations were performed in R.

AGB's distribution in large tropical trees

We took advantage of the segmented data produced by the Compartmentalized Model to look at the relative contribution of tree trunk biomass and tree crown biomass to the overall tree AGB in relation to DBH size. We aimed to explain the increasing variability in AGB estimates as tree size increases (Supp. Info. Figure S3). We log-transformed trunk biomass, crown biomass and DBH values and we computed linear models for trunk biomass and crown biomass following DBH size. Moreover, we explored the biomass allocation within tree crowns using the biomass data of each first-order branch estimated from the Compartmentalized Model. This second analysis explored the relative impact of branch fall and/or branch damage on the total AGB of large tropical trees. All calculations were performed in R.

Results

QSM's challenges

Tree size, vegetation density, and occlusion problems in the point cloud were the main challenges found in the QSM construction process. These effects often resulted in the poor separation of leaf tissues from wood tissues during the LeWoS segmentation and unsuitable point clouds for QSM reconstructions. For example, most of the trees in the Panama Plots produced LeWoS results that removed too much of the tree's woody component, leading to a point cloud missing too much information for QSM reconstruction (Figure 3). Also, in some cases, when the results of the LeWoS step were judged "suitable" (Figure 4), a manual intervention to remove more of the soft tissue was needed and in some cases point clouds still presented too much occlusion for successful QSM reconstructions.

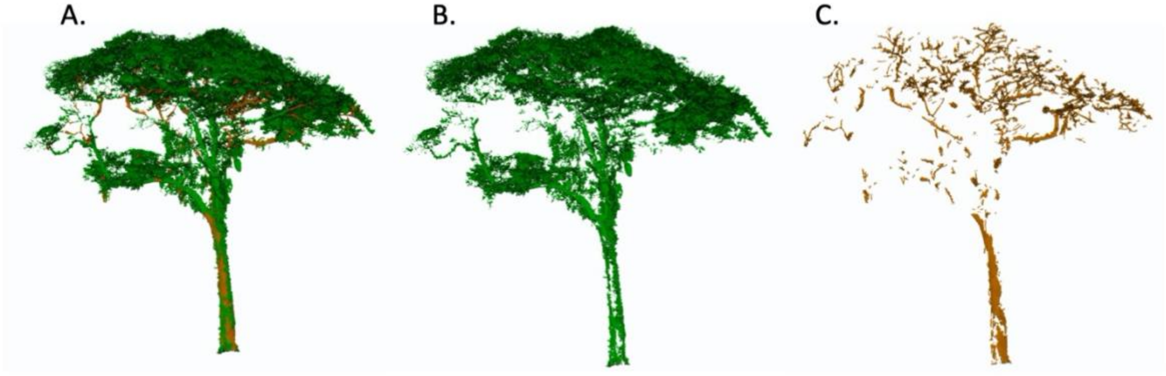

Figure 3: Unsuccessful Leaf-Wood Separation computation where the initial point cloud (panel A) was split into a soft-tissue point cloud (panel B) and a hard-tissue point cloud (panel C). In this example the separation led to removing too much of the point cloud considered as soft tissue, thus adding occlusion in the point cloud and affecting tree structure significantly.

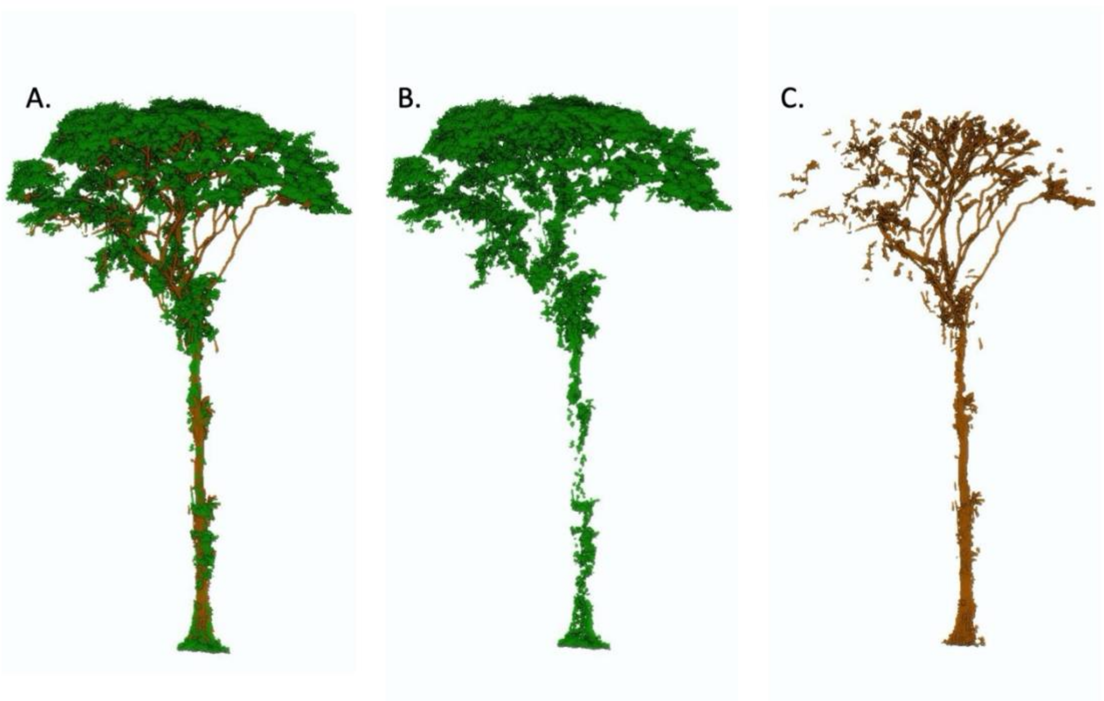

Figure 4: A successful Leaf-Wood Separation computation where the initial point cloud (panel A) was split into a soft-tissue point cloud (panel B) and a hard-tissue point cloud (panel C). The resulting hard-tissue point cloud represents the entire tree architecture but still contains soft tissues that were removed manually using the segmentation tool in CloudCompare.

In all of the Panama Plots, QSMs were not suitable for at least one or more large trees and prevented this method from providing AGB estimation at the plot level. In fact, even if a tree produced "suitable" LeWoS results, the point cloud, in five instances, still had too much occlusion and resulted in bad QSM reconstruction (Supp. Info. Figure S2). As an example, Panama Plot 17 contained three large trees. Using QSM, we successfully separated leaf and wood tissues for only one tree, which ruled out the possibility of providing a plot-level AGB estimate from QSM. Moreover, the only large tree that underwent a QSM reconstruction for Panama Plot 17 was deemed inaccurate from failing to reconstruct a first-order branch (Supp.

Info. Figure S2). In comparison, the Compartmentalized Model proved AGB estimates for all the large trees within this plot and resulted in a summed AGB plot value of 79,52 Mg (Figure 5).

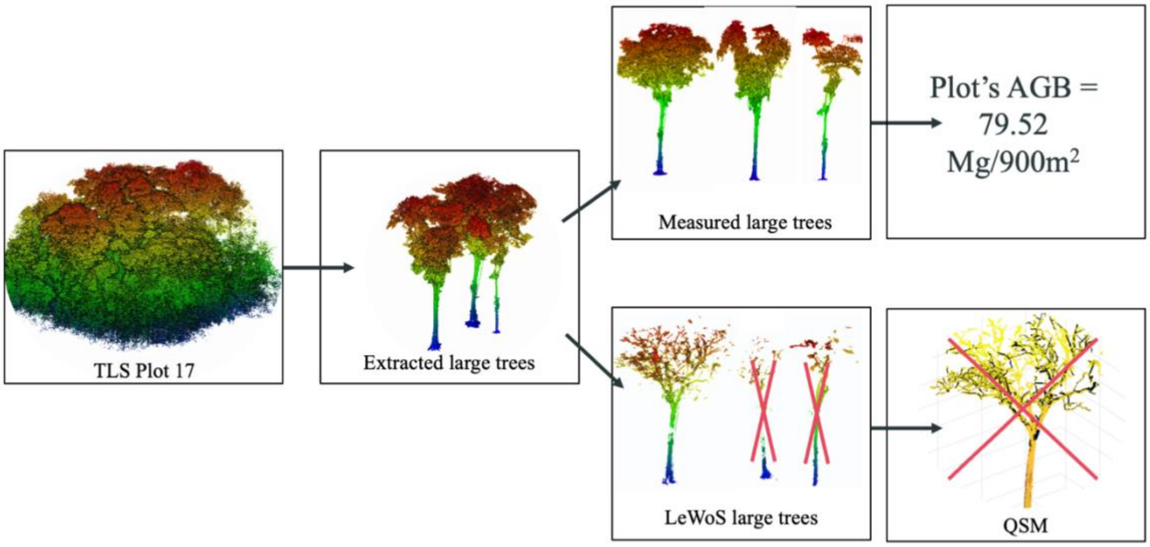

Figure 5: The process of extracting and measuring (top fork) or reconstructing QSM (bottom fork) for large trees using TLS plot scan to obtain plot AGB estimates with Compartmentalized Model (top fork) and QSM (bottom fork).

Models' agreement to QSM

We found that the Compartmentalized Model provided the best-fitted AGB estimations to the QSM reference values (slope = 1.12 and CCC = 0.89) (Figure 6). Following the Compartmentalized Model, Chave *et al.* (2005) pantropical equation for moist forests was the model that compared the closest to the QSM AGB reference values (slope =1.26; CCC = 0.82), closely followed by Chave *et al.* (2014) pantropical equation n.04 (slope = 1.27; CCC = 0.82). Ploton *et al.* (2016) model 03 was the model that compared the least with the QSM AGB reference values (slope = 1.86; CCC = 0.68). The Compartmentalized Model also showed the lowest variability (RMSE = 5.01), followed by Chave *et al.* (2005) and Chave *et al.* (2014) pantropical equations (RMSE = 6.86 and RMSE = 6.95, respectively). Ploton et al. (2016) model 3 showed slightly higher variability in its AGB estimates (RMSE = 13.79). The Compartmentalized Model also had the lowest bias of all models (Relative Bias = -0.91 %).

The Compartmentalized Model was found to be more accurate and precise than the other methods because it proved to be particularly good at estimating the AGB of the very large trees compared to the others. For example, when removing the trees of QSM AGB > 25Mg, all four models performed similarly (Supp. Info. Figure S4 and Table S3). However, the Compartmentalized Model performance improved significantly when the trees of QSM AGB > 25Mg were included compared to the other estimation methods. Furthermore, the Compartmentalized Model proved more accurate because it provided smaller AGB estimates than the other models that tended to overestimate trees' AGB compared to the reference values (Figure 9).

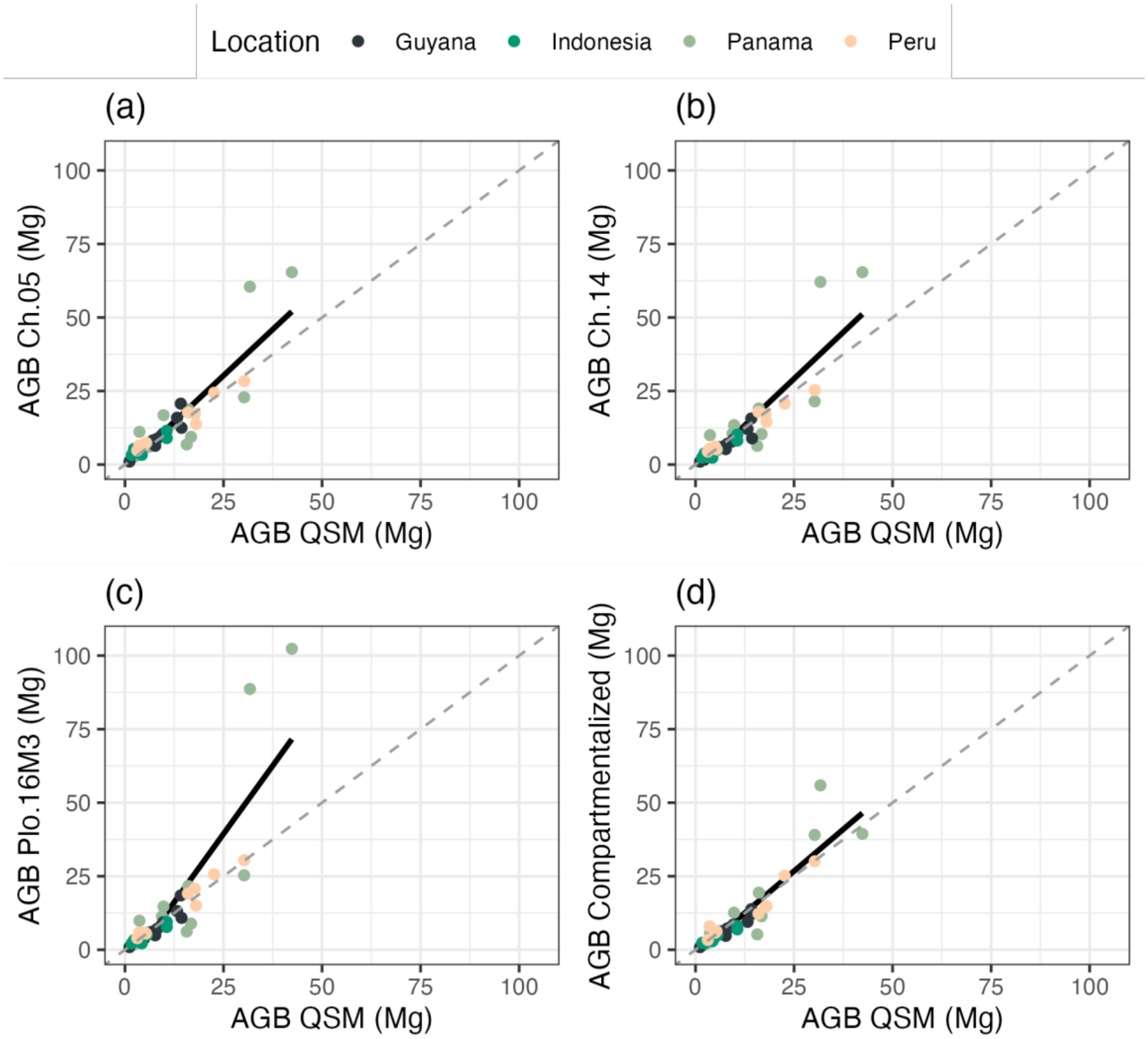

Figure 6: Scattered plot of the predicted tree AGB from (a) Chave et al. (2005) pantropical equation, (b) Chave et al. (2014) pantropical equation, (c) Ploton et al. (2016) model 3 and (d) the compartmentalized Model against the reference values of the quantitative structure models (QSM) AGB estimates. The solid black line represents a fitted linear regression between the predicted values from the equation or model and the reference value of the QSMs. The dashed grey line represents a 1:1 relationship. Tree measurements come from TLS scans of the Panama dataset and Gonzalez de Tanago (2018) dataset (n = 38). (see Table 3 for linear models' parameters).

Table 3: Models performance against QSM reconstructions. SE = standard error. R2 = coefficient of determination RMSE = root mean square error. CCC = concordance correlation coefficient. In all cases, the regression model has 38 points and, thus, 36 degrees of freedom.

	Regression parameters				Model performance				
	a	*b*	SE*a*	SE*b*	R^2	RMSE	CCC	Bias (abs)	Bias (%)
Chave 05	1.26	-1.15	0.11	1.64	0.78	6.86	0.82	69.19	15.68
Chave 14	1.27	-2.50	0.12	1.72	0.77	6.95	0.82	22.67	5.14
Plo.16M3	1.86	-7.00	0.19	2.88	0.72	13.79	0.63	111.89	25.36
Compartmentalized	1.14	-1.71	0.09	1.29	0.83	5.01	0.89	-4.04	-0.91

AGB's distribution in large tropical trees

To understand the increasing variability in AGB estimates with increasing tree size (Supp. Info. Figure S3), we looked at trunk and crown biomass following DBH size. Both large tropical tree trunk biomass and crown biomass increased exponentially with DBH size (log-transformed slope = 1.9760 ± 0.1012 and log-transformed slope = 2.1074 ± 0.1955, respectively) (Figure 7). However, large tropical tree trunks had significantly more biomass (mean = 7.89 Mg, SD = 7.26 Mg) than large tropical tree crowns (mean = 5.47 Mg, SD = 6.73 Mg) ($t = -4.216$; $p < 0.05$).

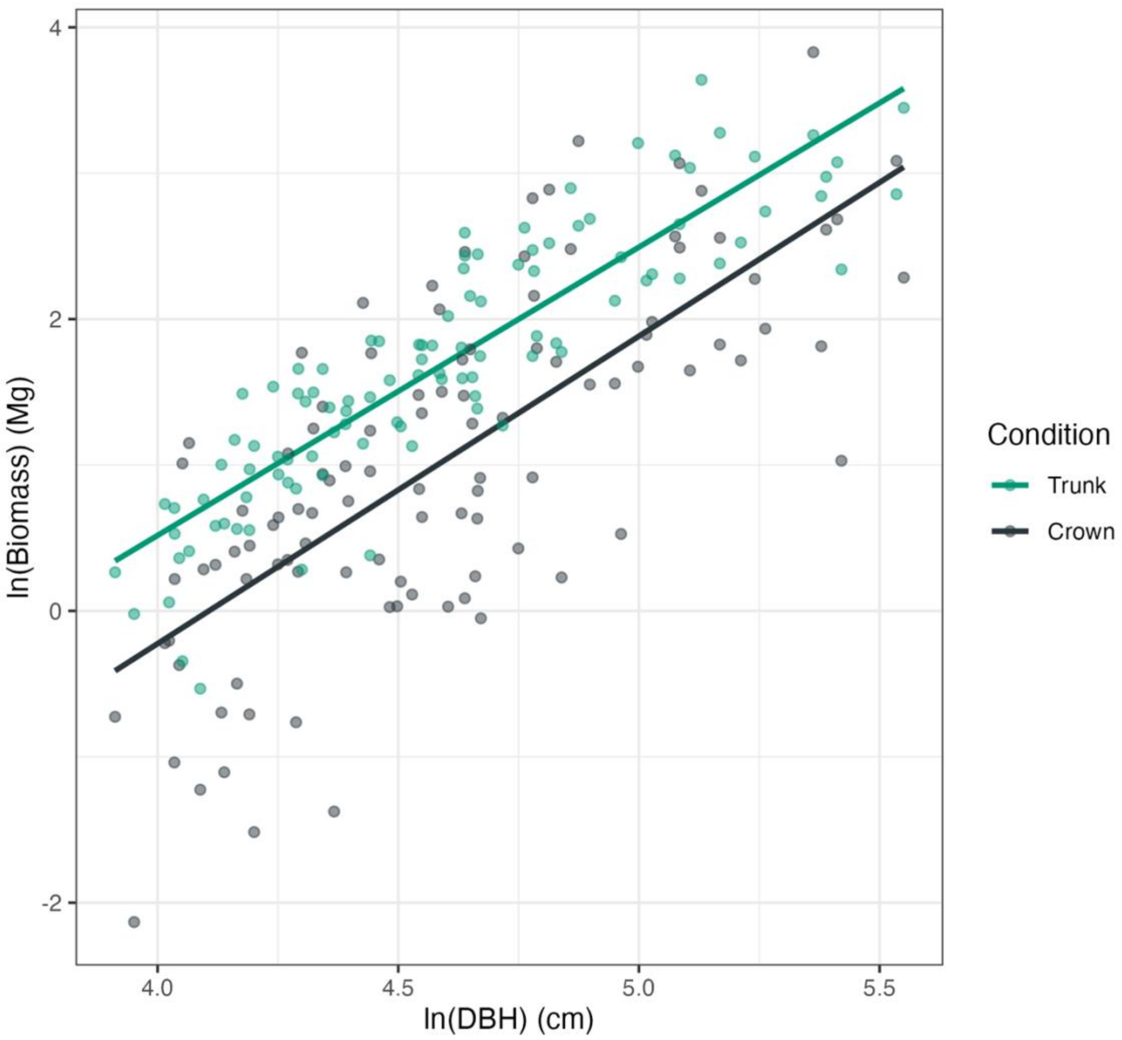

Figure 7: Log-transformed individual tree trunk biomass values are represented in green dots and green linear regression line (F = 381.4; $p < 0.05$). Log-transformed individual tree crown biomass values are in dark grey dots and dark grey linear regression line (F= 116.1; $p < 0.05$).

For the 104 large trees of our dataset, first-order branch count ranged from 2 to 7, with around 75% of the trees having 2 or 3 first-order branches. Only 25 large trees out of 104 had four or more first-order branches. First-order branches estimated biomass averaged 1.79 Mg (SD = 3.09 Mg) (Figure 8). The biggest branch of our dataset weighed 28.38 Mg and was found in a giant *Anacardium excelsum* of DBH = 213 cm that contained two first-order branches. In fact, the two biggest first-order branches were found on this tree, accounting for a total crown biomass of 46.04 Mg. The heaviest first-order branches (biomass > 5 Mg) were found in the biggest trees with four or fewer first-order branches. These results highlight the significant contribution of first-order branches to a tree's AGB.

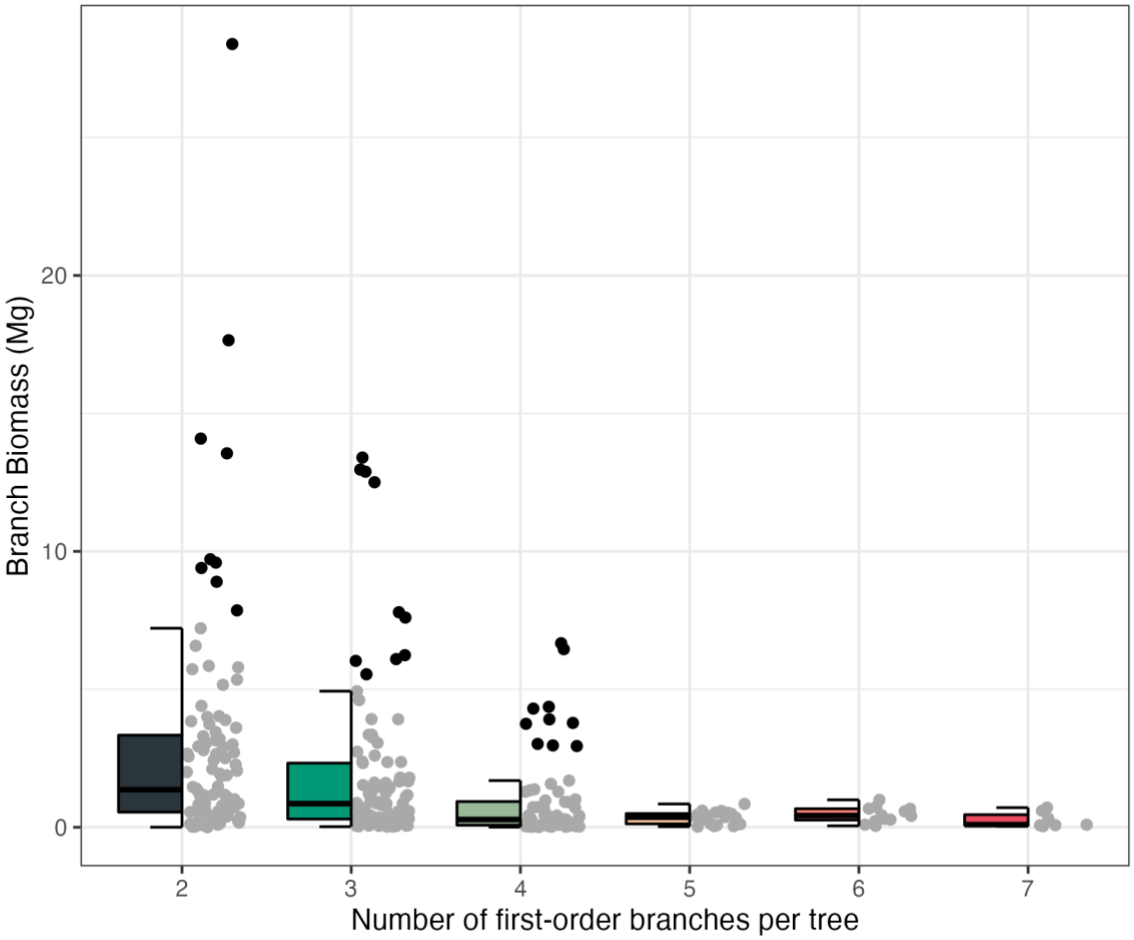

Figure 8: First-order branch biomass estimates coming from the Compartmentalized Model. The Boxplots are categorized and colored based on the number of branches in a tree crown. Boxes represent the interquartile range (25th and 75th percentile) with the median value represented by the middle line. Grey dots represent individual first-order branch biomass estimates within 1.5

times interquartile range and the black dots are individual first-order branch biomass outliers found outside 1.5 times interquartile range.

Discussion

The future of TLS, QSM and the Compartmentalized Model

Monitoring, reporting, and verifying is critical in any forest carbon offset program, such as Reducing Emissions from Deforestation and forests Degradation (REDD+) (Herold & Skutsch 2011). Forest sector evidence-based compensation programs rely on ground estimates of carbon stocks to calibrate remote sensing tools for predicting AGB at large scales (Goodman, Phillips & Baker 2014; Mascaro *et al.* 2014). Accurately estimating the AGB from the ground is essential as the accuracy of the remote sensing AGB prediction cannot surpass the accuracy of the calibration data (Clark & Kellner 2012). However, accurately estimating forest carbon stocks is problematic in forested regions with numerous large trees for two reasons: (1) large trees' AGB is difficult to estimate accurately and (2) little is known about their distribution, abundance, and dynamics (Lutz *et al.* 2012; Xu *et al.* 2016; Clark *et al.* 2019). TLS combined with QSM, theoretically, can address the first problem by providing accurate AGB estimates of large tropical trees (Gonzalez de Tanago *et al.* 2018; Lau *et al.* 2018; Momo Takoudjou *et al.* 2018; Lau *et al.* 2019). However, calibration data for remote sensing tools rely on plot AGB estimates (Goetz *et al.* 2009), and QSM estimates would have to be scaled up to the plot level in order to calibrate remote sensing tools. Tropical forests present many challenges to successfully compute QSM for all large trees found within a given forest plot. To our knowledge, QSMs have not yet provided AGB estimates at the plot level for evergreen tropical forests but rather for a few singled-out trees (e.g., Gonzalez de Tanago *et al.* 2018; Lau *et al.* 2018; Momo Takoudjou *et al.* 2018; Lau *et al.* 2019).

Similar to previous studies, we found that the main challenges of computing QSM came from occlusion problems in point clouds of tropical forests (Wilkes *et al.* 2017; Gonzalez de Tanago *et al.* 2018). QSM requires removing all vegetation from a tree before reproducing cylinders that mimic a tree's architecture (Calders *et al.* 2020). In evergreen tropical forests, it is impossible to think of doing leaf-wood separation manually on all trees. This process relies on automated leaf-wood separation algorithms (e.g., Leaf-Wood-Separation by Wang, Momo Takoudjou and Casella (2020)). We identified this step as one of the main challenges facing QSM. It prevented computing QSM for 61 trees out of 78 trees, for the Panama Plots dataset. Until we have advancements in TLS technologies and leaf-wood separation algorithms (Calders *et al.* 2015), estimating plot AGB using QSM in tropical evergreen forests will have to bypass the limits caused by occlusion and the mandatory leaf-wood separation steps. We suggest that a more simplistic approach with a lower level of tree compartmentalization, such as the Compartmentalized Model, bypasses these limits while providing tailored and accurate tree AGB estimates.

The Compartmentalized Model does not require a leaf-wood separation step and relies on simple tree measurements that are less affected by occlusion than QSM. Moreover, the Compartmentalized Model provides tailored AGB estimates that follow a tree's architecture providing a minimum level of compartmentalization. Most importantly, the Compartmentalized Model estimates compared the closest to the QSM values for the largest trees and could be applied to all 104 large trees of our dataset. In comparison, QSMs could be fitted to only 38 large trees. The Panama Plot 17 shows an example of a situation where QSM reconstruction was not possible for at least one or many large trees, thus preventing the QSM method from providing plot AGB estimates. In comparison, the Compartmentalized Model was applied to every large tree and could provide plot AGB estimates.

Challenges in estimating large trees' AGB

There could be many reasons why a tree's AGB estimate varies as size increases. Goodman, Phillips and Baker (2014) suggest the increasing contribution of the crown to a tree's AGB and its increasing complexity as its size increases explain the difficulty in estimating large tropical trees' AGB. For this reason, previous studies suggested that including crown measurements in allometric equations improved large trees' AGB estimates (e.g., Goodman, Phillips & Baker 2014; Ploton *et al.* 2016; Lau *et al.* 2019). Similar to others (e.g., Goodman, Phillips & Baker 2014; Kunz *et al.* 2019), our results show that the biomass of large tree crowns increases non-linear with tree DBH size. Different theories have tried to predict tree crown architecture, growth, and allometries (e.g. Metabolic Scaling Theory (MST) (West, Brown & Enquist 1997), competitive convergence (Iida *et al.* 2011), sphere packing (Taubert *et al.* 2015) (Supp. Info Table S2). These theories combine genetic, ecosystemic, and biological constraints with mixed success in explaining tree crowns' architecture (e.g., Muller-Landau *et al.* 2006; Blanchard *et al.* 2016; Shenkin *et al.* 2020). But, tree crown development is also controlled by stochastic disturbances that may overrule predictable genetic and competitive processes (Shenkin *et al.* 2020), making it difficult to conclude about general crown architecture, growth and allometry patterns.

The Compartmentalized Model allows us to examine individual first-order branch biomass to understand crown biomass distribution. We found that first-order branches contributed on average to 12 % of the total tree AGB, with even a more important contribution for large trees with few first-order branches. In fact, first-order branch biomass increased with tree size and decreased with the number of first-order branches per tree (Supp. Info. Figure S5). The heaviest first-order branches were found in the largest trees with four or fewer first-order branches. The heaviest branch of our dataset weighed 28.38 Mg, as much as one-third of some 1-ha-plots in disturbed forest plots for the Darien region (Mateo-Vega, Arroyo-Mora & Potvin 2019) and 39% of its overall tree AGB. Considering that stochastic events may control crown development (Shenkin *et al.* 2020) (i.e., number of branches and branch size) and that crown's contribution to trees' AGB increase with tree size, general allometric equations that don't include particular tree crown variables or first-order branch number and size should expect higher variability around AGB estimates of large trees. A single random disturbance affecting a large first-order branch would significantly impact a tree's overall AGB or even an entire plot's AGB depending on the size of this branch.

AGB estimation models like QSMs, the Compartmentalized Model and Ploton *et al.* (2016) benefit from providing tailored AGB estimates that consider crown size or the actual number of first-order branches on a tree. Consequently, such methods account for first-order branch fall and irregularities in tree crown architecture when estimating trees' AGB. However, Ploton *et al.* (2016) model 3, which uses crown metrics, performed well for the large trees of our dataset except for very large ones (i.e., QSM AGB > 25 Mg). For the trees of DBH > 150 cm, this equation overestimated the AGB compared to the other equations (Figure 9). Crown area and crown diameter, variables used in this model, are the most complicated metrics to collect in the field (Blanchard *et al.* 2016), which could lead to higher variability when used to calibrate such equations. Another reason why the Compartmentalized Model performed better for the largest trees is that AGB scales exponentially to the DBH. Therefore, AGB estimates coming from allometric equations using DBH-AGB allometry into account will inherently have increasing variability with increasing DBH size (Clark & Kellner 2012). Compared to the other equations, the Compartmentalized Model applies DBH-AGB allometry coefficients from Chave et al. (2014) at the branch level instead of at the trunk level. Branches have smaller diameters than DBHs which, by default, will lower the variability from those estimates (Supp. Info. Figure S3). Moreover, we found that the Compartmentalized Model underestimated the AGB of the largest trees compared to the other equations, which compared closer to the QSM reference values. The Compartmentalized Model also generated lower AGB estimates compared to the other equations (Figure 9).

Overall, AGB estimation models considering each tree-specific architecture seem to perform better than general allometric equations in predicting very large tree AGB partly because branch contribution to the AGB increases with tree size and the development of tree crown is affected by stochastic disturbances that are hardly predictable by genetic, ecosystemic, and biological processes. It is possible that some large trees of our dataset suffered from first-order branch fall and the AGB difference was only fully captured by tailored estimates like to Compartmentalized Model and QSM.

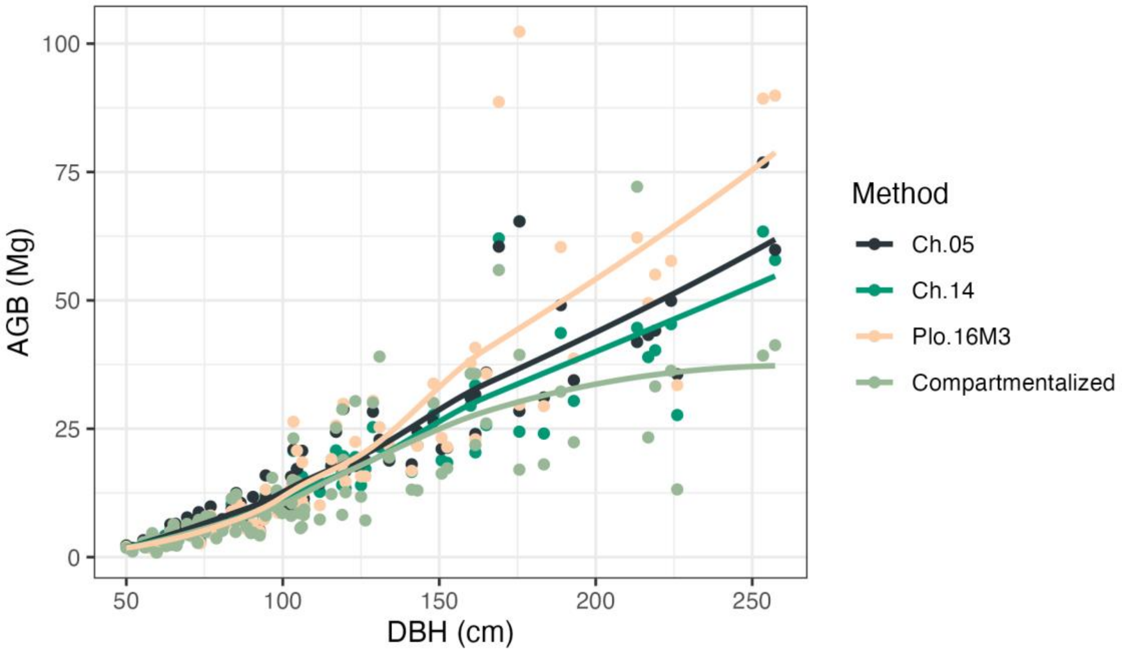

Figure 9: Estimated AGB (Mg) for all 104 TLS large trees (colored points) coming from Chave *et al.* (2005) pantropical equation, Chave *et al.* (2014) pantropical equation, Ploton *et al.* (2016) model 3 and the Compartmentalized Model. Solid lines represent a smoothed regression line across the scattered points.

Conclusion

So far, AGB estimates coming from QSM have been applied to individual trees in tropical evergreen forests with remarkable accuracy (e.g., Gonzalez de Tanago *et al.* 2018; Lau *et al.* 2018; Momo Takoudjou *et al.* 2018; Lau *et al.* 2019). However, we conclude that given the current technologies, computation tools, and challenges faced by QSM, tropical plot's AGB estimates coming from TLS data have to rely on a simplified estimation method with a suitable level of tree compartmentalization to avoid the challenges caused by occlusion problems (Liang *et al.* 2016). The Compartmentalized Model was developed based on these constraints and proved to be applicable to all TLS large trees of our forest plots. It opens the door to estimating tropical forests plot AGB using tailored AGB estimates of its largest trees with TLS data. We hope this model will serve forest carbon conservation initiatives to improve estimations of carbon emissions from deforestation and degradation in forested landscapes with a high density of large trees.

This study did not include buttress parameters in the Compartmentalized Model. The reason was to keep the model flexible to occlusion problems around some trees' buttresses. Nölke *et al.* (2015) mentioned a similar difficulty to computing QSMs in computing buttress AGB using TLS data. An alternative could be Mobile Laser Scanning which allows moving dynamically with the scanner around the targeted object and may provide occlusion-free TLS data for tree trunks. However, for the moment, these scanners have a smaller range than the RIEGL 400zi and will likely provide low-quality point clouds in the tree crowns (Bauwens *et al.* 2016). Nonetheless, buttressed trunks are another important source of variability when estimating large trees' AGB, and biomass models ignoring buttress parameters can lead to underestimation of tree trunks' AGB (Nogueira, Nelson & Fearnside 2006; Cushman *et al.* 2014). We encourage future studies to look into simple buttress parameters, independent of occlusion problems, or to look into using data from a combination of technologies that allow including buttress AGB in the Compartmentalized Model.

References

Ali, A., Lin, S.L., He, J.K., Kong, F.M., Yu, J.H. & Jiang, H.S. (2019) Big-sized trees overrule remaining trees' attributes and species richness as determinants of aboveground biomass in tropical forests. *Global Change Biology,* **25,** 2810-2824.

Allen, C.D., Macalady, A.K., Chenchouni, H., Bachelet, D., McDowell, N., Vennetier, M., Kitzberger, T., Rigling, A., Breshears, D.D., Hogg, E.H., Gonzalez, P., Fensham, R., Zhang, Z., Castro, J., Demidova, N., Lim, J.-H., Allard, G., Running, S.W., Semerci, A. & Cobb, N. (2010) A global overview of drought and heat-induced tree mortality reveals emerging climate change risks for forests. *Forest Ecology and Management,* **259,** 660-684.

Asner, G.P., Knapp, D.E., Broadbent, E.N., Oliveira, P.J., Keller, M. & Silva, J.N. (2005) Selective logging in the Brazilian Amazon. *Science,* **310,** 480-482.

Bastin, J.-F., Barbier, N., Couteron, P., Adams, B., Shapiro, A., Bogaert, J. & De Cannière, C. (2014) Aboveground biomass mapping of African forest mosaics using canopy texture analysis: toward a regional approach. *Ecological Applications,* **24,** 1984-2001.

Bastin, J.-F., Barbier, N., Réjou-Méchain, M., Fayolle, A., Gourlet-Fleury, S., Maniatis, D., De Haulleville, T., Baya, F., Beeckman, H. & Beina, D. (2015) Seeing Central African forests through their largest trees. *Scientific Reports,* **5,** 1-8.

Bastin, J.F., Rutishauser, E., Kellner, J.R., Saatchi, S., Pélissier, R., Hérault, B., Slik, F., Bogaert, J., De Cannière, C. & Marshall, A.R. (2018) Pan-tropical prediction of forest structure from the largest trees. *Global Ecology and Biogeography,* **27,** 1366-1383.

Bauwens, S., Bartholomeus, H., Calders, K. & Lejeune, P. (2016) Forest inventory with terrestrial LiDAR: A comparison of static and hand-held mobile laser scanning. *Forests,* **7,** 127.

Bennett, A.C., McDowell, N.G., Allen, C.D. & Anderson-Teixeira, K.J. (2015) Larger trees suffer most during drought in forests worldwide. *Nature plants,* **1,** 1-5.

Blanchard, E., Birnbaum, P., Ibanez, T., Boutreux, T., Antin, C., Ploton, P., Vincent, G., Pouteau, R., Vandrot, H. & Hequet, V. (2016) Contrasted allometries between stem diameter, crown area, and tree height in five tropical biogeographic areas. *Trees,* **30,** 1953-1968.

Brede, B., Terryn, L., Barbier, N., Bartholomeus, H.M., Bartolo, R., Calders, K., Derroire, G., Moorthy, S.M.K., Lau, A. & Levick, S.R. (2022) Non-destructive estimation of individual tree biomass: Allometric models, terrestrial and UAV laser scanning. *Remote Sensing of Environment,* **280,** 113180.

Burt, A., Disney, M., Raumonen, P., Armston, J., Calders, K. & Lewis, P. (2013) Rapid characterisation of forest structure from TLS and 3D modelling. *2013 IEEE International Geoscience and Remote Sensing Symposium-IGARSS*, pp. 3387-3390. IEEE.

Calders, K., Adams, J., Armston, J., Bartholomeus, H., Bauwens, S., Bentley, L.P., Chave, J., Danson, F.M., Demol, M. & Disney, M. (2020) Terrestrial laser scanning in forest ecology: Expanding the horizon. *Remote Sensing of Environment,* **251,** 112102.

Calders, K., Newnham, G., Burt, A., Murphy, S., Raumonen, P., Herold, M., Culvenor, D., Avitabile, V., Disney, M. & Armston, J. (2015) Nondestructive estimates of above-ground biomass using terrestrial laser scanning. *Methods in Ecology and Evolution,* **6,** 198-208.

Chave, J., Andalo, C., Brown, S., Cairns, M.A., Chambers, J.Q., Eamus, D., Fölster, H., Fromard, F., Higuchi, N. & Kira, T. (2005) Tree allometry and improved estimation of carbon stocks and balance in tropical forests. *Oecologia,* **145,** 87-99.

Chave, J., Réjou-Méchain, M., Búrquez, A., Chidumayo, E., Colgan, M.S., Delitti, W.B., Duque, A., Eid, T., Fearnside, P.M. & Goodman, R.C. (2014) Improved allometric models to estimate the aboveground biomass of tropical trees. *Global Change Biology,* **20,** 3177-3190.

Clark, D.B., Ferraz, A., Clark, D.A., Kellner, J.R., Letcher, S.G. & Saatchi, S. (2019) Diversity, distribution and dynamics of large trees across an old-growth lowland tropical rain forest landscape. *PloS one,* **14,** e0224896.

Clark, D.B. & Kellner, J.R. (2012) Tropical forest biomass estimation and the fallacy of misplaced concreteness. *Journal of Vegetation Science,* **23,** 1191-1196.

Cushman, K., Muller-Landau, H.C., Condit, R.S. & Hubbell, S.P. (2014) Improving estimates of biomass change in buttressed trees using tree taper models. *Methods in Ecology and Evolution,* **5,** 573-582.

Dassot, M., Constant, T. & Fournier, M. (2011) The use of terrestrial LiDAR technology in forest science: application fields, benefits and challenges. *Annals of forest science,* **68,** 959-974.

Disney, M.I., Boni Vicari, M., Burt, A., Calders, K., Lewis, S.L., Raumonen, P. & Wilkes, P. (2018) Weighing trees with lasers: advances, challenges and opportunities. *Interface Focus,* **8,** 20170048.

Ehbrecht, M., Seidel, D., Annighöfer, P., Kreft, H., Köhler, M., Zemp, D.C., Puettmann, K., Nilus, R., Babweteera, F. & Willim, K. (2021) Global patterns and climatic controls of forest structural complexity. *Nature communications,* **12,** 519.

Esquivel-Muelbert, A., Baker, T.R., Dexter, K.G., Lewis, S.L., Brienen, R.J., Feldpausch, T.R., Lloyd, J., Monteagudo-Mendoza, A., Arroyo, L. & Álvarez-Dávila, E. (2019) Compositional response of Amazon forests to climate change. *Global Change Biology,* **25,** 39-56.

Goetz, S.J., Baccini, A., Laporte, N.T., Johns, T., Walker, W., Kellndorfer, J., Houghton, R.A. & Sun, M. (2009) Mapping and monitoring carbon stocks with satellite observations: a comparison of methods. *Carbon balance and management,* **4,** 1-7.

Gonzalez de Tanago, J., Lau, A., Bartholomeus, H., Herold, M., Avitabile, V., Raumonen, P., Martius, C., Goodman, R.C., Disney, M. & Manuri, S. (2018) Estimation of above-ground biomass of large tropical trees with terrestrial LiDAR. *Methods in Ecology and Evolution,* **9,** 223-234.

Goodman, R.C., Phillips, O.L. & Baker, T.R. (2014) The importance of crown dimensions to improve tropical tree biomass estimates. *Ecological Applications,* **24,** 680-698.

Gora, E.M. & Esquivel-Muelbert, A. (2021) Implications of size-dependent tree mortality for tropical forest carbon dynamics. *Nature plants,* **7,** 384-391.

Guillemot, J., Kunz, M., Schnabel, F., Fichtner, A., Madsen, C.P., Gebauer, T., Härdtle, W., von Oheimb, G. & Potvin, C. (2020) Neighbourhood-mediated shifts in tree biomass allocation drive overyielding in tropical species mixtures. *New Phytologist,* **228,** 1256-1268.

Guzmán Q, J.A., Sharp, I., Alencastro, F. & Sánchez-Azofeifa, G.A. (2020) On the relationship of fractal geometry and tree–stand metrics on point clouds derived from terrestrial laser scanning. *Methods in Ecology and Evolution,* **11,** 1309-1318.

Hackenberg, J., Spiecker, H., Calders, K., Disney, M. & Raumonen, P. (2015) SimpleTree—an efficient open source tool to build tree models from TLS clouds. *Forests,* **6,** 4245-4294.

Henning, J.G. & Radtke, P.J. (2006) Ground-based laser imaging for assessing three-dimensional forest canopy structure. *Photogrammetric Engineering & Remote Sensing,* **72,** 1349-1358.

Herold, M. & Skutsch, M. (2011) Monitoring, reporting and verification for national REDD+ programmes: two proposals. *Environmental Research Letters,* **6,** 014002.

Holopainen, M., Vastaranta, M., Kankare, V., Räty, M., Vaaja, M., Liang, X., Yu, X., Hyyppä, J., Hyyppä, H. & Viitala, R. (2011) Biomass estimation of individual trees using stem and crown diameter TLS measurements. *ISPRS-International Archives of the Photogrammetry, Remote Sensing and Spatial Information Sciences,* **3812,** 91-95.

Hopkinson, C., Chasmer, L., Young-Pow, C. & Treitz, P. (2004) Assessing forest metrics with a ground-based scanning lidar. *Canadian Journal of Forest Research,* **34,** 573-583.

Iida, Y., Kohyama, T.S., Kubo, T., Kassim, A.R., Poorter, L., Sterck, F. & Potts, M.D. (2011) Tree architecture and life-history strategies across 200 co-occurring tropical tree species. *Functional Ecology,* **25,** 1260-1268.

Kaasalainen, S., Krooks, A., Liski, J., Raumonen, P., Kaartinen, H., Kaasalainen, M., Puttonen, E., Anttila, K. & Mäkipää, R. (2014) Change detection of tree biomass with terrestrial laser scanning and quantitative structure modelling. *Remote Sensing,* **6,** 3906-3922.

Keeton, W.S. & Franklin, J.F. (2005) Do remnant old-growth trees accelerate rates of succession in mature Douglas-fir forests? *Ecological Monographs,* **75,** 103-118.

Kunz, M., Barrios, H.E., Dan, M., Dogirama, I., Gennaretti, F., Mathieu, G., Koller, A., Madsen, C., Lana, G. & Ortega, A. (2022) Bacurú Drõa: Indigenous Forest Custody as an Effective Climate Change Mitigation Option. A case study from Darién, Panama. *Frontiers in Climate***,** 231.

Kunz, M., Fichtner, A., Härdtle, W., Raumonen, P., Bruelheide, H. & von Oheimb, G. (2019) Neighbour species richness and local structural variability modulate aboveground allocation patterns and crown morphology of individual trees. *Ecology letters,* **22,** 2130-2140.

Lau, A., Bentley, L.P., Martius, C., Shenkin, A., Bartholomeus, H., Raumonen, P., Malhi, Y., Jackson, T. & Herold, M. (2018) Quantifying branch architecture of tropical trees using terrestrial LiDAR and 3D modelling. *Trees,* **32,** 1219-1231.

Lau, A., Calders, K., Bartholomeus, H., Martius, C., Raumonen, P., Herold, M., Vicari, M., Sukhdeo, H., Singh, J. & Goodman, R.C. (2019) Tree biomass equations from terrestrial LiDAR: A case study in Guyana. *Forests,* **10,** 527.

Liang, X., Kankare, V., Hyyppä, J., Wang, Y., Kukko, A., Haggrén, H., Yu, X., Kaartinen, H., Jaakkola, A. & Guan, F. (2016) Terrestrial laser scanning in forest inventories. *ISPRS Journal of Photogrammetry and Remote Sensing,* **115,** 63-77.

Lindenmayer, D., Messier, C. & Sato, C. (2016) Avoiding ecosystem collapse in managed forest ecosystems. *Frontiers in Ecology and the Environment,* **14,** 561-568.

Lindenmayer, D.B. & Laurance, W.F. (2017) The ecology, distribution, conservation and management of large old trees. *Biological Reviews,* **92,** 1434-1458.

Lindenmayer, D.B., Laurance, W.F. & Franklin, J.F. (2012) Global decline in large old trees. *Science,* **338,** 1305-1306.

Lutz, J.A., Furniss, T.J., Johnson, D.J., Davies, S.J., Allen, D., Alonso, A., Anderson-Teixeira, K.J., Andrade, A., Baltzer, J. & Becker, K.M. (2018) Global importance of large-diameter trees. *Global Ecology and Biogeography,* **27,** 849-864.

Lutz, J.A., Larson, A.J., Swanson, M.E. & Freund, J.A. (2012) Ecological importance of large-diameter trees in a temperate mixed-conifer forest. *PloS one,* **7,** e36131.

Mascaro, J., Asner, G.P., Knapp, D.E., Kennedy-Bowdoin, T., Martin, R.E., Anderson, C., Higgins, M. & Chadwick, K.D. (2014) A tale of two "forests": Random Forest machine learning aids tropical forest carbon mapping. *PloS one,* **9,** e85993.

Mateo-Vega, J., Arroyo-Mora, J.P. & Potvin, C. (2019) Tree aboveground biomass and species richness of the mature tropical forests of Darien, Panama, and their role in global climate change mitigation and biodiversity conservation. *Conservation Science and Practice,* **1,** e42.

Meakem, V., Tepley, A.J., Gonzalez-Akre, E.B., Herrmann, V., Muller-Landau, H.C., Wright, S.J., Hubbell, S.P., Condit, R. & Anderson-Teixeira, K.J. (2018) Role of tree size in moist tropical forest carbon cycling and water deficit responses. *New Phytologist,* **219,** 947-958.

Momo Takoudjou, S., Ploton, P., Sonké, B., Hackenberg, J., Griffon, S., De Coligny, F., Kamdem, N.G., Libalah, M., Mofack, G.I. & Le Moguédec, G. (2018) Using terrestrial laser scanning data to estimate large tropical trees biomass and calibrate allometric models: A comparison with traditional destructive approach. *Methods in Ecology and Evolution,* **9,** 905-916.

Muller-Landau, H.C., Condit, R.S., Chave, J., Thomas, S.C., Bohlman, S.A., Bunyavejchewin, S., Davies, S., Foster, R., Gunatilleke, S. & Gunatilleke, N. (2006) Testing metabolic ecology theory for allometric scaling of tree size, growth and mortality in tropical forests. *Ecology letters,* **9,** 575-588.

Nepstad, D.C., Tohver, I.M., Ray, D., Moutinho, P. & Cardinot, G. (2007) Mortality of large trees and lianas following experimental drought in an Amazon forest. *Ecology,* **88,** 2259-2269.

Newnham, G.J., Armston, J.D., Calders, K., Disney, M.I., Lovell, J.L., Schaaf, C.B., Strahler, A.H. & Danson, F.M. (2015) Terrestrial laser scanning for plot-scale forest measurement. *Current Forestry Reports,* **1,** 239-251.

Nogueira, E.M., Nelson, B.W. & Fearnside, P.M. (2006) Volume and biomass of trees in central Amazonia: influence of irregularly shaped and hollow trunks. *Forest Ecology and Management,* **227,** 14-21.

Nölke, N., Fehrmann, L., Surati Jaya, I., Tiryana, T., Seidel, D. & Kleinn, C. (2015) On the geometry and allometry of big-buttressed trees-a challenge for forest monitoring: new insights from 3D-modeling with terrestrial laser scanning. . *iForest-Biogeosciences and Forestry,* **8,** 574.

Ploton, P., Barbier, N., Takoudjou Momo, S., Réjou-Méchain, M., Boyemba Bosela, F., Chuyong, G., Dauby, G., Droissart, V., Fayolle, A. & Goodman, R.C. (2016) Closing a gap in tropical forest biomass estimation: taking crown mass variation into account in pantropical allometries. *Biogeosciences,* **13,** 1571-1585.

R Development Core Team (2022) R: A language and environment for statistical computing. R Foundation for Statistical Computing, Vienna, Austria.

Raumonen, P., Åkerblom, M., Kaasalainen, M., Casella, E., Calders, K. & Murphy, S. (2015) Massive-scale tree modelling from TLS data. *ISPRS Annals of Photogrammetry, Remote Sensing & Spatial Information Sciences,* **2**.

Réjou-Méchain, M., Tanguy, A., Piponiot, C., Chave, J. & Hérault, B. (2017) biomass: an r package for estimating above-ground biomass and its uncertainty in tropical forests. *Methods in Ecology and Evolution,* **8,** 1163-1167.

Shenkin, A., Bentley, L.P., Oliveras, I., Salinas, N., Adu-Bredu, S., Marimon-Junior, B.H., Marimon, B.S., Peprah, T., Choque, E.L. & Trujillo Rodriguez, L. (2020) The influence of ecosystem and phylogeny on tropical tree crown size and shape. *Frontiers in Forests and Global Change,* **3,** 501757.

Slik, J.F., Paoli, G., McGuire, K., Amaral, I., Barroso, J., Bastian, M., Blanc, L., Bongers, F., Boundja, P. & Clark, C. (2013) Large trees drive forest aboveground biomass variation in moist lowland forests across the tropics. *Global Ecology and Biogeography,* **22,** 1261-1271.

Srinivasan, S., Popescu, S.C., Eriksson, M., Sheridan, R.D. & Ku, N.-W. (2014) Multi-temporal terrestrial laser scanning for modeling tree biomass change. *Forest Ecology and Management,* **318,** 304-317.

Taubert, F., Jahn, M.W., Dobner, H.-J., Wiegand, T. & Huth, A. (2015) The structure of tropical forests and sphere packings. *Proceedings of the National Academy of Sciences,* **112,** 15125-15129.

Wang, D., Momo Takoudjou, S. & Casella, E. (2020) LeWoS: A universal leaf-wood classification method to facilitate the 3D modelling of large tropical trees using terrestrial LiDAR. *Methods in Ecology and Evolution,* **11,** 376-389.

West, G.B., Brown, J.H. & Enquist, B.J. (1997) A general model for the origin of allometric scaling laws in biology. *Science,* **276,** 122-126.

Wilkes, P., Lau, A., Disney, M., Calders, K., Burt, A., de Tanago, J.G., Bartholomeus, H., Brede, B. & Herold, M. (2017) Data acquisition considerations for terrestrial laser scanning of forest plots. *Remote Sensing of Environment,* **196,** 140-153.

Xu, L., Saatchi, S.S., Yang, Y., Yu, Y. & White, L. (2016) Performance of non-parametric algorithms for spatial mapping of tropical forest structure. *Carbon balance and management,* **11,** 1-14.

Zanne, A.E., Lopez-Gonzalez, G., Coomes, D.A., Ilic, J., Jansen, S., Lewis, S.L., Miller, R.B., Swenson, N.G., Wiemann, M.C. & Chave, J. (2009) Global wood density database.

Funding

We would like to thank the NSERC Discovery Grant (Canada), CP’s Canada Research Chair, NSERC Canada Graduate Scholarship and FRQNT *Bourse de formation à la maîtrise* for funding this project.

Acknowledgments

We thank RIEGL Laser Measurement Systems GmbH for providing additional batteries for the field and technical support. We thank the SENAFRONT for their service in providing transport logistics and safety support in the field. We thank Camilo Alejo, Helen Muller-Landau, Jerome Chave and K.C. Cushman for their comment on the manuscript. We also thank the technical assistance of Anne Bienert and Norman Döring at Technische Universität Dresden.

Author Contributions

Mathieu Guillemette, Matthias Kunz and Catherine Potvin conceived the original idea for this study. Karl Friedrich Reich, Goddert von Oheimb and Jose Gonzalez de Tanago contributed to the ideas and further refinement. Alexis Ortega, Catherine Potvin, Francisco Solis, José Pari-Pari, Jose Gonzalez de Tanago and Matthias Kunz are responsible for collecting the field data. Alexandra Koller, Inga Freshse, Jose Gonzalez de Tanago, Matthias Kunz and Mathieu Guillemette performed that data processing and analysis. Mathieu Guillemette led the writing of the manuscript, with all other co-authors making significant contributions.

Conflict of Interest

The authors declare that the research was conducted in the absence of any commercial or financial relationships that could be construed as a potential conflict of interest.

Supplementary Information

Data acquisition and tree measurements

For the Panama Plots, fifteen to eighteen scans were performed in each plot using a RIEGL VZ-400i scanner with full-waveform analysis capabilities and a range up to 800 m. Scan design was focused on scanning the whole plot rather than individual trees. We scanned each plot at 15 different positions from the plot border to its center to optimize coverage (Figure S1). Vertical and horizontal angular location was 0.04. For Gonzalez de Tanago *et al.* (2018) dataset, eight to thirteen scans were performed in each plot also using a RIEGL VZ-400i. Similarly to the Panama Plots design, Gonzalez de Tanago *et al.* (2018) scan design was optimized for plot scanning and not for individual trees. Each scan had an angular resolution of 0.06.

For the Panama Plots data, large trees were extracted manually from the TLS point clouds using RiScan software. For Gonzalez de Tanago *et al.* (2018) each point cloud contained already extracted large trees. We measured DBH, tree height, trunk height, trunk top diameter, crown diameter, first-order branch diameter, and first-order branch length for a total of 104 TLS tropical large trees; 78 from the Panama Plots and 26 from Gonzalez de Tanago *et al.* (2018). All measurements were performed in the software CloudCompare v.2.11. Trunk top diameter is defined as the diameter at the top of the trunk before the trunks divide into first-order branches. First-order branches are defined as the first main branches where the tree trunk divides. First-order branch diameter was measured using the distance between two points perpendicular to the branch location. First-order branch length was measured by the distance between two points from the extremity of the branch to its division at the trunk. DBH was measured by estimating the diameter of a fitted plane surface around the tree trunk using CloudCompare's 2D polygon tool. Other measures were taken using the "distance between points" tool in CloudCompare.

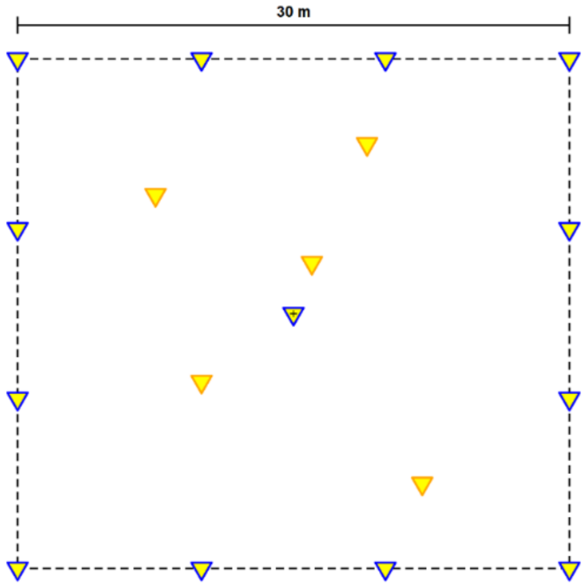

Figure S1: Example of TLS scan design inside 30 x 30 m plots (dashed line). Triangles show regular scan positions (blue stroke) and additional freely selected scan positions (orange stroke) for optimized scan coverage.

Other QSM studies in tropical forests

Previous studies have computed QSMs for tropical large trees, except for Brede *et al.* (2022) (Table S1). However the sample size of these studies was relatively small and none of these studies provided plot AGB estimates, but rather specific trees' AGB estimates.

Table S1 : Previously published scientific articles with Quantitative Structure Models (QSM) for tropical trees.

Datasets	*n* harvested trees	n QSM trees	DBH range (cm)	H range (m)	Instrument	Results
(Gonzalez de Tanago *et al.* 2018)	29	29	37.2 to 128.8	24.8 to 48.87	Riegl Vz-400	QSM provides accurate tree volume estimates (RMSE < 2.89 ; $R^2 > 0.90$) outperforming allometric models.
(Lau *et al.* 2018)	9	9	61.3 to 97.0	18.8 to 29.9	Riegl Vz-400	QSM reconstructs 95% of all branches > 30cm and 97% of tree volume.
(Lau *et al.* 2019)	26	72	16.7 to 128.7	16.4 to 51.6	Riegl Vz-400	Allometric models with crown metrics perform better than models with H, especially for large trees.
(Momo Takoudjou *et al.* 2018)	61	61	10.8 to 186.6	12.6 to 52.8	Leica C10	QSM provides accurate and unbiased volume estimation (RMSE < 2.81% and $R^2 >$ 0.98).
(Brede *et al.* 2022)	171	171	8.0 to 158.8	10.4 to 44.6	Riegl Vz-400	QSM was successfully used to calibrate allometric equations combining TLS and UAV-LS.

Theories for tree crown development

Table S2: Summary of theories behind tree crown size and architecture.

Theory	Summary	Authors
Metabolic Scaling Theory (MST)	The MST predicts that scaling relationships follow a 3/4 power law for metabolic	(West, Brown & Enquist 1997)

	rates. It assumes that biological systems minimize energy dissipation in transporting material through their bodies which regulates allometries.	
Competitive Convergence	The Competitive Convergence theory suggests environmental and competitive factors rule tree allometry in tropical forests, resulting in architectural convergence and equalizing effects. Proving that general allometric equations can be used to estimate trees' AGB.	(Iida *et al.* 2011)
Sphere Packing	The Sphere Packing theory suggests that stochastic packing of tree crowns in forest canopy by random placement of trees, competition for space, and mortality explain tree allometries.	(Taubert *et al.* 2015)

Challenges in computing QSM

In this study, we removed five QSM reconstructions because of point clouds that had too much occlusion after the LeWoS process, which resulted in an inaccurate QSM reconstruction where at least one first-order branch could not be reconstructed (Figure S2).

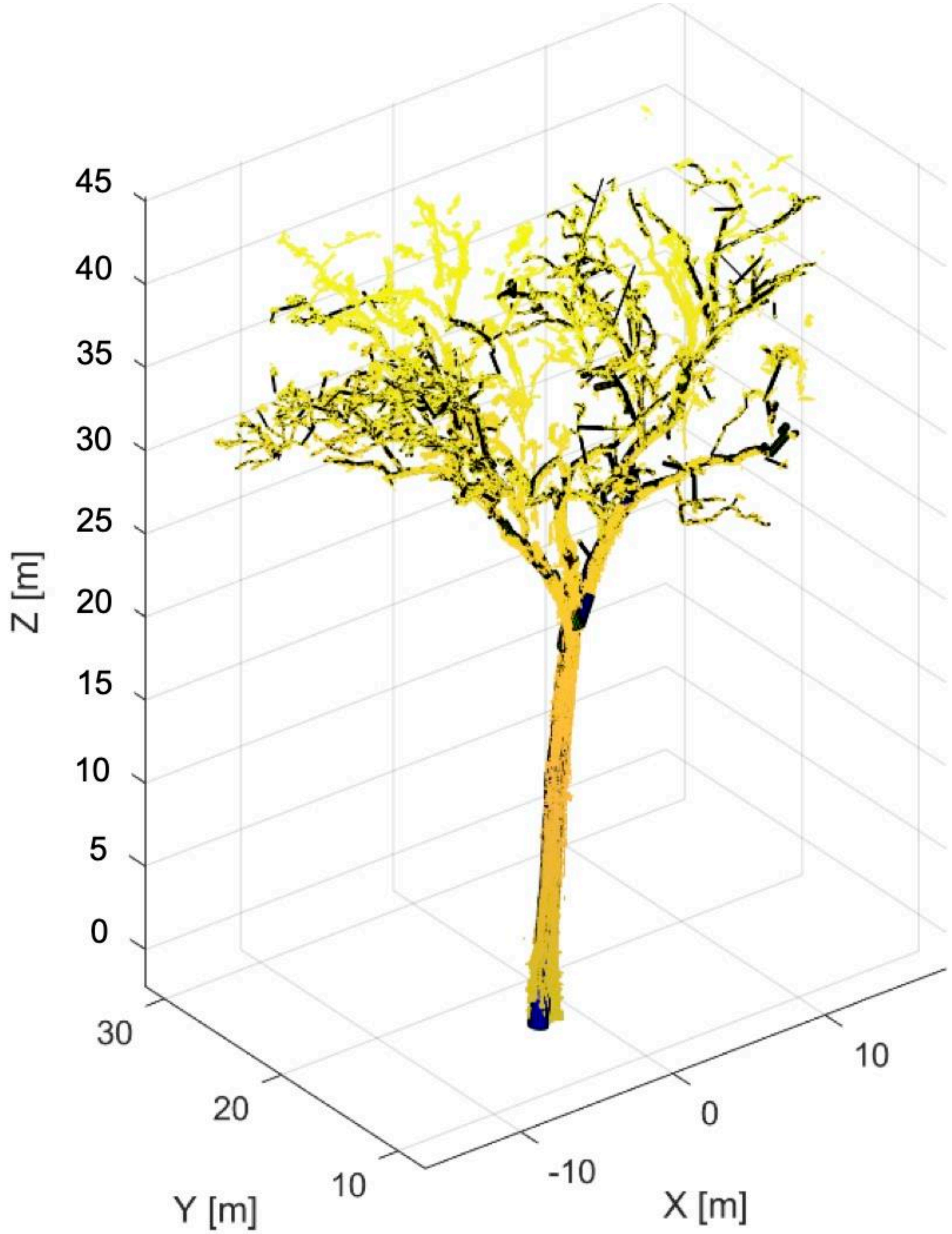

Figure S2: QSM reconstruction (dark colored cylinders) and tree point cloud (yellow) of tree17_02 where we see missing reconstruction of a second order branch in the crown center, a limited definition of crown reconstruction and the difficulty to capture the buttressed trunk.

Models' performances

To look at the variability in AGB estimates between the 4 models and the reference values coming from QSM reconstructions, we plotted the residuals of each model on a y-axis with the log-transformed referenced QSM-AGB on the x-axis. We found that for each model, the residuals increased with the referenced AGB. This result suggests that all models do not follow a homoscedastic pattern and that variability increases with tree size. Across all models, the Compartmentalized Model had the lowest residual range distribution (variability) in particular for the top four largest trees (QSM AGB > 25Mg) compared to the other models.

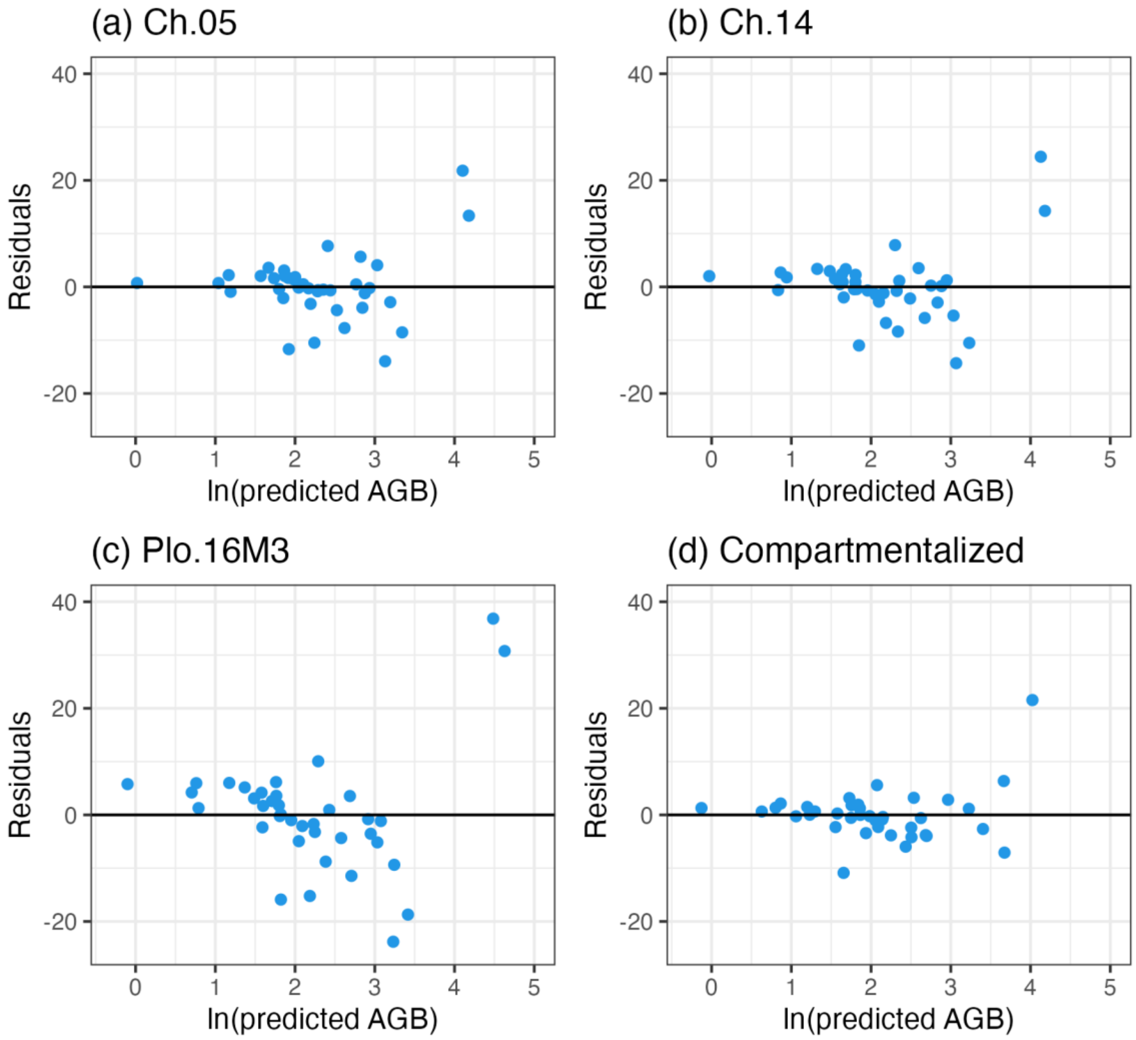

Figure S3: Residuals from Chave *et al.* (2005) pantropical equation estimates compared to the reference values of the QSM reconstruction (panel a) and for Chave *et al.* (2014) pantropical equation (panel b), Ploton *et al.* (2016) model 3 (panel 3) and the Compartmentalized Model (panel c)

The linear regressions plotted using all 38 large trees that had available QSM reconstructions were influenced by four very large trees of QSM AGB > 25 Mg. To understand the models' performance for the other large trees, we removed the 4 largest trees (QSM AGB > 25 Mg) and performed the same analysis as described in 2.3.1.

We found that the performance of the different models changed when removing the 4 largest trees. Ploton *et al.* (2016) model 3 became the model with the closest 1:1 fit with the referenced values (slope = 0.94) followed by the Compartmentalized (slope = 0.82), Chave *et al.* (2005) (slope = 0.81) and Chave *et al.* (2014) (slope = 0.79) (Figure S4). However, Ploton *et al.* (2016) had higher variability (RMSE = 3.30) than the Compartmentalized (RMSE = 2.87) which led that the Compartmentalized Model having the highest CCC (0.86) even though it had a slope further from a 1:1 relationship than Ploton *et al.* (2016) model 3. Overall, all four models had CCC that were close to each other (Table S3) suggesting that they performed similarly for the large trees of QSM AGB < 25 Mg.

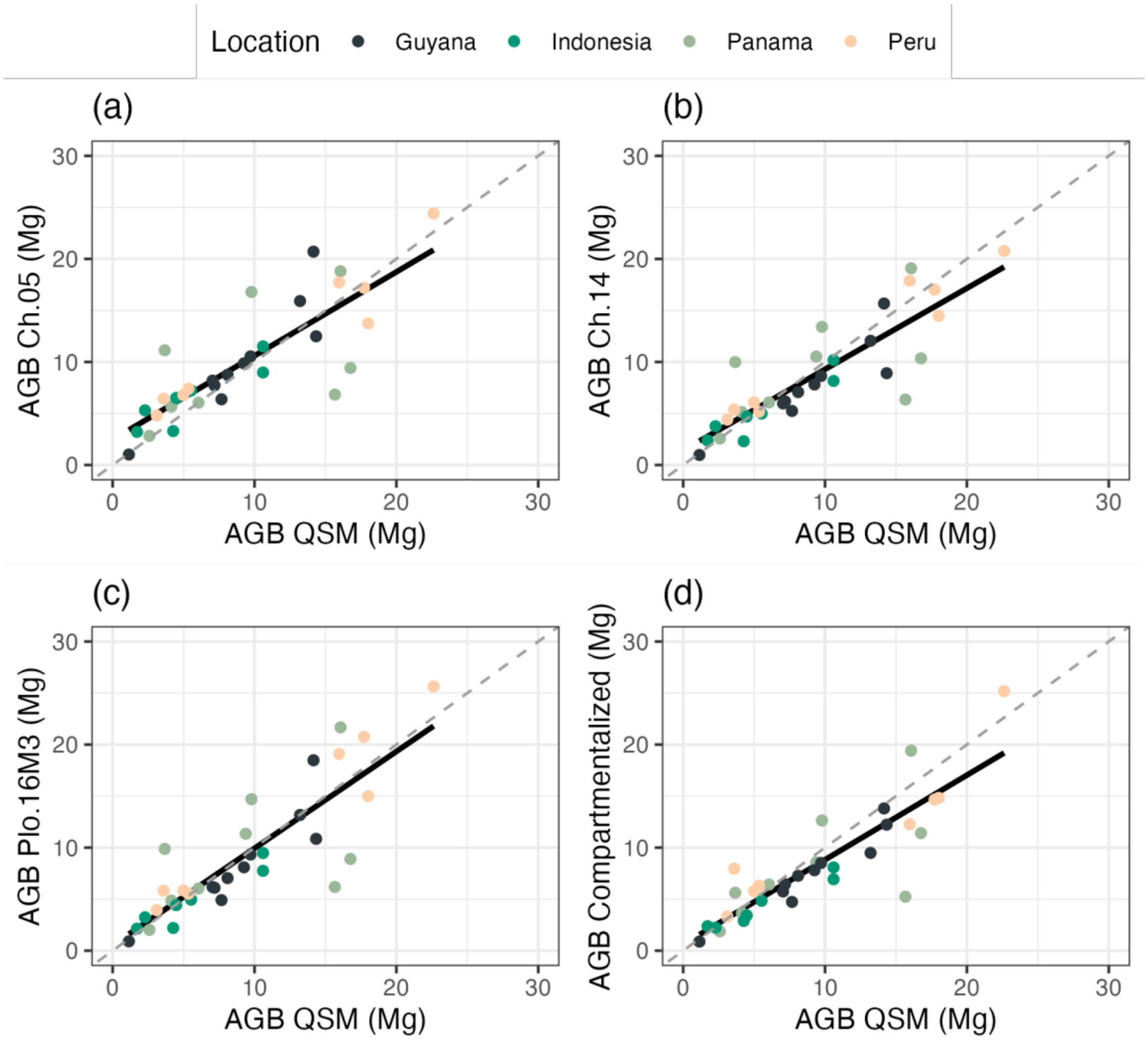

Figure S4: Scattered plot of the predicted tree AGB from (a) Chave *et al.* (2005) pantropical equation, (b) Chave *et al.* (2014) pantropical equation, (c) Ploton *et al.* (2016) model 3 and (d) the compartmentalized method against the reference values of the quantitative structure models (QSM) AGB estimates. The solid black line represents a fitted linear regression between the predicted values from the equation or model and the reference value of the QSMs. The dashed grey line represents a 1:1 relationship. Tree measurements come from TLS scans of the Panama dataset and Gonzalez de Tanago *et al.* (2018) dataset. Trees of QSM AGB > 25 Mg were removed (n = 34) (see Table S3 for linear models' parameters).

Table S3: Models performance against QSM reconstructions. SE = standard error. R^2 = coefficient of determination RMSE = root mean square error. CCC = concordance correlation coefficient. In all cases, trees of QSM AGB > 25 Mg were removed and there are 34 points and thus 32 degrees of freedom in the regression model.

	Regression parameters				Model performance				
	a	*b*	SE*a*	SE*b*	R^2	RMSE	CCC	Bias (abs)	Bias (%)
Chave 05	0.81	2.47	0.10	1.03	0.69	3.30	0.82	26.68	8.70
Chave 14	0.79	1.42	0.08	0.86	0.75	2.85	0.86	-17.10	-5.57
Plo.16M3	0.94	0.53	0.10	1.08	0.73	3.22	0.85	-0.12	-0.12
Compartmentalized	0.82	0.62	0.84	1.13	0.77	2.87	0.86	-33.95	-11.07

First-order branches' biomass

To understand the drivers of the first-order branch biomass, we plotted the distribution of first-order branch biomass following trees' DBH by the number of first-order branches per tree as a category. We found that the first-order branch biomass increases with DBH size and decreases with the number of first-order branches per tree. The biggest first-order branches were found in the largest trees of our dataset with the lowest number of first-order branches in their crown.

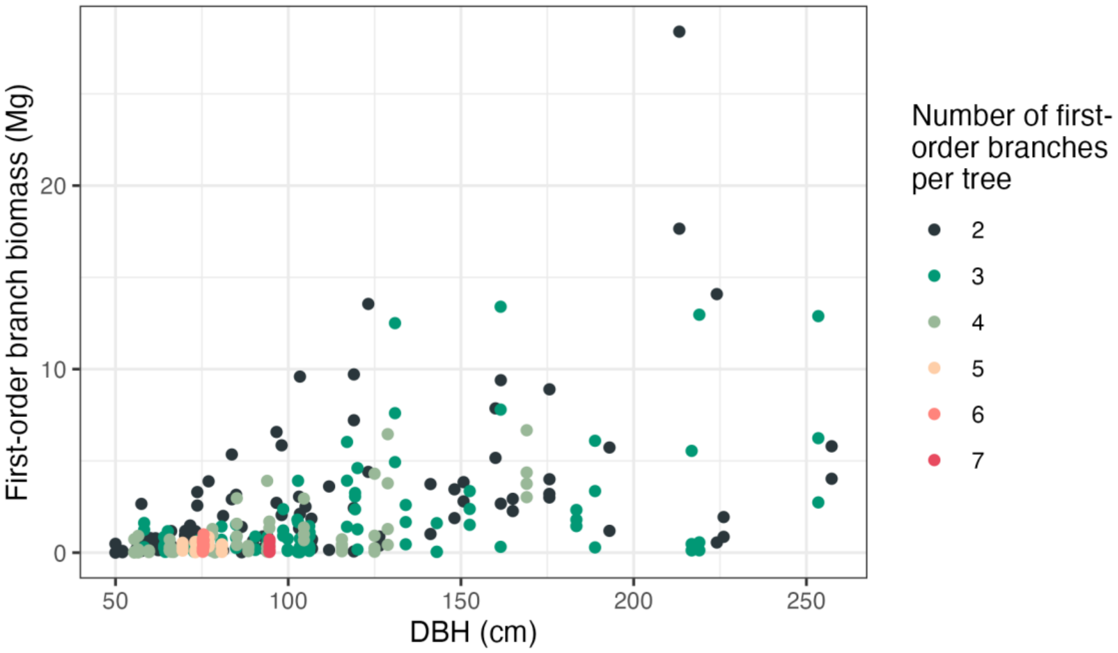

Figure S5: Biomass (Mg) distribution of first-order branches following trees' DBH for the 104 TLS trees.

Supplementary References

Brede, B., Terryn, L., Barbier, N., Bartholomeus, H.M., Bartolo, R., Calders, K., Derroire, G., Moorthy, S.M.K., Lau, A. & Levick, S.R. (2022) Non-destructive estimation of individual tree biomass: Allometric models, terrestrial and UAV laser scanning. *Remote Sensing of Environment,* **280,** 113180.

Chave, J., Andalo, C., Brown, S., Cairns, M.A., Chambers, J.Q., Eamus, D., Fölster, H., Fromard, F., Higuchi, N. & Kira, T. (2005) Tree allometry and improved estimation of carbon stocks and balance in tropical forests. *Oecologia,* **145,** 87-99.

Chave, J., Réjou-Méchain, M., Búrquez, A., Chidumayo, E., Colgan, M.S., Delitti, W.B., Duque, A., Eid, T., Fearnside, P.M. & Goodman, R.C. (2014) Improved allometric models to estimate the aboveground biomass of tropical trees. *Global Change Biology,* **20,** 3177-3190.

Gonzalez de Tanago, J., Lau, A., Bartholomeus, H., Herold, M., Avitabile, V., Raumonen, P., Martius, C., Goodman, R.C., Disney, M. & Manuri, S. (2018) Estimation of above-ground biomass of large tropical trees with terrestrial LiDAR. *Methods in Ecology and Evolution,* **9,** 223-234.

Iida, Y., Kohyama, T.S., Kubo, T., Kassim, A.R., Poorter, L., Sterck, F. & Potts, M.D. (2011) Tree architecture and life-history strategies across 200 co-occurring tropical tree species. *Functional Ecology,* **25,** 1260-1268.

Lau, A., Bentley, L.P., Martius, C., Shenkin, A., Bartholomeus, H., Raumonen, P., Malhi, Y., Jackson, T. & Herold, M. (2018) Quantifying branch architecture of tropical trees using terrestrial LiDAR and 3D modelling. *Trees,* **32,** 1219-1231.

Lau, A., Calders, K., Bartholomeus, H., Martius, C., Raumonen, P., Herold, M., Vicari, M., Sukhdeo, H., Singh, J. & Goodman, R.C. (2019) Tree biomass equations from terrestrial LiDAR: A case study in Guyana. *Forests,* **10,** 527.

Momo Takoudjou, S., Ploton, P., Sonké, B., Hackenberg, J., Griffon, S., De Coligny, F., Kamdem, N.G., Libalah, M., Mofack, G.I. & Le Moguédec, G. (2018) Using terrestrial laser scanning data to estimate large tropical trees biomass and calibrate allometric models: A comparison with traditional destructive approach. *Methods in Ecology and Evolution,* **9,** 905-916.

Ploton, P., Barbier, N., Takoudjou Momo, S., Réjou-Méchain, M., Boyemba Bosela, F., Chuyong, G., Dauby, G., Droissart, V., Fayolle, A. & Goodman, R.C. (2016) Closing a gap in tropical forest biomass estimation: taking crown mass variation into account in pantropical allometries. *Biogeosciences,* **13,** 1571-1585.

Taubert, F., Jahn, M.W., Dobner, H.-J., Wiegand, T. & Huth, A. (2015) The structure of tropical forests and sphere packings. *Proceedings of the National Academy of Sciences,* **112,** 15125-15129.

West, G.B., Brown, J.H. & Enquist, B.J. (1997) A general model for the origin of allometric scaling laws in biology. *Science,* **276,** 122-126.

Linking Statement

In Chapter 1 of this thesis, I focused on the challenges in estimating the aboveground biomass (AGB) of large tropical trees and how it can affect our ability to scale up accurate estimates of AGB at the plot and landscape levels. In Chapter 2, I turn to the landscape level and focus on the impact of large tropical tree abundance and distribution patterns on the spatial variation of forest carbon stocks. I also discuss the implications of large tropical tree density and distribution patterns on sampling protocols for forest carbon monitoring programs. The first and second chapters of this thesis answer important questions regarding two sources of uncertainties when estimating forest carbon stocks: (1) the estimation methods at the tree level and (2) the sampling protocols at the landscape level.

Chapter 2: Large tree density, distribution pattern and carbon stocks' spatial variation in a neotropical intact forest

Mathieu Guillemette[1]*, Matthias Kunz[2], Jorge Valdez[3], Alexis Ortega[4], Camilo Alejo[1], Rolando Pérez[3], Salomon Aguila[3], David Mitre[3], Catherine Potvin[1,3]

[1]Neotropical Lab, Department of Biology, McGill University, Montréal, Québec, Canada

[2]Institute of General Ecology and Environmental Protection, Technische Universität Dresden, Germany

[3]Smithsonian Tropical Research Institute, Panama City, Republic of Panama

[4]Tierras Colectivas Emberá del Rio Balsas, Manené, Panama

*** Correspondance:**

Mathieu Guillemette

mathieu.guillemette@mail.mcgill.ca

Keywords: Tropical forests, Intact forests, Carbon uncertainties, MRV, REDD+, Bacurú Drõa, Indigenous research, Darién.

Introduction

Large trees play an important role in forest structure, diversity and complexity (Lindenmayer, Laurance & Franklin 2012; Lutz *et al.* 2012). They supply habitat refugia for many species and they can act as biodiversity hotspots (Dean, Milton & Jeltsch 1999). Moreover, they influence forests' succession patterns and rates (Keeton & Franklin 2005) and account for a large portion of the world's forest carbon stocks and fluxes (Lutz *et al.* 2018; Piponiot *et al.* 2022). In fact, it is suggested that the world's forests could not stock large amounts of aboveground carbon without the presence of large trees (Lutz *et al.* 2018) and numerous studies (e.g., Lutz *et al.* 2012; Slik *et al.* 2013; Bastin *et al.* 2015; Bastin *et al.* 2018; Mateo-Vega, Arroyo-Mora & Potvin 2019) have shown that despite their relatively low number, large trees represent the bulk of forest plot's aboveground biomass (AGB).

Large trees and intact tropical forests present a great challenge when it comes to estimating their carbon stock. Intact forests are defined as seamless mosaics of at least 500 km^2 with no signs of human intervention (Potapov *et al.* 2008; Potapov *et al.* 2017). They typically consist of large unfragmented areas of old-growth or primary forests (Potapov *et al.* 2017), providing the environmental conditions for large trees (Lindenmayer & Laurance 2017). At the tree level, large tropical trees' carbon stock is difficult to estimate accurately because of the inherent uncertainties of the allometric equations, which are calibrated from data on destructively harvested trees that invariably includes relatively few large trees (Chave *et al.* 2014; Goodman, Phillips & Baker 2014; Gonzalez de Tanago *et al.* 2018; Lutz *et al.* 2018). Uncertainties around AGB estimates derived from allometric equations are carried out at the landscape level through scaling-up processes (Clark & Kellner 2012). Moreover, large trees control the spatial distribution of forested landscape carbon stocks (Slik *et al.* 2013; Bastin *et al.* 2018; Lutz *et al.* 2018). However, large trees' spatial distribution patterns and abundance remain elusive worldwide (Lutz *et al.* 2012; Lutz *et al.* 2018; Clark *et al.* 2019; de Lima *et al.* 2022). According to Mitchard *et al.* (2013), the largest uncertainties in current carbon maps come from the spatial distribution of carbon and from the spatial pattern of forest cover change.

Studying large tree distribution and abundance is increasingly urgent because they are rapidly declining due to logging pressure (Lindenmayer, Messier & Sato 2016) and the increased environmental impacts of climate change (Allen *et al.* 2010; Lindenmayer, Laurance & Franklin 2012; Bennett *et al.* 2015; Clark *et al.* 2019). Variation in the abundance of large trees among plots in the Darien region of Panama was explained in large part by selective logging pressure (Mateo-Vega, Arroyo-Mora & Potvin 2019). Large trees are also more susceptible to die from hydraulic failure caused by drought than smaller trees (Allen *et al.* 2010; Bennett *et al.* 2015). With the warming climate, tropical forests are expected to become warmer and drier with even more severe El Niño events, resulting in higher large tree mortality (Allen *et al.* 2010; Bennett *et al.* 2015; Meakem *et al.* 2018). Climate change may lead to lasting decreases in the abundance of large trees, thereby reducing forest carbon stocks (Gora & Esquivel-Muelbert 2021).

There are multiple definitions for large trees depending on the ecosystem, species, and environmental conditions (Lindenmayer & Laurance 2017). In general, large trees are of reproductive age, tall enough to reach the upper canopy, and larger than the majority of the woody stem of the forest (Lutz *et al.* 2018). The definition of a large tree is arbitrary and depends on the purpose of the study (Ali & Wang 2021). Numerous studies refer to large trees by setting a fixed diameter at breast height (DBH) threshold, but other approaches have also been used (e.g., using the top 1 % of measured stems or the top quantile (Ali *et al.* 2019; Ali *et al.* 2020; Ali & Wang 2021)). Here, we used different DBH thresholds to compare our results with a broad range of other studies. In the region where we work, previous studies have defined “large trees” as trees of DBH ≥ 50 (Mateo-Vega *et al.* 2017; Meakem *et al.* 2018; Mateo-Vega, Arroyo-Mora & Potvin 2019). Moreover, to compare with other studies in Central America (e.g., Clark & Clark 1996), we further consider “very large trees” as trees of DBH ≥ 70 cm and “giant trees” as trees of DBH ≥ 100 cm to compare with data coming for remote sensing analysis (Kunz *et al.* 2022).

In 2017, Mateo-Vega, Arroyo-Mora and Potvin (2019) conducted a field campaign to estimate the AGB of Darién’s forests, already considered the richest forest in Panama in terms of AGB (Asner *et al.* 2013). Of the 30 one-hectare (ha) plots that were monitored by Mateo-Vega, Arroyo-Mora and Potvin (2019), the *Tierras Colectivas del Rio Balsas* stood out from the other regions as it contained the highest AGB value. In 2019, an exploratory field expedition established 20 0.09-ha (900 m^2) plots to collect forest inventory data and terrestrial laser scan (TLS) data across the *Tierras Colectivas del Rio Balsas*. This expedition was co-led by local Indigenous Emberá technicians in collaboration with McGill’s Neotropical Lab to target forest locations that Emberá knowledge holders and traditional authorities consider as their “best forests”. They reported numerous large trees, including some of the largest trees recorded in Central America (Kunz *et al.* 2022). In 2022, a long-term permanent forest plot of 10 ha was established under the *Bacurú Drõa* project (Old-Growth Forests in Emberá), a partnership between the Emberá Indigenous peoples of the *Tierras Colectivas del Rio Balsas*, the Neotropical ecology laboratory of McGill University and the Smithsonian Tropical Research Institute (STRI). Here, we aim to (1) analyze the *Bacurú Drõa* Permanent Plot forest structure and diversity, (2) elucidate large tropical trees’ spatial distribution patterns within the plot and beyond and (3) report on the abundance of large trees for the intact tropical forests of the Balsas river. These results will underline the implication of large tree contagion and heterogeneous forest structure for developing forest monitoring sampling protocols.

Materials and Methods

Study site

This study takes place in the *Tierras Colectivas del Rio Balsas* located in the South-Eastern portion of Darién's province, in Panama, and home of the Emberá Indigenous people (Figure 1). The Choco-Darién region bridges Central and South America and is the only gap in the Pan-American highway, making this region hard to access. It is considered one of the last frontiers on Earth (Bryant, Nielsen & Tangley 1997). The Darién is a global biodiversity hot spot host to numerous endemic species (Davis, Heywood & Hamilton 1997) and high forest carbon stocks (Mateo-Vega, Arroyo-Mora & Potvin 2019). The Choco-Darién region, including almost the entirety of the Balsas territory, constitutes the single largest area of intact primary forest in Central America, according to the latest GlobalForestWatch data (Hansen *et al.* 2013; Kunz *et al.* 2022).

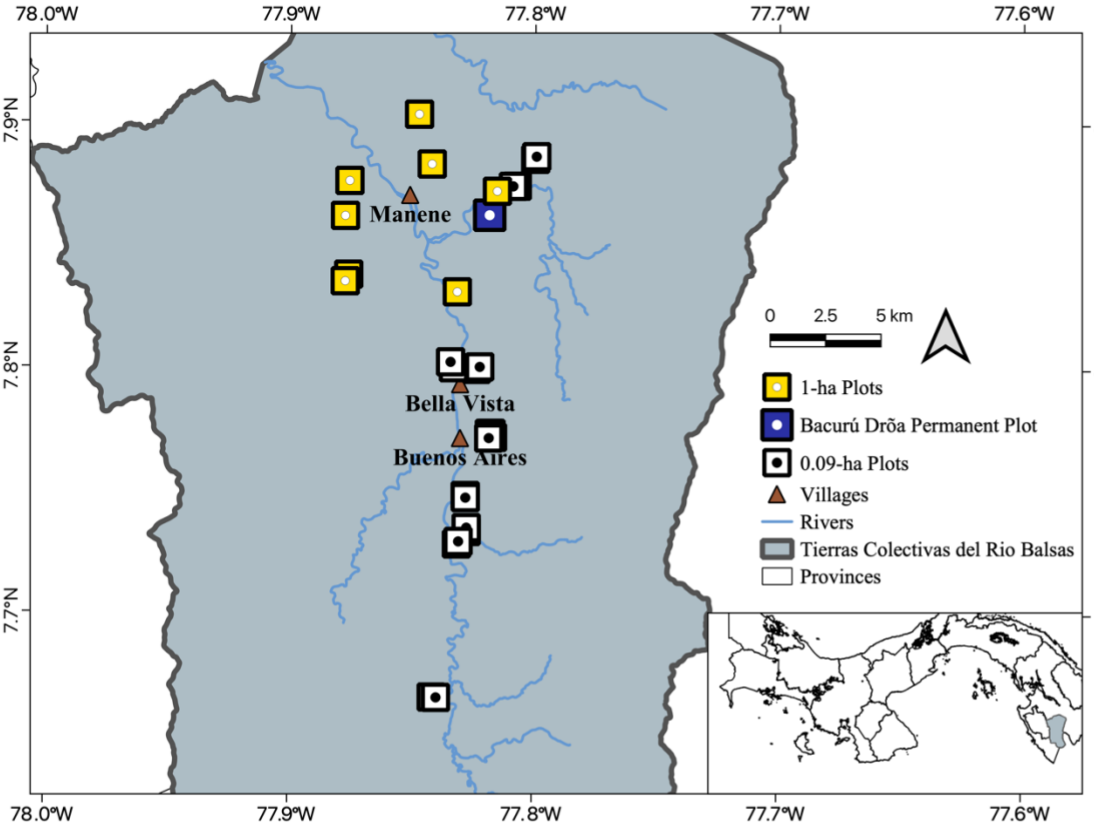

Figure 1: Map close-up on the *Tierras Colectivas del Rio Balsas* with the centroids of the 0.09-ha plots presented in Kunz et al. (2022), 1-ha plots from Mateo-Vega et al. (2019) and the *Bacurú Drõa* Permanent Plot (10 ha) as well as the main villages and rivers. Marker size is not to scale.

Bacurú Drõa Permanent Plot

The *Bacurú Drõa* Permanent Plot (Figure 2) was established following the ForestGEO standardized methodology (Condit 1998) after a 9-day training of lead Emberá technicians by ForestGEO professionals (Co-authors SA, DM and RP). The 10-ha plot followed a grid pattern of 20 m by 20 m quadrats forming 1-ha rectangle subplots of 20 x 500 m oriented south to north

(Supp. Info. Figure S1). The plot was established using a Ushikata Tracon S-25 optical theodolite and measuring tapes to establish the 20 x 20 m quadrats while controlling for slope. The plot was oriented to magnetic north at the time of its installation, ~7° deviation to the west of due north (Kunz *et al.* 2022).

All trees of diameter at breast height (DBH) ≥10 cm were tagged, measured and mapped. Manual mapping on the ground was performed by trained Emberá field technicians using measuring tapes and a compass, giving each tree an x-y coordinate location inside its attributed 20 x 20 m quadrat. Later, the mapped trees were digitalized using ArcGIS (Figure 2). Moreover, each tree was tagged and identified to its lowest taxa possible by co-authors JV, SA, RP and local Emberá botanists giving scientific and Emberá names to each tree. Tree DBHs were measured using diameter tapes and ladders were used when buttressed trees were encountered to ensure measuring above the buttress. In the case of a buttressed tree, the height at which the diameter was measured was also recorded. For multi-stem trees, each stem DBH was measured and stems were numbered separately under the same tree tag number.

We calculated three stand-level metrics from the DBH measurements: DBH coefficient of variation (CV), basal area, and estimated aboveground biomass (AGB), and we quantified the contributions of large trees to both basal area and AGB. We used DBH CV as a surrogate for forest structure. We calculated the plot's basal area, the summed cross-sectional area of tree trunks, because this is a convenient and widely used indicator of wood volume. Unlike AGB, basal area is not affected by the inherent uncertainties associated with using allometric equations and assigning wood densities (Lutz *et al.* 2013). Therefore, the basal area is easily compared among studies and is generally preferred in forestry (Lutz *et al.* 2013). We calculated AGB carbon stocks because these are of prime interest in the climate change mitigation domain (Chenost *et al.* 2010). We first calculated AGB dry mass using the pantropical equation based on DBH only (no height) (Chave *et al.* 2014), as implemented in the BIOMASS package (Réjou-Méchain *et al.* 2017) in R, with wood densities from the Global Wood Density database (Zanne *et al.* (2009). We then converted AGB dry mass to AGB carbon using the carbon-mass-ratio value of 0.461 by Elias and Potvin (2003) derived from a study on 32 tree species in Panama.

Equation 1: Pantropical equation from Chave *et al.* (2014) where AGB is tree aboveground biomass (in kg dry mass), DBH is diameter at breast height (cm), WD is wood density (g/cm^3) assigned from taxonomic identity, and E is a measure of environmental stress based on climate averages for the location.

$$AGB = exp(-2.024 - 0.896 * E + 0.920 * log(WD) + 2.795 * log(DBH) - 0.0461 * (log(DBH))^2))$$

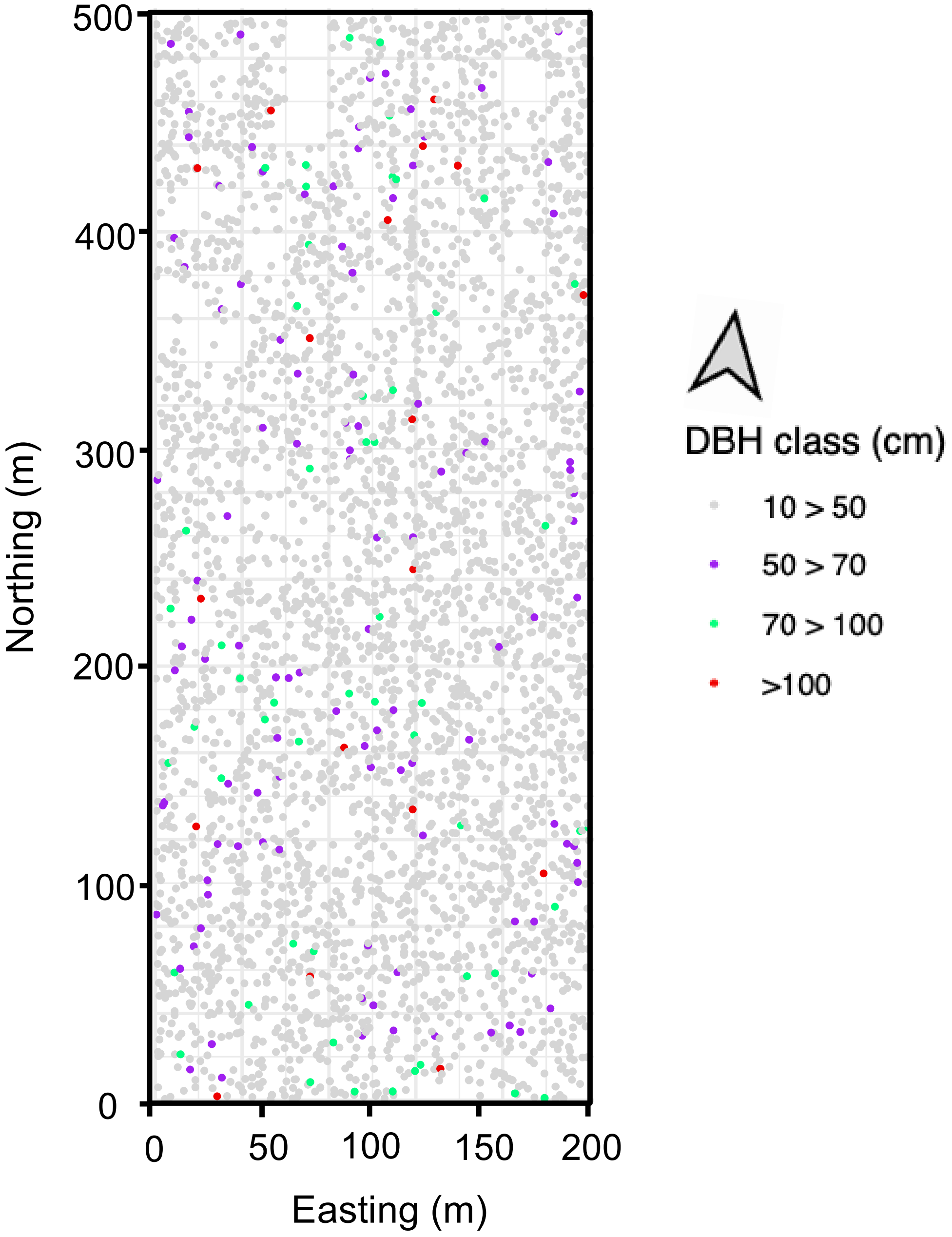

Figure 2: Map of the *Bacurú Drõa* Permanent Plot, showing censused trees by DBH size class category.

In addition, we analyzed the spatial distribution pattern of the large trees (≥50 cm DBH), very large trees (≥70 cm DBH) and giant trees (≥100 cm DBH) within the plot. Specifically, we counted the number of trees of each size class in rectangular subplots, choosing 12 quadrats of 0.83 ha each as a scale large enough to mostly avoid 0 values and small enough to divide the area and control for environmental factors (Baddeley & Turner 2005). For the large and very large trees, we further performed a quadrat test (Baddeley 2008), testing if trees were randomly distributed among rectangular subplots, or if they were more clustered or more regularly distributed than would be expected under a homogenous Poisson process (Supp. Info. 6.2). We did not perform a quadrat test for the giant trees because the sample size was too small (n = 18) and the quadrat count revealed quadrats with 0 giant trees. The results of the quadrat-test were inspected with a Pearson X^2 goodness of fit test to reveal if the distribution pattern was clustered, random or regular. These spatial distribution analyses were done in R4.2.1 (R Development Core Team 2022) using Spatstat package (Baddeley & Turner 2005).

Landscape analyses

We complemented our analysis of large tree distribution on the *Bacurú Drõa* Permanent Plot with a landscape-level analysis. For this, we used data from Kunz *et al.* (2022), who identified a preliminary 220 large tree crowns followed by an additional 860 over a concave hull area of 20 100 ha within the *Tierras Colectivas del Rio Balsas* from high-resolution satellite images (PlanetScope and Sentinel-2) (Figure 3). We refer to these trees as the “RS” trees for consistency with Kunz *et al.* (2022). In this study, we added another 92 RS trees after a secondary inspection by co-author MK following the same method. In their study, Kunz *et al.* (2022) conducted ground-truthing that tested for true-positive results (i.e., validating on the ground potential giant trees identified via remote sensing). They reached 66 RS trees out of the preliminary 220 and confirmed the presence of all trees. They reported DBH ranging between 65 to 350 cm with only six trees with DBH < 100 cm, leaving a 90% true-positive detection rate of giant trees for the RS tree survey. Moreover, we take advantage of the *Bacurú Drõa* Permanent Plot to test for false-negative (i.e., large trees present on the ground that were not spotted during the survey of the satellite image bank). We compared the RS trees to the giant trees (DBH ≥ 100 cm) found inside the *Bacurú Drõa* Permanent Plot.

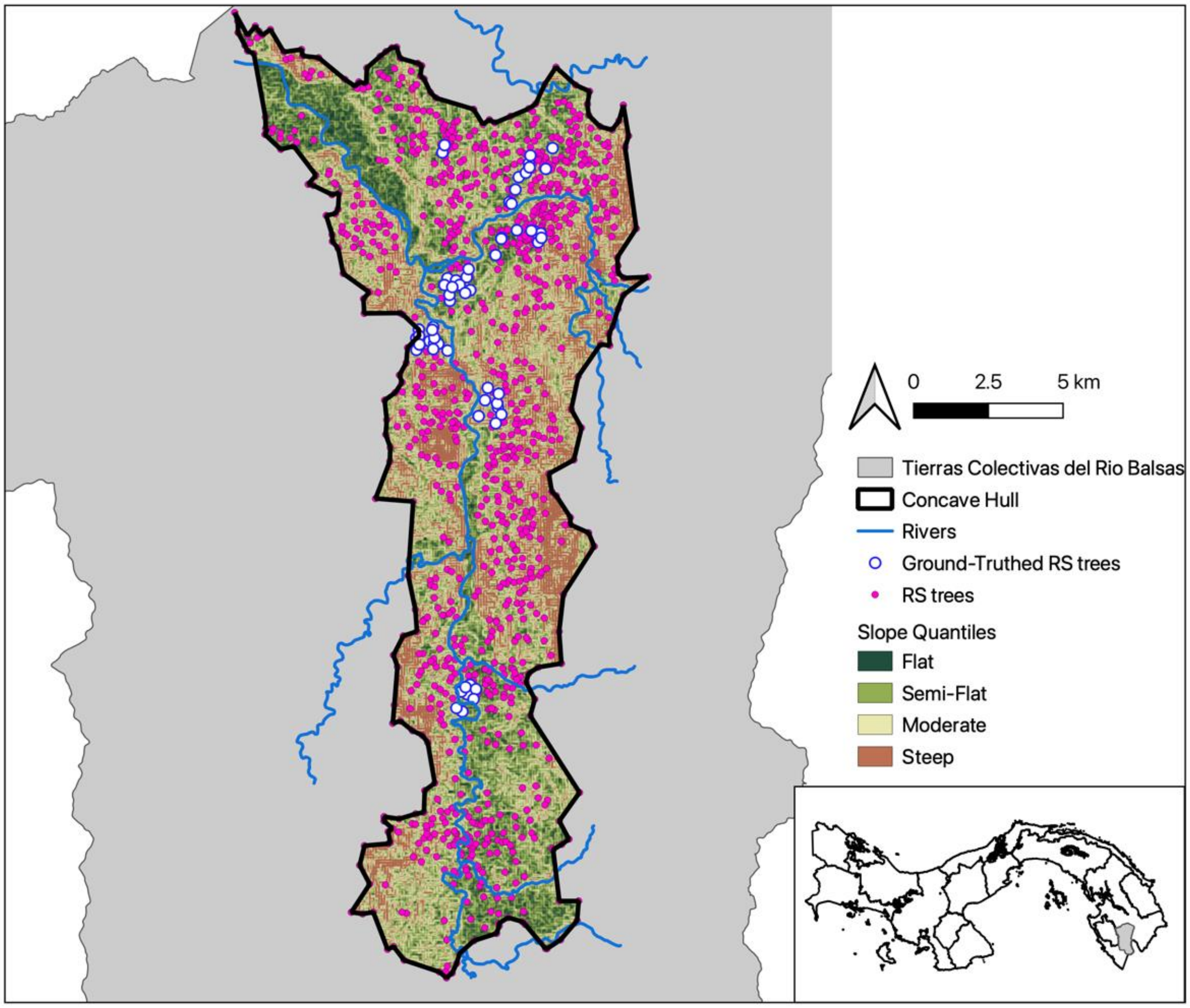

Figure 3: Location of the RS trees (pink dots) and ground-validated RS trees (White/blue dots) within the concave hull area of interest (20 100 ha). Data from Kunz *et al.* (2022) with the additional 92 RS trees. Slope quantiles are flat (0 – 2.9°), semi-flat (2.9 - 8.6°), moderate (8.6 – 17.3°) and steep (17.3 – 60.9°).

Building on the results of Kunz *et al.* (2022) reporting that ground-validated RS trees grew on slopes up to 20° angle, we aimed to understand the abundance of large trees at the landscape level according to the slope category in which they are located. To do so, we calculated a quadrat-count of all the RS trees by slope categories (Figure 3). Terrain slope is known to affect large tree distribution and abundance (Lindenmayer & Laurance 2017) and compared to the *Bacurú Drõa* Permanent Plot, where the terrain was relatively flat (elevation ranging from 110 m to 130 m), the terrain slope at the landscape level is more heterogeneous (0° to < 60°). Therefore, we defined quadrat polygons based on slope categories and counted the number of trees within each quadrat. Slope categories were defined by quantiles so they have equal total area (5 025 ha): 1st quantile: flat (0 – 2.9°), 2nd quantile: semi-flat (2.9 - 8.6°), third quantile: moderate (8.6 – 17.3°) and fourth quantile: steep (17.3 – 60.9°). Moreover, as for the *Bacurú Drõa* Permanent Plot, we tested the distribution pattern of the RS trees against a homogenous Poisson point process to see if their distribution was clustered, random or regular. In addition, we performed a quadrat-test, using the same slope quantiles as for the quadrat-count. The Slope Terrain Model was built using the Raster package in R from the digital elevation model (STRM 90). The quadrat-count and quadrat-test were also performed in R using the Spatstat package.

To further the analysis of the impact of large tree distribution on carbon stock spatial variability, we estimated the carbon stock of the entire *Tierras Colectivas del Rio Balsas* using forest inventory data of three datasets: the 10-ha *Bacurú Drõa* Permanent Plot, the twenty 0.09-ha plots monitored by Kunz *et al.* (2022) and the eight 1-ha plots censused by Mateo-Vega, Arroyo-Mora and Potvin (2019). The 0.09-ha Plots were established in locations considered their "best forest" by the Emberá, thus containing an abundance of large trees (Figure 1). In these 0.09-ha plots, DBHs and tree heights were measured for all trees of DBH ≥ 10 cm and tree species, genus or family was identified to the lowest taxonomic level possible (Kunz *et al.* 2022). The 1-ha Plots were established to sample disturbed forests from traditional selective logging activities that are not detectable from remote sensing (3 plots), and undisturbed forests distributed in the north-west part of the *Tierras Colectivas del Rio Balsas* (5 plots, Figure 1). In these 1-ha plots, DBHs were measured only for trees with DBH ≥ 50 cm at the 1-ha level while all trees of 10 cm > DBH < 50 cm were measured in 4 subplots of 12 x 12 m at each corner of the 1-ha plots (Mateo-Vega, Arroyo-Mora & Potvin 2019). Tree species, genus or family were identified to the lowest taxonomical level possible. We calculated individual tree AGB and carbon stocks following the same methods as described above for the *Bacurú Drõa* Permanent Plot.

Once we obtained the carbon stock value for each of the three types of plots, we transformed them into a carbon density value per hectare by dividing them by the total area of each plot. For each 1-ha plot, we calculated the carbon density for trees 10-50 cm within the subplots, and added it to the carbon density value for trees with DBH ≥ 50 cm for the entire 1-ha plot. We used the "Stratify and Multiple" method to provide the total carbon stock estimate for the *Tierras Colectivas del Rio Balsas*. The Stratify and Multiply method consists in using field biomass inventory data to carbon density value per hectare and extrapolating the result to a given area of forested ground cover obtained by satellite images (Goetz *et al.* 2015). In addition to the three estimates of the total carbon stocks found within the *Tierras Colectivas del Rio Balsas* intact forest, we present a fourth estimate of carbon stock coming from the weighted average by total monitored area for the three carbon density values.

Results

Bacurú Drõa **Permanent Plot's tree diversity and forest structure**

The *Bacurú Drõa* Permanent Plot contained a total of 3698 individual trees of DBH ≥ 10 cm with a total of 4101 stems when accounting for multi-stem trees. To date, 57 % of the trees have been identified at the species level. Trees that could not be confidently identified by the field team were collected and brought to the Smithsonian Tropical Research Institute and the University of Panama herbarium for further identification. Overall, 1590 trees are still to be identified, including 68 individuals in the large tree size category (DBH ≥ 50 cm). A total of 129 tree species were identified in the 10 ha of the *Bacurú Drõa* Permanent Plot, of which 27 species were present in the large tree community (DBH ≥ 50 cm). The six most common species for all trees of DBH ≥ 10 cm were *Inga oerstediana*, *Pterocarpus rohrii*, *Cecropia insignis*, *Gustavia superba*, *Cecropia obtusifolia* and *Sorocea affinis* in descending order and the six most common species for the large tree community (DBH ≥ 50 cm) were *Pterocarpus rohrii*, *Luehea seemannii*, *Terminalia oblonga*, *Inga oerstediana*, *Ceiba pentandra* and *Apeiba tibourbou* in descending order (Table 1). *Pterocarpus rohrii* and *Inga oerstediana* are the only two species present in the top six most dominant species of the large tree community that were also amongst the top six species for all the trees.

Table 1 : The six most dominant tree species and families for all the trees and for the large tree community of the *Bacurú Drõa* Permanent Plot with their respective number of trees, DBH average and standard deviation and their population's proportion of individuals in the large tree community. Species are presented by order of abundance.

Species	Emberá name	Number of trees	Number of large trees	Mean DBH (cm)	Standard Deviation DBH (cm)	Proportion of large trees (%)
Pterocarpus rohrii	Guanchiru	220	20	25.8	17.7	9
Luehea seemannii	Purru	40	19	47.9	31.8	48
Terminalia oblonga	Guayabillo	16	9	48.7	32.2	56
Inga oerstediana	Ugujo	221	8	23.3	11.6	4
Ceiba pentandra	Bongo	21	8	49.7	42.2	38
Apeiba tibourbou	Tejiru bacuru	52	8	29.92	19.8	15
Cecropia insignis	Eborro	162	2	20.0	8.3	1
Sorocea affinis	Quera tubu	112	1	15.7	6.1	1
Gustavia superba	Paco	136	0	14.9	5.5	0
Cecropia obtusifolia	Buriala	117	0	17.3	6.2	0

The *Bacurú Drõa* Permanent Plot presented a high level of forest structural heterogeneity in terms of tree size representation with a DBH CV equal to 72.3%. The plot contained 185 large trees (DBH ≥ 50 cm), 73 very large trees (DBH ≥ 70 cm) and 18 giant trees (DBH ≥ 100 cm). The largest tree found within the *Bacurú Drõa* Permanent Plot was a *Dipteryx oleifera* (Soiba in Emberá) with a DBH of 160.4 cm. The basal area per hectare for all trees was equal to 2038 m^2. The carbon density per hectare for the plot, when considering all trees, was equal to 99.4 Mg/ha.

The large tree community accounted for 4.5 % of the tree stems, 39 % of the basal area and 53 % of the carbon stock of all the trees found within the plot, and included 16% of the tree species.

Large trees and very large trees were clustered within the plot ($X^2 = 42.495$; p-value < 0.05 and $X^2 = 22.178$; p-value < 0.05). The 12 quadrats of 0.83 ha encompassed between 7 and 36 large trees, 2 to 11 very large trees and 0 to 3 giant trees (Figure 4). The highest density of large trees was found in the southwest part of the plot (Supp. Info. Figure S3).

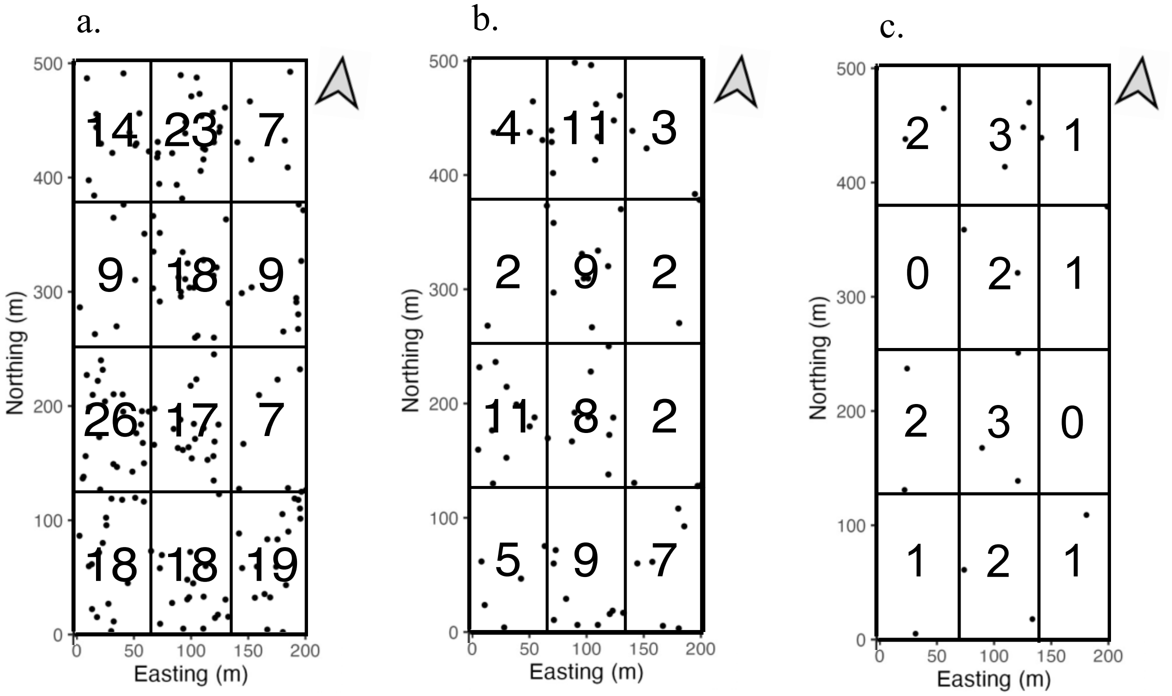

Figure 4: Large trees (DBH ≥ 50 cm) distribution and overlayed quadrat-count (panel a). Very large trees (DBH ≥ 70 cm) distribution and overlayed quadrat-count (panel b). Giant trees (DBH ≥ 100 cm) distribution and overlayed quadrat-count+ (panel c).

RS trees false-negative analysis

We used the giant trees (DBH ≥ 100 cm) from the inventory dataset of the *Bacurú Drõa* Permanent Plot to test for false-negative results in the RS tree survey. The *Bacurú Drõa* Permanent Plot had 18 giant trees. Out of these 18 giant trees, the RS survey located three giant trees within the plot, leaving 15 false-negative results and a detection rate of 16.67 % (Figure 5). The three trees detected by remote sensing were the three largest trees of the plot: a *Dipteryx oleifera* (DBH =160.4 cm), a *Luehea semennii* (DBH = 148.4 cm) and a *Ceiba pentendra* (DBH = 134.6 cm).

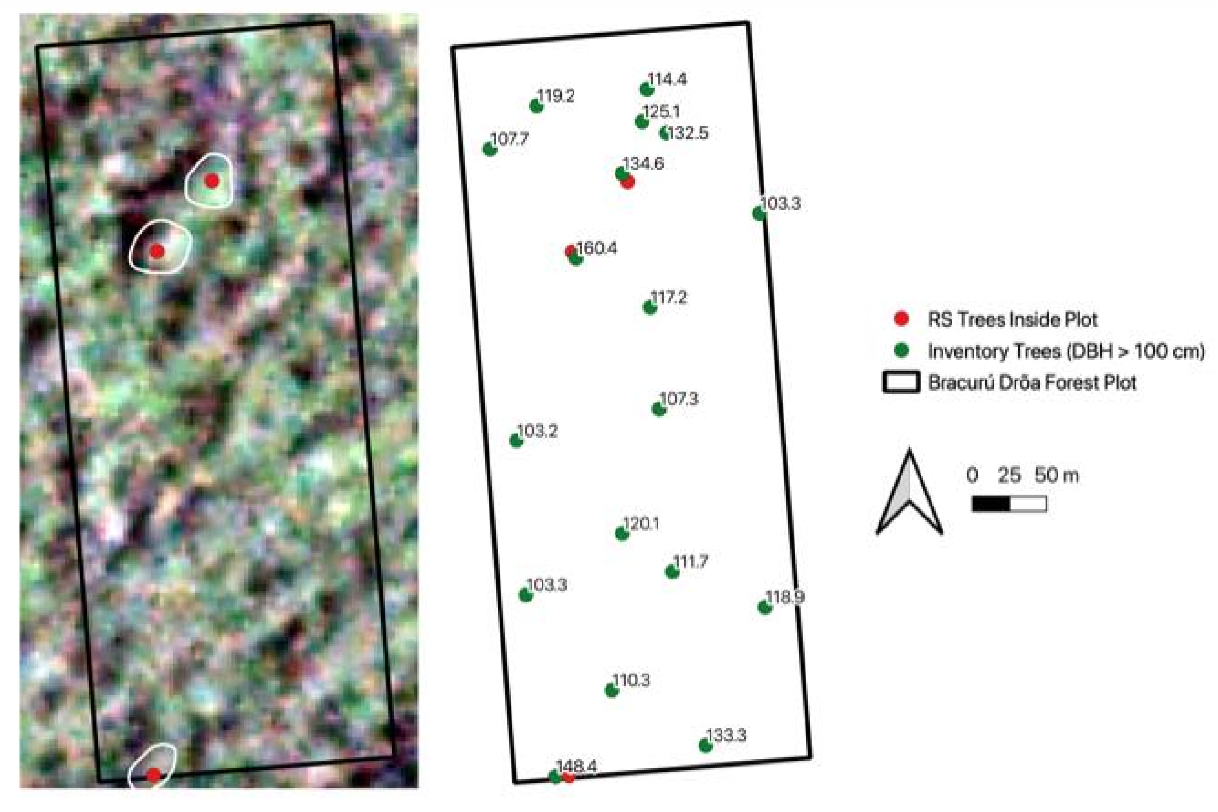

Figure 5: The *Bacurú Drõa* Permanent Plot with the RS trees identified (red dots) using satellite image analysis on the left and the evaluation against ground census data for trees of DBH ≥ 100

cm from inventory data of the *Bacurú Drõa* Permanent Plot with their DBH measurements identified in centimeters on the right. The satellite image on this map comes from PlanetScope 4-Band Scene (10/13/2018).

Landscape giant tree abundance, distribution pattern and carbon stocks

At the landscape level, the 1172 giant trees detected from the remote sensing survey followed a clustered distribution pattern ($X^2 = 119.53$; p-value < 0.05). Of the four quantiles of slope that were evaluated, most RS trees were found in semi-flat and moderate terrain (n = 400 and n = 342, respectively), with fewer trees in flat terrain (n=249) and fewest in steep terrain (n = 181). Overall, the RS analysis suggests an abundance of 0.0583 giant trees (DBH ≥ 100 cm) per hectare within the concave hull (20 100 ha). When correcting for the false-negative detection rate (16.67 %) and true-positive rate (95.45%), we estimate the abundance of giant trees at the landscape level would be around 0.33 giant trees per hectare.

The average carbon density varied among the plot types. Whereas the carbon density for the *Bacurú Drõa* Permanent Plot was 99.5 Mg/ha and 158.1 Mg/ha for the 1-ha Plots, it was 669.5 Mg/ha for the 0.09-ha plots which were selectively located in the “best forests” (i.e., abundant large trees). When considering the total area monitored for all the plots used in this study (19.8 ha), the weighted average carbon density is 175 Mg/ha (Table 2). It is important to note that the carbon density value per ha of the 0.09-ha Plots was extrapolated to the area of one hectare and likely biased towards higher values than the reality because these small plots were located in targeted areas of “best forests” (i.e., abundant large trees). It is unlikely that these pockets of high carbon density found within the 30 x 30m plots extended to the total area of one hectare. Nonetheless, on average, the 0.09-ha Plots had more than half the AGB found in the 1-

ha plot of Mateo-Vega, Arroyo-Mora and Potvin (2019) and found inside the 1-ha subplots of the *Bacurú Drõa* Permanent Plot.

The total area of *Tierras Colectivas del Rio Balsas* represents 127 350 ha, of which 117 637 ha constitutes intact forest, according to Global Forest Watch (Hansen *et al.* 2013). Only 891 ha are considered non-forest land and 8363 ha are regarded as other forest types (Hansen *et al.* 2013). The total area representing the intact forest inside the *Tierras Colectivas del Rio Balsas* under 500 m of elevation was 38 208 ha (Supp. Info. Figure S2). Using the weighted average carbon density value (175.0 Mg/ha), we found a total carbon stock estimate of over 6.6 million tons of carbon for the area of interest. Depending on the different carbon density estimates coming from the inventory sampling datasets, the total carbon stocks can be significantly different, ranging from ~ 25.58 million tons of carbon for the 0.09-ha Plots, ~ 6.04 million tons of carbon for the 1-ha Plots and ~ 3.08 million tons of carbon for the *Bacurú Drõa* Permanent Plot.

Table 2: Average carbon stocks for all the plots inventoried inside Balsa river territory and total carbon stocks following the Stratify and Multiply method for the area covered by intact forests according to Global Forest Watch data (Hansen *et al.* 2013).

Data	**C Density (Mg/ha)**	**Standard Deviation C Density (Mg/ha)**	**Total C stock (Mg/ha)**	**Standard Deviation on C Stock (Mg/ha)**	**Total Area Monitored (ha)**
0.09-ha plots	669.5	409.0	25.58×10^6	15.63×10^6	1.8
1-ha plots	158.1	40.2	6.04×10^6	1.54×10^6	8
Bacurú Drõa Permanent Plot	99.5	23.6	3.80×10^6	0.90×10^6	10
Weighted Average	175.0	65.4	6.69×10^6	2.50×10^6	19.8

Discussion

Abundance and distribution pattern of large trees

Other studies have reported on the density of large trees in tropical forests. Harris *et al.* (2021) reported an abundance of 5.2 to 12.5 very large trees (DBH ≥ 80 cm) per hectare in the Republic of Congo; Clark and Clark (1996) reported 8.9 very large trees (DBH ≥ 70 cm) per hectare in La Selva; Costa Rica, and 10.6 very large trees (DBH ≥ 70 cm) per hectare in the 50-ha plot of Barro Colorado Island, Panama, in the 1995 census. However, Clark and Clark (1996) noted that Panamanian forests are extremely dynamic at large scales and when we looked at the 2010 census, we found that the very large tree (DBH ≥ 70 cm) density per hectare decreased to 7.72. The *Bacurú Drõa* Permanent Plot exhibits a similar abundance with 7.3 very large trees per hectare. On the other hand, we found that the giant tree density of the *Bacurú Drõa* Permanent Plot was lower than the giant tree density of the 50-ha Plot on BCI (1.8/ha vs. 2.44/ha respectively). This result was unexpected, given the previous studies reported that the *Tierras Colectivas del Rio Balsas* was a land of giant trees (Mateo-Vega, Arroyo-Mora & Potvin 2019; Kunz *et al.* 2022).

Moreover, we found that large trees and very large trees of the *Bacurú Drõa* Permanent Plot and giant trees over the landscape were distributed in clusters. The clustered distribution affected the spatial variation of carbon stocks and led to pockets of high carbon density surrounded by areas of lower carbon density. The 0.09-ha Plots located in forested regions described as their “best forests” by the Emberá highlight this finding. The carbon density per hectare inside the 0.09-ha plots was 6.5 times higher than the carbon density found within the *Bacurú Drõa* Permanent Plot and around four times higher than the carbon density found inside

Mateo-Vega, Arroyo-Mora and Potvin (2019) 1-ha Plots. Inversely, the *Bacurú Drõa* Permanent Plot illustrates the opposite of this situation. The plot was located in a region of the landscape with abundant giant trees (Figure 3). However, a zoomed-out visual inspection reveals that the plot falls in between clusters of giant trees (Supp. Info. Figure S4). This finding can explain the lower carbon density inside the *Bacurú Drõa* Permanent Plot compared to the other plots and to the > 130 Mg/ha suggested by Asner *et al.* (2013) airborne LiDAR survey.

At the landscape level, our study focused on: (1) estimating the false-negative detection rate for the RS tree survey and the limits affecting our ability to detect giant trees from satellite imagery and (2) what is the spatial distribution and abundance of giant trees at the landscape level. Our detection rate analysis of the RS trees at the landscape level (20 100 ha) revealed a true-positive detection rate of 90% and a false-negative detection rate of 16.67%. Accounting for both detection rates, the analysis yielded an abundance of giant trees (DBH ≥ 100 cm) of 0.32/ha. This is lower than the giant tree density of 1.8/ha found inside the *Bacurú Drõa* Permanent Plot, suggesting that the remote sensing survey possibly underestimated the abundance of giant trees.

Identifying tree crowns using 2D satellite images relies on our ability to distinguish large tree crowns from the surrounding canopy. While previous studies have successfully used high-resolution (< 10 m) satellite images to identify individual tree crowns and canopy gaps (e.g., Asner *et al.* 2002; Read 2003; Clark *et al.* 2004; Palace *et al.* 2008; Barbier *et al.* 2010), it has also proved to be challenging (Asner *et al.* 2002; Palace *et al.* 2008). The difficulty of manually distinguishing neighboring trees and separating adjacent crowns results in larger-than-reality crown identification (Asner *et al.* 2002). It may also explain why six RS trees were smaller than

100 cm DBH. Moreover, shadows in the images from emergent tree crowns can help identify overstory trees and obscure sections of other large tree crowns, leading to false-negative results (Clark *et al.* 2004). Finally, the 66 ground-truthed RS trees encompassed six species with a strong bias for *Ceiba pentandra* and *Dipteryx oleifera*, representing over 75 % of the individuals. This result suggests for a species bias in identifying giant trees from remote sensing and also suggest that some species may be harder to identify as giant trees than others. Overall, our detection rate analysis of the RS tree survey suggests that we underestimated the number of giant trees inside the *Tierras Colectivas del Rio Balsas*.

Other remote sensing tools such as airborne LiDAR and very high-resolution drone imagery are being used to identify individual tree crowns, canopy gaps or forest AGB (e.g., Popescu, Wynne & Nelson 2003; Getzin, Wiegand & Schöning 2012; Dash *et al.* 2017; Meyer *et al.* 2018; Celes *et al.* 2020). Airborne LiDAR provides 3D data, eliminating shadow problems and providing more accurate measurements that can be used to directly estimate forest AGB from large tree crowns (e.g., Meyer *et al.* 2018). However, airborne LiDAR is considerably more expensive and is more scarce than satellite imagery (Palace *et al.* 2008). On the other hand, very high-resolution drone imagery or drone LiDAR are financially more accessible and can have a quick revisit time compared to airborne LiDAR (Banu, Borlea & Banu 2016). But, despite rapid improvement in drones, flight time and heavy data acquisition significantly limit the total area that can be monitored (Torresan *et al.* 2017). Compared to these technologies, high-resolution satellite images allow studying large trees over large areas at a reasonable cost with a short revisit time.

Large tree distribution pattern's impacts on sampling protocols

We found that different sampling protocols can draw significantly different carbon density estimates in heterogeneous forest landscapes. Perret *et al.* (2022) explain that in the case of aggregated populations, to capture the spatial variability adequately, the sampling plots have to be larger than the clusters' size or the sampling protocol requires multiple sampling plots distributed in a pattern to capture the spatial variability. Initially, to monitor forests, the Food and Agriculture Organization (FAO) recommended reducing fieldwork as much as possible because of its costs and making the greatest possible use of remote sensing data combined with 0.5-ha plots (FAO 1981). However, the accuracy of ≤ 1-ha plots to monitor forest carbon stocks and large trees has been challenged because large tree density may be too low to be captured by a ≤ 1 ha area (Wagner *et al.* 2010; Lutz *et al.* 2012; Lutz 2015; Ali & Wang 2021). This problem is also aggravated when monitoring heterogeneous forest landscapes because small sampling plots will likely miss aggregated populations (Phillips *et al.* 2003; Baraloto *et al.* 2013).

Numerous authors focusing on plot size and sample design have proposed alternative methods to monitor forest carbon stocks accurately. Studies debate the cost and benefits of multiple small plots (e.g., 0.5-ha modified Gentry plots (Baraloto *et al.* 2013) versus large individual plots of 2 ha (Wagner *et al.* 2010) or > 4 ha (Lutz *et al.* 2012). There is no consensus on what is the best sampling protocol yet. Still, studies agree that studying large trees, dynamic processes and heterogenous forest landscapes (i.e., with aggregated populations and/or rare species) requires larger plots (Baraloto *et al.* 2013; Rejou-Mechain *et al.* 2014; Ali & Wang 2021; Perret *et al.* 2022). Moreover, they agree that when studying heterogeneous ecosystems, small (<1 ha) multi-plot methods risk overemphasizing certain habitats across the study area

(Phillips *et al.* 2003; Baraloto *et al.* 2013), while systematic sampling or balance sampling designs will outperform random sampling designs (FAO 1981; McGarvey, Burch & Matthews 2016; Perret *et al.* 2022).

Our understanding of forest ecological phenomenon from sampling plots also depends on the total monitored area (Bellehumeur & Legendre 1998; Lutz 2015). The total monitored area represents the sum of each plot's area that is established within the study area. For example, in this study, it constitutes the sum of the *Bacurú Drõa* Permanent Plot (10 ha), the 0.09-ha Plots (1.8 ha) and the 1-ha Plots (8 ha) for a total area of 19.8 ha. To our knowledge, there is no specific recommendation pertaining to the minimum monitored area required when establishing carbon density value in REDD+ projects. Yet, the total monitored area is an important source of uncertainty in carbon finance programs (Grassi *et al.* 2008). For example, in this study, we monitored a relative total area 15 times larger than the relative total monitored area coming from Panama REDD+ Reference Level of Emission's proposal (MiAmbiente 2018). To estimate Balsas' carbon density value, we exceeded the total monitored area of most carbon finance initiatives. Yet, our weighted average carbon density estimate presents a relative standard deviation of 37%, raising important concerns about the uncertainties around carbon density established from smaller sample sizes.

In addition, contrary to previous studies suggesting that large trees are more abundant on flat low elevation terrain (i.e., elevation lower than 129 m but with no details on "flat" terrain) (Clark *et al.* 2019) but similar to the study of Mascaro *et al.* (2011) on tall trees and carbon stock in BCI, we found that giant trees were more abundant in semi-flat and moderate slope terrains. Shenkin *et al.* (2019) explain that in some conditions, slope and aspect can help provide a sheltered environment to winds and favor the establishment of large trees. But, environmental factors can only partly explain the presence or absence of large trees as local factors such as competition and predation can also influence the distribution of large trees (Lutz *et al.* 2012). Cuni-Sanchez *et al.* (2021) also challenged the idea of large trees decreasing abundance with slope and elevation. They found that large trees were abundant in African Montane Forests, resulting in higher carbon stock values in this ecosystem than the expected default values of the Intergovernmental Panel on Climate Change (IPCC). These results highlight the importance of monitoring all types of terrain to accurately estimate forest carbon stocks (Goetz *et al.* 2015).

Conclusion

In conclusion, our results raise concerns about how to monitor forest carbon stocks accurately. Failing to capture the spatial variation of carbon density from the ground will lead to systematic errors in large-scale carbon stock estimates (Chave *et al.* 2004; Clark & Kellner 2012) and can significantly impact payments from carbon finance programs (Pelletier, Kirby & Potvin 2012). This study highlights the importance of understanding the spatial distribution of forest carbon stocks to have a better understanding of the world's carbon budget (Mascaro *et al.* 2014). We encourage future efforts to guide monitoring protocols on efficient sampling protocols to capture carbon spatial variability and, particularly, to inform on the total monitored area needed to monitor forest carbon stocks accurately when considering forest structure heterogeneity.

References

Ali, A., Lin, S.L., He, J.K., Kong, F.M., Yu, J.H. & Jiang, H.S. (2019) Big-sized trees overrule remaining trees' attributes and species richness as determinants of aboveground biomass in tropical forests. *Global Change Biology,* **25,** 2810-2824.

Ali, A., Sanaei, A., Li, M., Nalivan, O.A., Pour, M.J., Valipour, A., Karami, J., Aminpour, M., Kaboli, H. & Askari, Y. (2020) Big-trees–Energy mechanism underlies forest diversity and aboveground biomass. *Forest Ecology and Management,* **461,** 117968.

Ali, A. & Wang, L.-Q. (2021) Big-sized trees and forest functioning: Current knowledge and future perspectives. *Ecological Indicators,* **127,** 107760.

Allen, C.D., Macalady, A.K., Chenchouni, H., Bachelet, D., McDowell, N., Vennetier, M., Kitzberger, T., Rigling, A., Breshears, D.D., Hogg, E.H., Gonzalez, P., Fensham, R., Zhang, Z., Castro, J., Demidova, N., Lim, J.-H., Allard, G., Running, S.W., Semerci, A. & Cobb, N. (2010) A global overview of drought and heat-induced tree mortality reveals emerging climate change risks for forests. *Forest Ecology and Management,* **259,** 660-684.

Asner, G.P., Mascaro, J., Anderson, C., Knapp, D.E., Martin, R.E., Kennedy-Bowdoin, T., van Breugel, M., Davies, S., Hall, J.S. & Muller-Landau, H.C. (2013) High-fidelity national carbon mapping for resource management and REDD+. *Carbon balance and management,* **8,** 7.

Asner, G.P., Palace, M., Keller, M., Pereira Jr, R., Silva, J.N. & Zweede, J.C. (2002) Estimating canopy structure in an Amazon forest from laser range finder and IKONOS satellite observations 1. *Biotropica,* **34,** 483-492.

Baddeley, A. (2008) Analysing spatial point patterns in R. pp. 199. University of Western Australia.

Baddeley, A. & Turner, R. (2005) Spatstat: an R package for analyzing spatial point patterns. *Journal of statistical software,* **12,** 1-42.

Banu, T.P., Borlea, G.F. & Banu, C. (2016) The use of drones in forestry. *Journal of Environmental Science and Engineering B,* **5,** 557-562.

Baraloto, C., Molto, Q., Rabaud, S., Hérault, B., Valencia, R., Blanc, L., Fine, P.V. & Thompson, J. (2013) Rapid simultaneous estimation of aboveground biomass and tree diversity across Neotropical forests: a comparison of field inventory methods. *Biotropica,* **45,** 288-298.

Barbier, N., Couteron, P., Proisy, C., Malhi, Y. & Gastellu-Etchegorry, J.-P. (2010) The variation of apparent crown size and canopy heterogeneity across lowland Amazonian forests. *Global Ecology and Biogeography,* **19,** 72-84.

Bastin, J.-F., Barbier, N., Réjou-Méchain, M., Fayolle, A., Gourlet-Fleury, S., Maniatis, D., De Haulleville, T., Baya, F., Beeckman, H. & Beina, D. (2015) Seeing Central African forests through their largest trees. *Scientific Reports,* **5,** 1-8.

Bastin, J.F., Rutishauser, E., Kellner, J.R., Saatchi, S., Pélissier, R., Hérault, B., Slik, F., Bogaert, J., De Cannière, C. & Marshall, A.R. (2018) Pan-tropical prediction of forest structure from the largest trees. *Global Ecology and Biogeography,* **27,** 1366-1383.

Bellehumeur, C. & Legendre, P. (1998) Multiscale sources of variation in ecological variables: modeling spatial dispersion, elaborating sampling designs. *Landscape Ecology,* **13,** 15-25.

Bennett, A.C., McDowell, N.G., Allen, C.D. & Anderson-Teixeira, K.J. (2015) Larger trees suffer most during drought in forests worldwide. *Nature plants,* **1,** 1-5.

Bryant, D., Nielsen, D. & Tangley, L. (1997) The Last Frontier Forests: Ecosystems and Economies on the Edge–WRI. *Washington, DC.*

Celes, C., Araujo, R., Broadbent, E.N., Almeyda Zambrano, A. & Muller-Landau, H.C. (2020) High-resolution drone LiDAR reveals ecological drivers of decadal canopy tree crown growth on Barro Colorado Island, Panama. *AGU Fall Meeting Abstracts*, pp. B116-0008.

Chave, J., Condit, R., Aguilar, S., Hernandez, A., Lao, S. & Perez, R. (2004) Error propagation and scaling for tropical forest biomass estimates. *Philosophical Transactions of the Royal Society of London. Series B: Biological Sciences,* **359,** 409-420.

Chave, J., Réjou-Méchain, M., Búrquez, A., Chidumayo, E., Colgan, M.S., Delitti, W.B., Duque, A., Eid, T., Fearnside, P.M. & Goodman, R.C. (2014) Improved allometric models to estimate the aboveground biomass of tropical trees. *Global Change Biology,* **20,** 3177-3190.

Chenost, C., Gardette, Y., Demenois, J., Grondard, N., Perrier, M. & Waemere, M. (2010) Les marchés du carbone forestier. *UNEP, ONFI, AFD, BioCF.*

Clark, D.B. & Clark, D.A. (1996) Abundance, growth and mortality of very large trees in neotropical lowland rain forest. *Forest Ecology and Management,* **80,** 235-244.

Clark, D.B., Ferraz, A., Clark, D.A., Kellner, J.R., Letcher, S.G. & Saatchi, S. (2019) Diversity, distribution and dynamics of large trees across an old-growth lowland tropical rain forest landscape. *PloS one,* **14,** e0224896.

Clark, D.B. & Kellner, J.R. (2012) Tropical forest biomass estimation and the fallacy of misplaced concreteness. *Journal of Vegetation Science,* **23,** 1191-1196.

Clark, D.B., Read, J.M., Clark, M.L., Cruz, A.M., Dotti, M.F. & Clark, D.A. (2004) Application of 1-M and 4-M resolution satellite data to ecological studies of tropical rain forests. *Ecological Applications,* **14,** 61-74.

Condit, R. (1998) *Tropical forest census plots: methods and results from Barro Colorado Island, Panama and a comparison with other plots*. Springer Science & Business Media.

Cuni-Sanchez, A., Sullivan, M.J., Platts, P.J., Lewis, S.L., Marchant, R., Imani, G., Hubau, W., Abiem, I., Adhikari, H. & Albrecht, T. (2021) High aboveground carbon stock of African tropical montane forests. *Nature,* **596,** 536-542.

Dash, J.P., Watt, M.S., Pearse, G.D., Heaphy, M. & Dungey, H.S. (2017) Assessing very high resolution UAV imagery for monitoring forest health during a simulated disease outbreak. *ISPRS Journal of Photogrammetry and Remote Sensing,* **131,** 1-14.

Davis, S., Heywood, V. & Hamilton, A. (1997) World Wide Fund for Nature; International Union for Conservation of Nature and Natural Resources (Eds.) Centres of Plant Diversity: A Guide and Strategy for Their Conservation; World Wide Fund for Nature (WWF) and ICUN-World Conservation Union: Cambridge, UK, 1994. *Google Scholar*.

de Lima, R.B., Görgens, E.B., Batista, A.P.B., da Silva, D.A.S., de Oliveira, C.P. & de Sousa, C.S.C. (2022) Diversity and Big Tree Patterns in the Brazilian Amazon. *Diversity,* **14,** 503.

Dean, W., Milton, S. & Jeltsch, F. (1999) Large trees, fertile islands, and birds in arid savanna. *Journal of Arid Environments,* **41,** 61-78.

Elias, M. & Potvin, C. (2003) Assessing inter-and intra-specific variation in trunk carbon concentration for 32 neotropical tree species. *Canadian Journal of Forest Research,* **33,** 1039-1045.

FAO (1981) *Manual of Forest Inventory: With Special Reference to Mixed Tropical Forests*.

Getzin, S., Wiegand, K. & Schöning, I. (2012) Assessing biodiversity in forests using very high-resolution images and unmanned aerial vehicles. *Methods in Ecology and Evolution,* **3,** 397-404.

Goetz, S.J., Hansen, M., Houghton, R.A., Walker, W., Laporte, N. & Busch, J. (2015) Measurement and monitoring needs, capabilities and potential for addressing reduced emissions from deforestation and forest degradation under REDD+. *Environmental Research Letters,* **10,** 123001.

Gonzalez de Tanago, J., Lau, A., Bartholomeus, H., Herold, M., Avitabile, V., Raumonen, P., Martius, C., Goodman, R.C., Disney, M. & Manuri, S. (2018) Estimation of above-ground biomass of large tropical trees with terrestrial LiDAR. *Methods in Ecology and Evolution,* **9,** 223-234.

Goodman, R.C., Phillips, O.L. & Baker, T.R. (2014) The importance of crown dimensions to improve tropical tree biomass estimates. *Ecological Applications,* **24,** 680-698.

Gora, E.M. & Esquivel-Muelbert, A. (2021) Implications of size-dependent tree mortality for tropical forest carbon dynamics. *Nature plants,* **7,** 384-391.

Grassi, G., Monni, S., Federici, S., Achard, F. & Mollicone, D. (2008) Applying the conservativeness principle to REDD to deal with the uncertainties of the estimates. *Environmental Research Letters,* **3,** 035005.

Hansen, M.C., Potapov, P.V., Moore, R., Hancher, M., Turubanova, S.A., Tyukavina, A., Thau, D., Stehman, S.V., Goetz, S.J. & Loveland, T.R. (2013) High-resolution global maps of 21st-century forest cover change. *Science,* **342,** 850-853.

Harris, D.J., Ndolo Ebika, S.T., Sanz, C.M., Madingou, M.P. & Morgan, D.B. (2021) Large trees in tropical rain forests require big plots. *Plants, People, Planet,* **3,** 282-294.

Keeton, W.S. & Franklin, J.F. (2005) Do remnant old-growth trees accelerate rates of succession in mature Douglas-fir forests? *Ecological Monographs,* **75,** 103-118.

Kunz, M., Barrios, H.E., Dan, M., Dogirama, I., Gennaretti, F., Mathieu, G., Koller, A., Madsen, C., Lana, G. & Ortega, A. (2022) Bacurú Drõa: Indigenous Forest Custody as an Effective Climate Change Mitigation Option. A case study from Darién, Panama. *Frontiers in Climate***,** 231.

Lindenmayer, D., Messier, C. & Sato, C. (2016) Avoiding ecosystem collapse in managed forest ecosystems. *Frontiers in Ecology and the Environment,* **14,** 561-568.

Lindenmayer, D.B. & Laurance, W.F. (2017) The ecology, distribution, conservation and management of large old trees. *Biological Reviews,* **92,** 1434-1458.

Lindenmayer, D.B., Laurance, W.F. & Franklin, J.F. (2012) Global decline in large old trees. *Science,* **338,** 1305-1306.

Lutz, J.A. (2015) The evolution of long-term data for forestry: large temperate research plots in an era of global change. *Northwest Science,* **89,** 255-269.

Lutz, J.A., Furniss, T.J., Johnson, D.J., Davies, S.J., Allen, D., Alonso, A., Anderson-Teixeira, K.J., Andrade, A., Baltzer, J. & Becker, K.M. (2018) Global importance of large-diameter trees. *Global Ecology and Biogeography,* **27,** 849-864.

Lutz, J.A., Larson, A.J., Freund, J.A., Swanson, M.E. & Bible, K.J. (2013) The importance of large-diameter trees to forest structural heterogeneity. *PloS one,* **8,** e82784.

Lutz, J.A., Larson, A.J., Swanson, M.E. & Freund, J.A. (2012) Ecological importance of large-diameter trees in a temperate mixed-conifer forest. *PloS one,* **7,** e36131.

Mascaro, J., Asner, G.P., Knapp, D.E., Kennedy-Bowdoin, T., Martin, R.E., Anderson, C., Higgins, M. & Chadwick, K.D. (2014) A tale of two "forests": Random Forest machine learning aids tropical forest carbon mapping. *PloS one,* **9,** e85993.

Mascaro, J., Asner, G.P., Muller-Landau, H.C., van Breugel, M., Hall, J. & Dahlin, K. (2011) Controls over aboveground forest carbon density on Barro Colorado Island, Panama. *Biogeosciences,* **8,** 1615-1629.

Mateo-Vega, J., Arroyo-Mora, J.P. & Potvin, C. (2019) Tree aboveground biomass and species richness of the mature tropical forests of Darien, Panama, and their role in global climate change mitigation and biodiversity conservation. *Conservation Science and Practice,* **1,** e42.

Mateo-Vega, J., Potvin, C., Monteza, J., Bacorizo, J., Barrigón, J., Barrigón, R., López, N., Omi, L., Opua, M. & Serrano, J. (2017) Full and effective participation of indigenous peoples in forest monitoring for reducing emissions from deforestation and forest degradation (REDD+): trial in Panama's Darién. *Ecosphere,* **8,** e01635.

McGarvey, R., Burch, P. & Matthews, J.M. (2016) Precision of systematic and random sampling in clustered populations: habitat patches and aggregating organisms. *Ecological Applications,* **26,** 233-248.

Meakem, V., Tepley, A.J., Gonzalez-Akre, E.B., Herrmann, V., Muller-Landau, H.C., Wright, S.J., Hubbell, S.P., Condit, R. & Anderson-Teixeira, K.J. (2018) Role of tree size in moist tropical forest carbon cycling and water deficit responses. *New Phytologist,* **219,** 947-958.

Meyer, V., Saatchi, S., Clarck, D., Keller, M., Vicent, G., Ferraz, A., Espírito-Santo, F., Oliveira, M.d., Kaki, D. & Chave, J. (2018) Canopy area of large trees explains aboveground biomass variations across neotropical forest landscapes. *Embrapa Acre-Artigo em periódico indexado (ALICE).*

MiAmbiente (2018) Nivel de Referencia de Emisiones Forestales de Panamá. pp. 95.

Mitchard, E.T., Saatchi, S.S., Baccini, A., Asner, G.P., Goetz, S.J., Harris, N.L. & Brown, S. (2013) Uncertainty in the spatial distribution of tropical forest biomass: a comparison of pan-tropical maps. *Carbon balance and management,* **8,** 1-13.

Palace, M., Keller, M., Asner, G.P., Hagen, S. & Braswell, B. (2008) Amazon forest structure from IKONOS satellite data and the automated characterization of forest canopy properties. *Biotropica,* **40,** 141-150.

Pelletier, J., Kirby, K.R. & Potvin, C. (2012) Significance of carbon stock uncertainties on emission reductions from deforestation and forest degradation in developing countries. *Forest Policy and Economics,* **24,** 3-11.

Perret, J., Charpentier, A., Pradel, R., Papuga, G. & Besnard, A. (2022) Spatially balanced sampling methods are always more precise than random ones for estimating the size of aggregated populations. *Methods in Ecology and Evolution,* **13,** 2743-2756.

Phillips, O.L., Martínez, R.V., Vargas, P.N., Monteagudo, A.L., Zans, M.-E.C., Sánchez, W.G., Cruz, A.P., Timaná, M., Yli-Halla, M. & Rose, S. (2003) Efficient plot-based floristic assessment of tropical forests. *Journal of tropical ecology,* **19,** 629-645.

Piponiot, C., Anderson-Teixeira, K.J., Davies, S.J., Allen, D., Bourg, N.A., Burslem, D.F., Cárdenas, D., Chang-Yang, C.H., Chuyong, G. & Cordell, S. (2022) Distribution of biomass dynamics in relation to tree size in forests across the world. *New Phytologist,* **234,** 1664-1677.

Popescu, S.C., Wynne, R.H. & Nelson, R.F. (2003) Measuring individual tree crown diameter with lidar and assessing its influence on estimating forest volume and biomass. *Canadian journal of remote sensing,* **29,** 564-577.

Potapov, P., Hansen, M.C., Laestadius, L., Turubanova, S., Yaroshenko, A., Thies, C., Smith, W., Zhuravleva, I., Komarova, A. & Minnemeyer, S. (2017) The last frontiers of wilderness: Tracking loss of intact forest landscapes from 2000 to 2013. *Science advances,* **3,** e1600821.

Potapov, P., Yaroshenko, A., Turubanova, S., Dubinin, M., Laestadius, L., Thies, C., Aksenov, D., Egorov, A., Yesipova, Y. & Glushkov, I. (2008) Mapping the world's intact forest landscapes by remote sensing. *Ecology and Society,* **13.**

R Development Core Team (2022) R: A language and environment for statistical computing. R Foundation for Statistical Computing, Vienna, Austria.

Read, J.M. (2003) Spatial analyses of logging impacts in Amazonia using remotely sensed data. *Photogrammetric Engineering & Remote Sensing,* **69,** 275-282.

Rejou-Mechain, M., Muller-Landau, H.C., Detto, M., Thomas, S.C., Toan, T.L., Saatchi, S.S., Barreto-Silvia, J., Bourg, N.A., Bunyavejchewin, S. & Butt, N. (2014) Local spatial structure of forest biomass and its consequences for remote sensing of carbon stocks. *Biogeosciences Discussions,* **11,** 5711.

Réjou-Méchain, M., Tanguy, A., Piponiot, C., Chave, J. & Hérault, B. (2017) biomass: an r package for estimating above-ground biomass and its uncertainty in tropical forests. *Methods in Ecology and Evolution,* **8,** 1163-1167.

Shenkin, A., Chandler, C.J., Boyd, D.S., Jackson, T., Disney, M., Majalap, N., Nilus, R., Foody, G., bin Jami, J. & Reynolds, G. (2019) The world's tallest tropical tree in three dimensions. *Frontiers in Forests and Global Change,* **2,** 32.

Slik, J.F., Paoli, G., McGuire, K., Amaral, I., Barroso, J., Bastian, M., Blanc, L., Bongers, F., Boundja, P. & Clark, C. (2013) Large trees drive forest aboveground biomass variation in moist lowland forests across the tropics. *Global Ecology and Biogeography,* **22,** 1261-1271.

Torresan, C., Berton, A., Carotenuto, F., Di Gennaro, S.F., Gioli, B., Matese, A., Miglietta, F., Vagnoli, C., Zaldei, A. & Wallace, L. (2017) Forestry applications of UAVs in Europe: A review. *International Journal of Remote Sensing,* **38,** 2427-2447.

Wagner, F., Rutishauser, E., Blanc, L. & Herault, B. (2010) Effects of plot size and census interval on descriptors of forest structure and dynamics. *Biotropica,* **42,** 664-671.

Zanne, A.E., Lopez-Gonzalez, G., Coomes, D.A., Ilic, J., Jansen, S., Lewis, S.L., Miller, R.B., Swenson, N.G., Wiemann, M.C. & Chave, J. (2009) Global wood density database.

Supplementary Information

ForestGEO forest plot design

The ForestGEO program or Center for Tropical Forest Studies (CTFS), in Panama, has established numerous forest plots over the year including the notorious 50-ha plot found on Barro Colorado Island (BCI) (Condit 1998). ForestGEO has a pre-established surveying method to establish new forest plots and ensure data standardization. Forest plots are oriented south to north in subplots of 20 x 20m with each 10 m marked on the ground with PVC tubes. This method ensures an accurate tree mapping of all monitored trees and helps to reorient oneself and find the trees marked during the next census.

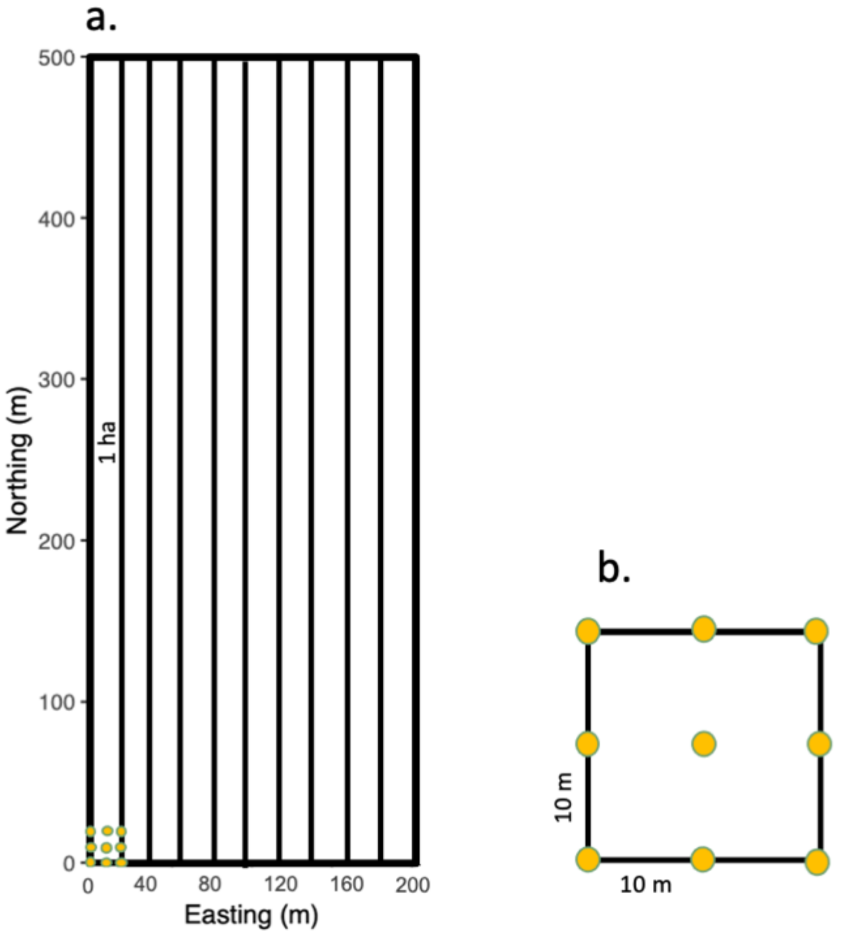

Figure S1 : ForestGEO forest plot design. Panel a shows the 10 ha *Bacurú Drõa* Permanent Plot with each subplot of 1 ha. Panel b shows a zoom-in on the 20 x 20 m squares surveyed on the ground and marked with PVC tubes to move north until completing a 1-ha-subplot.

Poisson distribution point pattern

Trees were considered as discrete entities represented in a point pattern in a two-dimensional space. Basic random point pattern distribution follows a Poisson distribution where the number of points falling in a given area (A) follows a Poisson's probability based on the intensity parameters (λ), which represents the point density (Caillaud *et al.* 2010) (Equation S1). Point patterns can be analyzed by comparing the intensity in the point patterns to a Poisson distribution where the intensity is constant and points independent and randomly distributed (Baddeley 2008). The alternative suggests that points are dependent and will follow a low-intensity pattern where points group with each other (clustered point pattern) or a high-intensity pattern where points avoid each other (regular point pattern).

Equation S1 : Homogeneous point density equation where intensity units are a number of points per area.

$$\lambda = \frac{n\ (x)}{A}$$

The area of interest within the *Tierras Colectivas del Rio Balsas*

We used Java Script 5 m contour lines for Panama to calculate the area of interest to extrapolate our carbon density value to total carbon stock estimates. The area of interest constitutes the area of elevation lower than 500 m and of intact forests found inside the *Tierras Colectivas del Rio Balsas*. We found that the total area of < 500 m inside the territory was equal to 47 461 ha (Figure S2). Moreover, according to Global Forest Watch (GFW), the *Tierras Colectivas del Rio Balsas'* total area of Intact Forests is equal to 117 636 ha, Other Forest Cover is equaled to 8363 ha and Other Land is equaled to 861 ha (Hansen *et al.* 2013). Using this data, we calculated that the intact forest cover within the area of and of elevation < 500 m (i.e., 47 461 ha) was equaled to 38 208 ha. Therefore, we used the value of 38 208 ha to estimate the total carbon stock of the *Tierras Colectivas del Rio Balsas*.

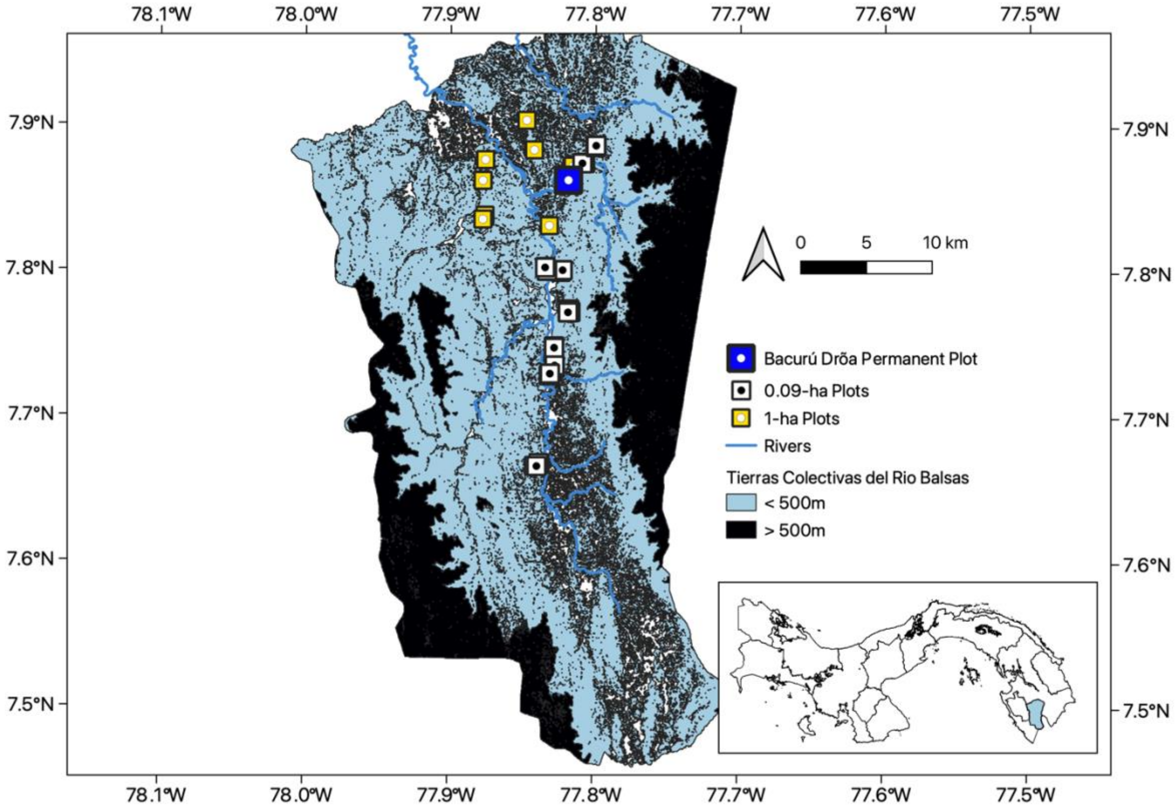

Figure S2: Map of the *Tierras Colectivas del Rio Balsas* categorized by the area above 500 m (black) and below 500 m (blue) and with the location of the inventory data plots.

Large tree density analysis

We performed a kernel density analysis to get a spatial impression of the density of the large trees inside the *Bacurú Drõa* Permanent Plot. The results show that the southwest portion of the plot has the highest density of large trees with clusters in the north-central part, south-central part and south-eastern part of the plot.

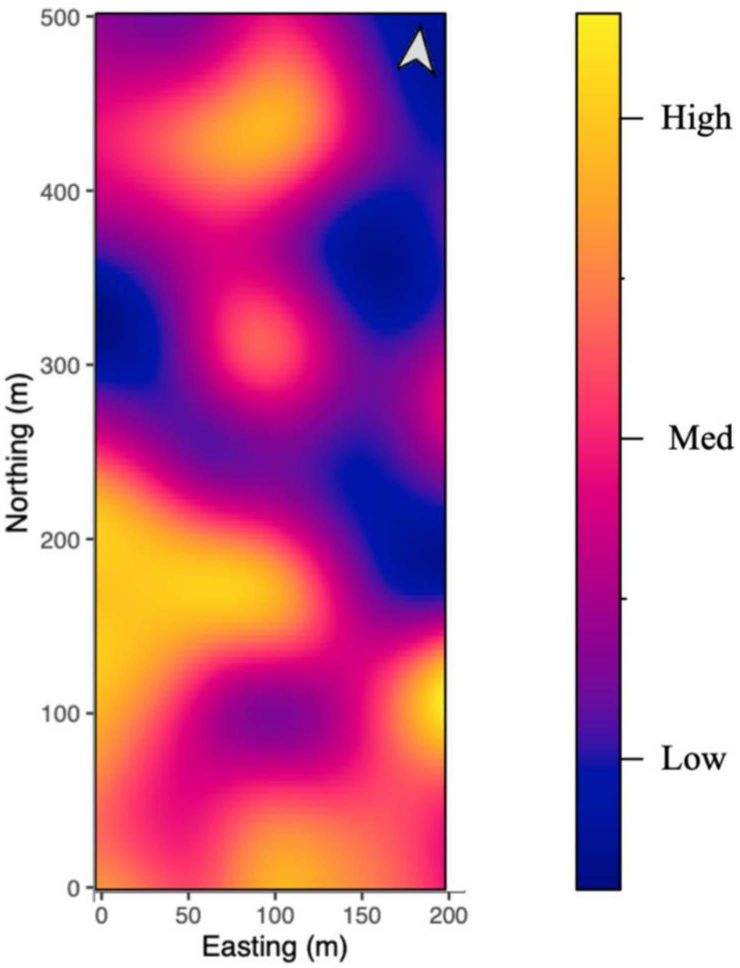

Figure S3: Kernel density plot of the large tree community of the *Bacurú Drõa* Permanent plot. Warm colors represent a higher density of large trees and cold colors represent a lower density.

The *Bacurú Drõa* Permanent Plot between clusters of RS trees

We performed a Kernel Density interpolation using the RS trees to illustrate the clusters of large trees at the landscape level. The Kernel density interpolation was performed in QGIS, setting the radius parameters at 300 m and the X and Y pixel value at 25 m. The *Bacurú Drõa* Permanent Plot was located between clusters of RS trees. It contained only 3 giant trees detected from the RS tree survey. However, if the plot would have been established 200 m west, it could have contained up to 8 RS trees (Supp. Info. Figure S5). Conserving the same true-positive detection rate of 90% and a false-negative detection rate of 16.67%, this scenario would have led the *Bacurú Drõa* Permanent Plot "true" giant tree community to 43 instead of 8. On the contrary, if the plot was moved further west, it could have contained 0 RS, leading to a "true" giant tree community of 0.

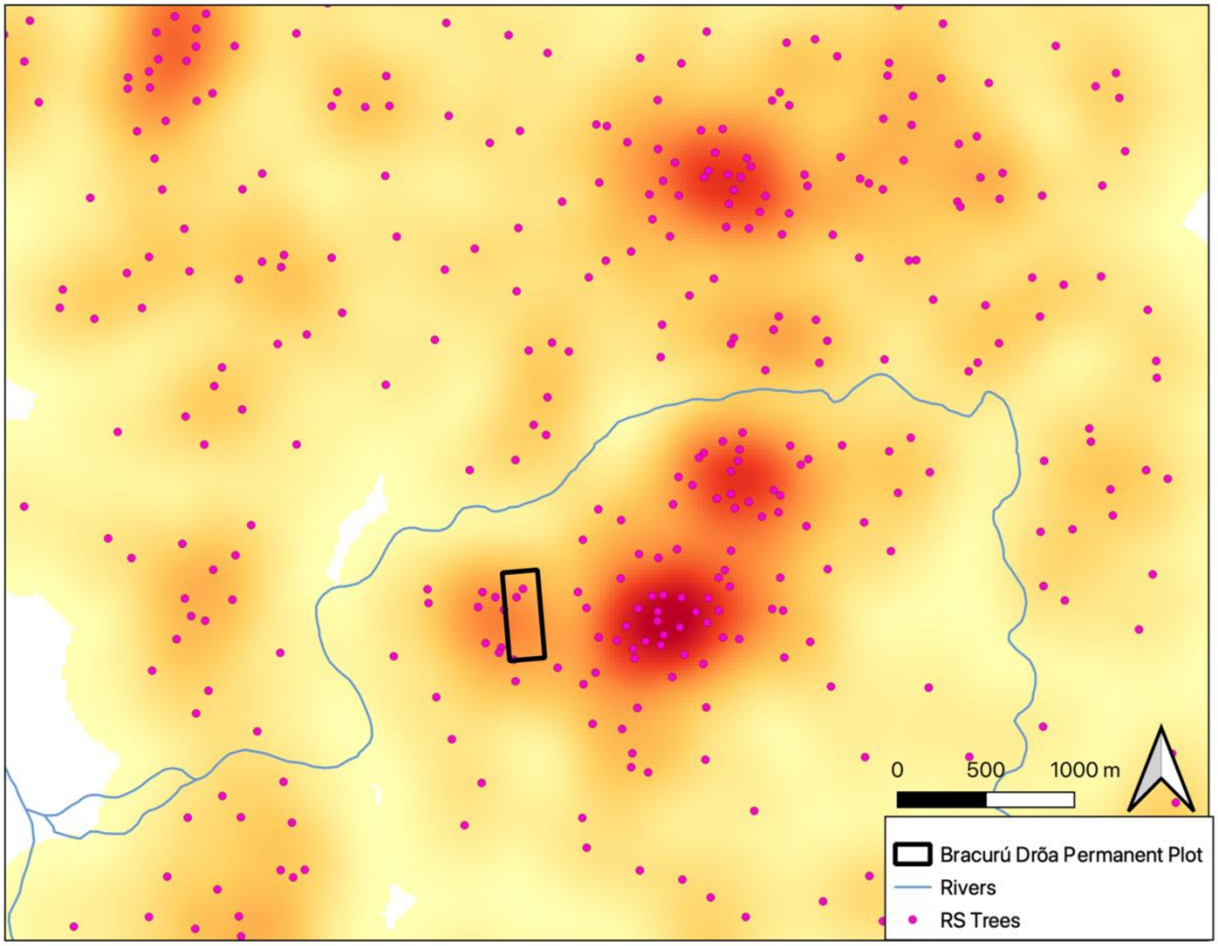

Figure S4: The *Bacurú Drõa* Permanent Plot location between clusters of giant trees presented using a Kernel Density interpolation using the RS trees.

Research limits

Our research did not employ automated tree crown detection algorithms (e.g., Palace *et al.* 2008) to identify RS trees, making it difficult to ensure that sampling efforts were consistent across the area of interest. Kunz *et al.* (2022) did not monitor the detection time of RS trees, even if they had, it would still be challenging to confirm that the effort was equivalent since human eyes become better at locating large crowns. Therefore, monitoring the time spent on each subregion, for instance, would not translate into equal sampling efforts. To address this limitation, we recommend that future studies use automated detection algorithms to identify giant tree crowns in the *Tierras Colectivas del Rio Balsas* and compare the results with the RS tree survey.

Supplementary References

Baddeley, A. (2008) Analysing spatial point patterns in R. pp. 199. University of Western Australia.

Caillaud, D., Crofoot, M.C., Scarpino, S.V., Jansen, P.A., Garzon-Lopez, C.X., Winkelhagen, A.J., Bohlman, S.A. & Walsh, P.D. (2010) Modeling the spatial distribution and fruiting pattern of a key tree species in a neotropical forest: methodology and potential applications. *PloS one,* **5,** e15002.

Condit, R. (1998) *Tropical forest census plots: methods and results from Barro Colorado Island, Panama and a comparison with other plots*. Springer Science & Business Media.

Hansen, M.C., Potapov, P.V., Moore, R., Hancher, M., Turubanova, S.A., Tyukavina, A., Thau, D., Stehman, S.V., Goetz, S.J. & Loveland, T.R. (2013) High-resolution global maps of 21st-century forest cover change. *Science,* **342,** 850-853.

Kunz, M., Barrios, H.E., Dan, M., Dogirama, I., Gennaretti, F., Mathieu, G., Koller, A., Madsen, C., Lana, G. & Ortega, A. (2022) Bacurú Drõa: Indigenous Forest Custody as an Effective Climate Change Mitigation Option. A case study from Darién, Panama. *Frontiers in Climate*, 231.

Palace, M., Keller, M., Asner, G.P., Hagen, S. & Braswell, B. (2008) Amazon forest structure from IKONOS satellite data and the automated characterization of forest canopy properties. *Biotropica,* **40,** 141-150.

General Discussion and Conclusion

My Master's thesis advances our understanding of intact tropical forests role as natural climate solutions (NCS) by improving how to estimate accurately large tropical trees' aboveground biomass (AGB). The first chapter highlights the challenges that allometric equations and Quantitative Structure Models (QSM) face in estimating large tropical trees' AGB. To answer this problem, I developed the Compartmentalized Model, which uses digital point clouds of terrestrial laser scans (TLS) to provide accurate AGB estimates of all large tropical trees within forest plots. This was an important milestone for tailored AGB estimation methods using TLS technology because plot-level AGB estimates can be scaled up to the landscape and QSM or other tailored AGB estimation using TLS have never produced plot-level AGB estimates before. Moreover, using the Compartmentalized Model, I highlighted the important contribution of large tree crowns and first-order branches to the overall tree AGB. Because of this finding, I suggested that to obtain accurate AGB estimates, large tropical trees require tailored AGB estimation methods that capture individual tree crown variability.

The second chapter presents the distribution pattern and abundance of large, very large, and giant trees in the *Tierras Colectivas del Rio Balsas*. This chapter is, to my knowledge, the second study after de Lima *et al.* (2022), who worked in the Amazonian forest, to present large tropical tree distribution patterns in neotropical forests. In addition, this chapter discusses the impact of large tree clustering on the spatial distribution of forest carbon stocks by providing different carbon density values from different sampling protocols. Following these findings, I suggested that forest monitoring activities should consider forest structure heterogeneity before selecting a sampling protocol to adequately capture forest carbon stock spatial distribution and estimate accurately intact forests' carbon stocks.

Both of my chapters answer important questions regarding problems for accurately estimating intact tropical forests' carbon stocks. I also make recommendation for forest monitoring programs and fulfilled my objective to advance our understanding of the role of intact tropical forests as NCS. However, forests contain significant carbon stocks when they are old and also remove CO_2 from the atmosphere (Phillips & Brienen 2017). Therefore, fully comprehending the role of intact tropical forests as NCS requires understanding forest carbon fluxes within these forests. Traditionally, intact forests have been considered a negligible active carbon sink because CO_2 emissions from mortality and damages were thought to offset the carbon capture of trees' photosynthesis (Odum 1969). Recent studies have challenged this idea and suggested that intact forests can also be active carbon sinks (Zhou *et al.* 2006; Luyssaert *et al.* 2008; Phillips & Brienen 2017).

During one of the expeditions in the *Tierras Colectivas del Rio Balsas*, Kunz *et al.* (2022) found a fallen giant *Ceiba pentandra*. It provided the unique opportunity to measure its height directly and without the traditional vertical height measurement error factors since it laid horizontally across the river. Moreover, the research team took advantage of its position to collect a slice of the trunk to learn from its life history via growth ring analysis. The *C. pentandra*'s measured DBH was 270 cm and height was 71 m. At an age of approximately 204 years-old, according to its carbon-14 dating, it constitutes one of the largest trees measured in the *Tierras Colectivas del Rio Balsas* (Kunz *et al.* 2022).

In tropical forests, studying growth rings can be challenging because not all species are deciduous (Boninsegna *et al.* 1989) and for those that are (e.g., *C. pentandra*), accurately discerning growth rings can be difficult (Worbes 1995). Nonetheless, the growth ring analysis of the *C. pentandra* revealed that this tree continually grew each year at an average rate of 5.49 mm per year for the last 95 years (SD = 4.43 mm) (Figure 1). When transforming to carbon content using Chave *et al.* (2014) pantropical equation and Elias and Potvin (2003) 0.461 expansion factor ratio, the fallen *C. pentandra* grew steadily at an average rate of 0.152 tons of carbon per year (SD = 0.0024 Mg C/yr). At this rate, the *C. pentandra* doubled its carbon weight in 95 years.

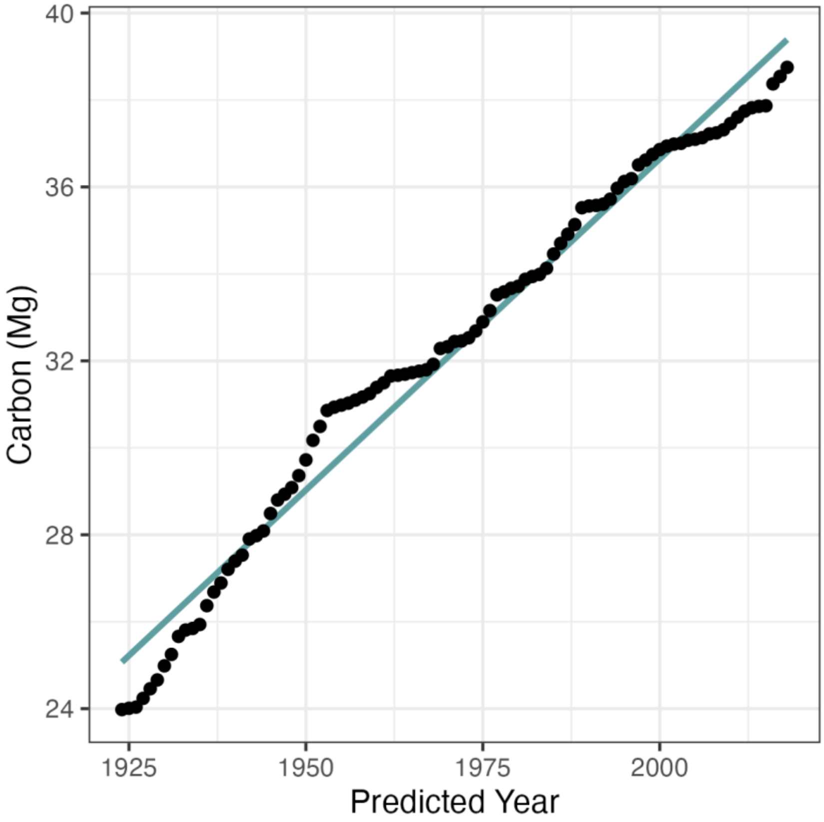

Figure 1: The fallen *Ceiba pentandra* yearly carbon uptake according to its growth ring analysis.

This result suggests, like others have (e.g., Sillett *et al.* 2010; Stephenson *et al.* 2014; Sillett *et al.* 2015), that large trees are sequestering an important amount of carbon despite their age and their size. However, answering if the entire intact forest of the *Tierras Colectivas del Rio Balsas* is an active carbon sink will require more data than just one tree. The balance of tree growth and recruitment vs. tree mortality and damages predicts if, as a whole, the aboveground portion of a standing forest is an active sink or source of carbon (Ligot *et al.* 2018; Yuan *et al.* 2019; Gora & Esquivel-Muelbert 2021). The *C. pentandra* suggests that the yearly carbon uptake of large and old trees can be significant. However, carbon losses from large tree death represent a massive carbon loss compared to the yearly gain (38.7 Mg lost vs. 0.125 Mg gained per year for the *C. pentandra*). Yet, large trees are generally old, stocking carbon for extended periods (Ali & Wang 2021) and large tree mortality rates are low compared to mortality rates of small trees (Thomas *et al.* 2013; Clark *et al.* 2019). Whether intact forests are active carbon sinks or sources is still debated today (Sheil *et al.* 2017).

The *Bacurú Drõa* project aims to establish a community-driven observatory of intact tropical forests to empower local communities and to advance knowledge on intact tropical forests through the data collected in the *Bacurú Drõa* Permanent Plot. However, answering dynamic processes such as forest carbon fluxes requires long-term data acquisition (Phillips & Brienen 2017) and will depend on the long-term viability of the *Bacurú Drõa* project to collect future census in the permanent plot.

My Master's thesis happened during the Covid-19 pandemic and the restriction on international travel. This unprecedented situation highlighted the importance of developing the autonomy of the local Emberá communities to conduct research to ensure the long-term sustainability of the *Bacurú Drõa* project. Historically, indigenous communities are disadvantaged regarding access to digital information and technologies (Samaras 2005) and the Covid-19 pandemic underlined this reality (Aissaoui 2022). The restrictions on international travel combined with this "digital divide" limited our ability to communicate with the technicians in Balsas. Moreover, non-user-friendly technologies such as high-end TLS complicated the autonomy of the Emberá technicians to collect data. I quickly realized that the digital divide jeopardized the project's long-term objectives. In fact, addressing the digital divide creates opportunities to develop a common language between stakeholders, to include traditional environmental knowledge, to decolonize datasets and to empower local communities (Brodnig & Mayer-Schönberger 2000; McMahon, LaHache & Whiteduck 2015; Toth, Smith & Giroux 2018). Following the Covid-19 pandemic, addressing the digital divide became one of the *Bacurú Drõa* project's objectives.

Currently, members of the project are training Emberá technicians on digital literacy and data processing on computers as well as terrestrial laser scanning with "user-friendly" iPad applications. I hope that my Master's thesis will inspire local Emberá youth and future graduate students to continue advancing our understanding of intact tropical forests and leading the way in indigenous participatory research. I wish the best to *the Bacurú Drõa* project and to the Emberá communities of the *Tierras Colectivas del Rio Balsas*.

Master’s Reference List

Aissaoui, N. (2022) The digital divide: a literature review and some directions for future research in light of COVID-19. *Global Knowledge, Memory and Communication,* **71,** 686-708.

Ali, A., Lin, S.L., He, J.K., Kong, F.M., Yu, J.H. & Jiang, H.S. (2019) Big-sized trees overrule remaining trees' attributes and species richness as determinants of aboveground biomass in tropical forests. *Global Change Biology,* **25,** 2810-2824.

Ali, A. & Wang, L.-Q. (2021) Big-sized trees and forest functioning: Current knowledge and future perspectives. *Ecological Indicators,* **127,** 107760.

Allan, J., Bansard, J., Jones, N., Luomi, M., Tan, J.M. & Sun, Y. (2021) Glasgow Climate Change Conference: 31 October–13 November 2021.

Atwoli, L., Erhabor, G.E., Gbakima, A.A., Haileamlak, A., Ntumba, J.-M.K., Kigera, J., Laybourn-Langton, L., Mash, R., Muhia, J. & Mulaudzi, F.M. (2022) COP27 Climate Change Conference: urgent action needed for Africa and the world. *The Lancet Oncology,* **23,** 1486-1488.

Baraloto, C., Molto, Q., Rabaud, S., Hérault, B., Valencia, R., Blanc, L., Fine, P.V. & Thompson, J. (2013) Rapid simultaneous estimation of aboveground biomass and tree diversity across Neotropical forests: a comparison of field inventory methods. *Biotropica,* **45,** 288-298.

Bastin, J.-F., Barbier, N., Couteron, P., Adams, B., Shapiro, A., Bogaert, J. & De Cannière, C. (2014) Aboveground biomass mapping of African forest mosaics using canopy texture analysis: toward a regional approach. *Ecological Applications,* **24,** 1984-2001.

Bastin, J.F., Rutishauser, E., Kellner, J.R., Saatchi, S., Pélissier, R., Hérault, B., Slik, F., Bogaert, J., De Cannière, C. & Marshall, A.R. (2018) Pan-tropical prediction of forest structure from the largest trees. *Global Ecology and Biogeography,* **27,** 1366-1383.

Berkes, F. & Davidson-Hunt, I.J. (2006) Biodiversity, traditional management systems, and cultural landscapes: examples from the boreal forest of Canada. *International Social Science Journal,* **58,** 35-47.

Boninsegna, J., Villalba, R., Amarilla, L. & Ocampo, J. (1989) Studies on tree rings, growth rates and age-size relationships of tropical tree species in Misiones, Argentina. *IAWA Journal,* **10,** 161-169.

Brodnig, G. & Mayer-Schönberger, V. (2000) Bridging the gap: the role of spatial information technologies in the integration of traditional environmental knowledge and western science. *The Electronic Journal of Information Systems in Developing Countries,* **1,** 1-15.

Chave, J., Réjou-Méchain, M., Búrquez, A., Chidumayo, E., Colgan, M.S., Delitti, W.B., Duque, A., Eid, T., Fearnside, P.M. & Goodman, R.C. (2014) Improved allometric models to estimate the aboveground biomass of tropical trees. *Global Change Biology,* **20,** 3177-3190.

Clark, D.B., Ferraz, A., Clark, D.A., Kellner, J.R., Letcher, S.G. & Saatchi, S. (2019) Diversity, distribution and dynamics of large trees across an old-growth lowland tropical rain forest landscape. *PloS one,* **14,** e0224896.

de Lima, R.B., Görgens, E.B., Batista, A.P.B., da Silva, D.A.S., de Oliveira, C.P. & de Sousa, C.S.C. (2022) Diversity and Big Tree Patterns in the Brazilian Amazon. *Diversity,* **14,** 503.

Dooley K., Keith H., Larson A., Catacora-Vargas G., Carton W., Christiansen K.L., Enokenwa Baa O., Frechette A., Hugh S., Ivetic N., Lim L.C., Lund J.F., Luqman M., Mackey B., Monterroso I., Ojha H., Perfecto I., Riamit K., Robiou du Pont Y. & V., Y. (2022) The Land Gap Report.

Drever, C.R., Cook-Patton, S.C., Akhter, F., Badiou, P.H., Chmura, G.L., Davidson, S.J., Desjardins, R.L., Dyk, A., Fargione, J.E. & Fellows, M. (2021) Natural climate solutions for Canada. *Science advances,* **7,** eabd6034.

Elias, M. & Potvin, C. (2003) Assessing inter-and intra-specific variation in trunk carbon concentration for 32 neotropical tree species. *Canadian Journal of Forest Research,* **33,** 1039-1045.

FAO (2018) La situation des forêts du monde 2018. Les forêts au service du développement durable. Rome. Licence: CC BY-NC-SA 3.0 IGO. Rome.

Fargione, J.E., Bassett, S., Boucher, T., Bridgham, S.D., Conant, R.T., Cook-Patton, S.C., Ellis, P.W., Falcucci, A., Fourqurean, J.W. & Gopalakrishna, T. (2018) Natural climate solutions for the United States. *Science advances,* **4,** eaat1869.

Friedlingstein, P., Jones, M.W., O'Sullivan, M., Andrew, R.M., Bakker, D.C., Hauck, J., Le Quéré, C., Peters, G.P., Peters, W. & Pongratz, J. (2022) Global carbon budget 2021. *Earth System Science Data,* **14,** 1917-2005.

Funk, J.M., Aguilar-Amuchastegui, N., Baldwin-Cantello, W., Busch, J., Chuvasov, E., Evans, T., Griffin, B., Harris, N., Ferreira, M.N., Petersen, K., Phillips, O., Soares, M.G. & van der Hoff, R.J.A. (2019) Securing the climate benefits of stable forests. *Climate Policy,* **19,** 845-860.

Goetz, S.J., Hansen, M., Houghton, R.A., Walker, W., Laporte, N. & Busch, J. (2015) Measurement and monitoring needs, capabilities and potential for addressing reduced emissions from deforestation and forest degradation under REDD+. *Environmental Research Letters,* **10,** 123001.

Gonzalez de Tanago, J., Lau, A., Bartholomeus, H., Herold, M., Avitabile, V., Raumonen, P., Martius, C., Goodman, R.C., Disney, M. & Manuri, S. (2018) Estimation of above-ground biomass of large tropical trees with terrestrial LiDAR. *Methods in Ecology and Evolution,* **9,** 223-234.

Goodman, R.C., Phillips, O.L. & Baker, T.R. (2014) The importance of crown dimensions to improve tropical tree biomass estimates. *Ecological Applications,* **24,** 680-698.

Gora, E.M. & Esquivel-Muelbert, A. (2021) Implications of size-dependent tree mortality for tropical forest carbon dynamics. *Nature plants,* **7,** 384-391.

Grassi, G., Monni, S., Federici, S., Achard, F. & Mollicone, D. (2008) Applying the conservativeness principle to REDD to deal with the uncertainties of the estimates. *Environmental Research Letters,* **3,** 035005.

Griscom, B.W., Adams, J., Ellis, P.W., Houghton, R.A., Lomax, G., Miteva, D.A., Schlesinger, W.H., Shoch, D., Siikamäki, J.V. & Smith, P. (2017) Natural climate solutions. *Proceedings of the National Academy of Sciences,* **114,** 11645-11650.

Hansen, M.C., Potapov, P.V., Moore, R., Hancher, M., Turubanova, S.A., Tyukavina, A., Thau, D., Stehman, S.V., Goetz, S.J. & Loveland, T.R. (2013) High-resolution global maps of 21st-century forest cover change. *Science,* **342,** 850-853.

Kunz, M., Barrios, H.E., Dan, M., Dogirama, I., Gennaretti, F., Mathieu, G., Koller, A., Madsen, C., Lana, G. & Ortega, A. (2022) Bacurú Drõa: Indigenous Forest Custody as an Effective Climate Change Mitigation Option. A case study from Darién, Panama. *Frontiers in Climate***,** 231.

Ligot, G., Gourlet-Fleury, S., Ouédraogo, D.Y., Morin, X., Bauwens, S., Baya, F., Brostaux, Y., Doucet, J.L. & Fayolle, A. (2018) The limited contribution of large trees to annual biomass production in an old-growth tropical forest. *Ecological Applications,* **28,** 1273-1281.

Lindenmayer, D., Messier, C. & Sato, C. (2016) Avoiding ecosystem collapse in managed forest ecosystems. *Frontiers in Ecology and the Environment,* **14,** 561-568.

Lindenmayer, D.B. & Laurance, W.F. (2017) The ecology, distribution, conservation and management of large old trees. *Biological Reviews,* **92,** 1434-1458.

Lindenmayer, D.B., Laurance, W.F. & Franklin, J.F. (2012) Global decline in large old trees. *Science,* **338,** 1305-1306.

Lutz, J.A., Furniss, T.J., Johnson, D.J., Davies, S.J., Allen, D., Alonso, A., Anderson-Teixeira, K.J., Andrade, A., Baltzer, J. & Becker, K.M. (2018) Global importance of large-diameter trees. *Global Ecology and Biogeography,* **27,** 849-864.

Lutz, J.A., Larson, A.J., Swanson, M.E. & Freund, J.A. (2012) Ecological importance of large-diameter trees in a temperate mixed-conifer forest. *PloS one,* **7,** e36131.

Luyssaert, S., Schulze, E.-D., Börner, A., Knohl, A., Hessenmöller, D., Law, B.E., Ciais, P. & Grace, J. (2008) Old-growth forests as global carbon sinks. *Nature,* **455,** 213-215.

Mackey, B., Keith, H., L Berry, S. & B Lindenmayer, D. (2008) *Green carbon: the role of natural forests in carbon storage*. ANU Press.

Mackey, B., Kormos, C.F., Keith, H., Moomaw, W.R., Houghton, R.A., Mittermeier, R.A., Hole, D. & Hugh, S. (2020) Understanding the importance of primary tropical forest protection as a mitigation strategy. *Mitigation and adaptation strategies for global change,* **25,** 763-787.

Mascaro, J., Asner, G.P., Knapp, D.E., Kennedy-Bowdoin, T., Martin, R.E., Anderson, C., Higgins, M. & Chadwick, K.D. (2014) A tale of two "forests": Random Forest machine learning aids tropical forest carbon mapping. *PloS one,* **9,** e85993.

Mateo-Vega, J., Arroyo-Mora, J.P. & Potvin, C. (2019) Tree aboveground biomass and species richness of the mature tropical forests of Darien, Panama, and their role in global climate change mitigation and biodiversity conservation. *Conservation Science and Practice,* **1,** e42.

McMahon, R., LaHache, T. & Whiteduck, T. (2015) Digital data management as indigenous resurgence in Kahnawà: Ke. *International Indigenous Policy Journal,* **6,** 1-19.

Muller-Landau, H.C., Condit, R.S., Chave, J., Thomas, S.C., Bohlman, S.A., Bunyavejchewin, S., Davies, S., Foster, R., Gunatilleke, S. & Gunatilleke, N. (2006) Testing metabolic ecology theory for allometric scaling of tree size, growth and mortality in tropical forests. *Ecology letters,* **9,** 575-588.

Odum, E.P. (1969) The Strategy of Ecosystem Development: An understanding of ecological succession provides a basis for resolving man's conflict with nature. *Science,* **164,** 262-270.

Pelletier, J., Busch, J. & Potvin, C. (2015) Addressing uncertainty upstream or downstream of accounting for emissions reductions from deforestation and forest degradation. *Climatic Change,* **130,** 635-648.

Pelletier, J., Kirby, K.R. & Potvin, C. (2012) Significance of carbon stock uncertainties on emission reductions from deforestation and forest degradation in developing countries. *Forest Policy and Economics,* **24,** 3-11.

Phillips, O.L. & Brienen, R.J.W. (2017) Carbon uptake by mature Amazon forests has mitigated Amazon nations' carbon emissions. *Carbon balance and management,* **12,** 1.

Potapov, P., Hansen, M.C., Laestadius, L., Turubanova, S., Yaroshenko, A., Thies, C., Smith, W., Zhuravleva, I., Komarova, A. & Minnemeyer, S. (2017) The last frontiers of wilderness: Tracking loss of intact forest landscapes from 2000 to 2013. *Science advances,* **3,** e1600821.

Redondo-Brenes, A. (2007) Growth, carbon sequestration, and management of native tree plantations in humid regions of Costa Rica. *New Forests,* **34,** 253-268.

Samaras, K. (2005) Indigenous Australians and the 'digital divide'. **55,** 84-95.

Seymour, F. (2020) Seeing the forests as well as the (trillion) trees in corporate climate strategies. *One Earth,* **2,** 390-393.

Sheil, D., Eastaugh, C.S., Vlam, M., Zuidema, P.A., Groenendijk, P., van der Sleen, P., Jay, A. & Vanclay, J. (2017) Does biomass growth increase in the largest trees? Flaws, fallacies and alternative analyses. *Functional Ecology,* **31,** 568-581.

Sillett, S.C., Van Pelt, R., Koch, G.W., Ambrose, A.R., Carroll, A.L., Antoine, M.E. & Mifsud, B.M. (2010) Increasing wood production through old age in tall trees. *Forest Ecology and Management,* **259,** 976-994.

Sillett, S.C., Van Pelt, R., Kramer, R.D., Carroll, A.L. & Koch, G.W. (2015) Biomass and growth potential of Eucalyptus regnans up to 100 m tall. *Forest Ecology and Management,* **348,** 78-91.

Sills, E.O., Atmadja, S.S., de Sassi, C., Duchelle, A.E., Kweka, D.L., Resosudarmo, I.A.P. & Sunderlin, W.D. (2014) *REDD+ on the ground: A case book of subnational initiatives across the globe*. Cifor.

Slik, J.F., Paoli, G., McGuire, K., Amaral, I., Barroso, J., Bastian, M., Blanc, L., Bongers, F., Boundja, P. & Clark, C. (2013) Large trees drive forest aboveground biomass variation in moist lowland forests across the tropics. *Global Ecology and Biogeography,* **22,** 1261-1271.

Smith, P., Ashmore, M.R., Black, H.I., Burgess, P.J., Evans, C.D., Quine, T.A., Thomson, A.M., Hicks, K. & Orr, H.G. (2013) The role of ecosystems and their management in regulating climate, and soil, water and air quality. *Journal of Applied Ecology,* **50,** 812-829.

Stephenson, N.L., Das, A., Condit, R., Russo, S., Baker, P., Beckman, N.G., Coomes, D., Lines, E., Morris, W. & Rüger, N. (2014) Rate of tree carbon accumulation increases continuously with tree size. *Nature,* **507,** 90-93.

Thomas, R.Q., Kellner, J.R., Clark, D.B. & Peart, D.R. (2013) Low mortality in tall tropical trees. *Ecology,* **94,** 920-929.

Toth, K., Smith, D. & Giroux, D. (2018) Indigenous peoples and empowerment via technology 1. *First Peoples Child & Family Review,* **13,** 21-33.

Watson, J.E., Evans, T., Venter, O., Williams, B., Tulloch, A., Stewart, C., Thompson, I., Ray, J.C., Murray, K. & Salazar, A. (2018) The exceptional value of intact forest ecosystems. *Nature ecology & evolution,* **2,** 599-610.

Worbes, M. (1995) How to measure growth dynamics in tropical trees a review. *IAWA Journal,* **16,** 337-351.

Yuan, Z., Ali, A., Jucker, T., Ruiz-Benito, P., Wang, S., Jiang, L., Wang, X., Lin, F., Ye, J. & Hao, Z. (2019) Multiple abiotic and biotic pathways shape biomass demographic processes in temperate forests. *Ecology,* **100,** e02650.

Zhou, G., Liu, S., Li, Z., Zhang, D., Tang, X., Zhou, C., Yan, J. & Mo, J. (2006) Old-growth forests can accumulate carbon in soils. *Science,* **314,** 1417-1417.